THE JOURNAL
OF
CHEMICAL PHYSICS

VOLUME 9 AUGUST, 1941 NUMBER 8

The Thermal Reaction Between Hydrogen and Oxygen

IV. Comparison of the Thermal and the Photochemical Reaction

O. OLDENBERG AND H. S. SOMMERS, JR.
Research Laboratory of Physics, Harvard University, Cambridge, Massachusetts
(Received March 31, 1941)

Some recent observations are compared with theories of the thermal and the photochemical reaction between hydrogen and oxygen. The conclusion is reached that for both cases the gas phase reaction observed at higher temperatures is best described by the Bonhoeffer-Haber chain.

I. PROBLEM

FOR the theoretical treatment of the hydrogen-oxygen combination the *photochemical* reaction has the advantage that the primary process is unquestionable: light generates free atoms, either H or O, in the gas phase at a measurable rate. Consequently, this process should lead to definite statements regarding the reactions of H or O atoms at various temperatures and pressures. The theory of the *thermal* reaction is more questionable since here the process starting the reaction is as difficult to ascertain as its further progress. Therefore, it seems worth while to apply some straightforward conclusions from the *photochemical* reaction to the questionable theory of the *thermal* reaction.

In Section II we shall summarize the various theories, some of them contradictory to each other. Our recent results showing that the thermal reaction is described by the Arrhenius law seem to lead to a decision between these theories. This will be discussed in the last section.

II. REVIEW OF FACTS AND THEORIES

A. The thermal reaction

The starting point of all theories is the discovery of Hinshelwood and Thompson[1] that at low temperatures, roughly below 500°C, the reaction takes place *at the surface*, while above this limit the reaction progresses largely in chains propagated *in the gas phase* and broken at the walls of the vessel. This hypothesis is necessary in order to explain the fact that the rate increases with either vessel size or addition of a foreign gas, which slows down the diffusion of the chain carriers to the walls. We are concerned almost exclusively with the gas phase reaction taking place at higher temperatures.

The facts of the *thermal* reaction and the theory of Lewis and von Elbe[2] have been discussed by these authors in a recent book. Since

[1] C. N. Hinshelwood and H. W. Thompson, Proc. Roy. Soc. **A118**, 170 (1928).

[2] B. Lewis and G. von Elbe, *Combustion, Flames, and Explosions of Gases* (Cambridge University Press, 1938). In the present paper we apply the numbers used in this book to the individual reactions.

they have been reviewed in this journal,[3,4] we shall summarize the reaction scheme only very briefly. The theory is based on Semenoff's[5] idea of explosions by branched chains, which are supposed to start in the gas phase by

$$H_2+M\rightarrow H+H+M. \qquad \text{XIII}$$

They continue in the gas phase by[6]

$$H+O_2\rightarrow OH+O, \qquad \text{II}$$

$$O+H_2\rightarrow OH+H, \qquad \text{III}$$

$$OH+H_2\rightarrow H_2O+H. \qquad \text{I}$$

They are broken in the gas phase by

$$H+O_2+M\rightarrow HO_2+M. \qquad \text{VI}$$

This last step, however, is chain breaking only if followed by

$$HO_2+\text{wall}\rightarrow\text{destruction}. \qquad \text{XII}$$

But for higher pressure or temperature, HO_2 may continue the chain in the gas phase by

$$HO_2+H_2\rightarrow H_2O+OH, \qquad \text{X}$$

or

$$HO_2+H_2\rightarrow H_2O_2+H. \qquad \text{XI}$$

As discussed in the book of Lewis and von Elbe, this set of reactions successfully describes a very complicated behavior, the steady reaction bordered *on both sides* by explosions, on the low pressure side by the second (or "upper") explosion limit, on the high pressure side by the third explosion limit. Furthermore, this set explains the shape of the $p-T$ diagram of the explosion limits[7] and the effects of varying the partial pressures.

Another theory describing the combustion of H_2 in the flame was introduced by Bonhoeffer and Haber[8] and modified by L. Farkas, Haber, and Harteck[9] to adapt it to processes in sensitized photochemical reactions. It applies also to the thermal reaction, but here its success is more limited in that it fails to give account of the second explosion limit; but it does describe the reaction above this limit, in particular its high order leading to the third explosion limit, experimentally investigated in detail by Prettre.[10] This scheme is as follows:

$$H_2+O_2\rightarrow OH+OH,$$
$$OH+H_2\rightarrow H_2O+H,$$
$$H+O_2+H_2\rightarrow H_2O+OH,$$
$$H+\text{wall}\rightarrow\text{destruction},$$
$$OH+\text{wall}\rightarrow\text{destruction}.$$

In order to take account of the formation of H_2O_2 observed in the same reaction, one supplements this scheme by

$$H+O_2+H_2\rightarrow H_2O_2+H.$$

(This step apparently describes the association of H_2+O_2 with H acting as a third body, carrying away some excess energy and momentum. More plausible seems the following interpretation. The chemical stability of H_2+O_2 is explained by the fact that any possible ordinary collision of H_2+O_2 leads to a configuration widely differing from the stable molecules H_2O_2 or H_2O. In a triple collision, however, the partners O_2, H and one of the H atoms belonging to the H_2 molecule may join in a configuration approaching the H_2O_2 structure. Such a triple collision would be expected to have a small steric factor.)

When accepting the scheme of Bonhoeffer and Haber for the thermal gas phase reaction one must ascribe the second explosion limit to some-

[3] B. Lewis and G. von Elbe, J. Chem. Phys. **7**, 710 (1939).
[4] O. Oldenberg and H. S. Sommers, Jr., J. Chem. Phys. **8**, 468 (1940).
[5] N. Semenoff, *Chemical Kinetics and Chain Reactions* (Oxford, Clarendon Press, 1935).
[6] The energies of the following reactions differ from the conventional values by small amounts when for the energy of dissociation of $OH\rightarrow O+H$ we apply the value of 100.9 ± 0.7 kcal. obtained recently by R. J. Dwyer, Phys. Rev. **59**, 928A (1941). To be published in detail later.
[7] For the third explosion limit this evidence was recently given by O. Oldenberg and H. S. Sommers, Jr., J. Chem. Phys. **7**, 279 (1939); *ibid.* **9**, 114 (1941); and H. R. Heiple and B. Lewis, J. Chem. Phys. **9**, 120 (1941). D. Frank-Kamenetzky, Acta Physicochim. U.R.S.S. **13**, 730 (1940), points out the agreement between our measurements of the third explosion limit and his theory which is based on the hypothesis of a *thermal* explosion. He concludes that it seems doubtless that the third explosion limit is of a thermal nature. Contrary to this statement, Heiple and Lewis interpret the same limit by a *branched chain* explosion but admit a superimposed thermal effect. In our paper referred to above we conclude that the investigation of the third explosion limit does not lend itself to a decision between the competing theories.
[8] K. F. Bonhoeffer and F. Haber, Zeits. f. physik. Chemie **137**, 263 (1928).
[9] L. Farkas, F. Haber and P. Harteck, Zeits. f. Elektrochemie **36**, 711 (1930). The application of their theory to the ammonia sensitized photochemical reaction of $2H_2+O_2$ has been disproved by Taylor and Salley (reference 15).
[10] M. Prettre, J. de chim. phys. **33**, 189 (1936).

thing else, presumably to the surface reaction, which is known to be superimposed on the gas phase reaction, exceeding it at low temperatures but completely obscured by it at high temperatures.

Finally, in a comparison of the theories of the thermal reaction, energy chains must be considered although, in general, chances for energy chains are supposed to be inferior.[11] An energy chain is a chain in which the large energy of activation required for the next step of the chain is stored up in a molecule in the shape of electronic excitation, vibration, rotation, or translation. All these types of energy, however, are liable to be dissipated by collisions and so changed into heat. Therefore the rate of an energy chain reaction is expected to be decreased by addition of an inert gas which can take away the energy of activation by impacts of the second kind. Experimentally, the opposite is the case in the reaction under discussion. Hinshelwood[12] observed an *increase* of rate with increasing pressure of a foreign gas (N_2, A, He). Prettre[10] confirmed this result using N_2 and A. This fact seems to exclude energy chains.

We found it desirable to do more experiments with helium as a foreign gas. The purpose was as follows: energy of activation stored up in a molecule is generally assumed to be *vibrational* energy because all other types of energy are supposed to have no appreciable lifetime. Vibrational energy, in particular of degrees of freedom connected with H atoms, is liable to be dissipated by collision with helium atoms. This follows from observations of the rates of monomolecular reactions and dispersion of sound.[11] Therefore He would be expected to reduce the length of an energy chain. No such effect could be observed as discussed in the preceding paper.* This experiment, therefore, furnishes an argument against energy chains with the energy stored up as *vibration*.

B. The photochemical reaction

As far as the *photochemical* reaction goes, we are interested only in its high temperature range for the sake of comparison with the thermal reaction just discussed.[13]

In order to test Semenoff's theory of branched chains,[5] Kistiakowsky[14] investigated the temperature coefficient of the "direct" photochemical combination of $2H_2+O_2$ started by O atoms, varying the temperature over as wide a range as possible. (He illuminated the gas mixture with light of a wave-length near 1720A and so dissociated O_2 molecules.)

Taylor and Salley[15] measured the temperature coefficient of the same photochemical reaction but started it by H atoms. (They "sensitized" the mixture by adding a trace of mercury vapor, illuminated with the resonance line of mercury, and so dissociated H_2 molecules by impacts of the second kind.) Taylor and Salley found that the two investigations, although starting from different atoms, H and O, respectively, lead to the same results. These are as follows. Both reactions obey the Arrhenius law up to the same temperature limit of 490°, showing appreciably the same constant value of the activation energy (3,000–5,000 cal./mole). Above this limit both show nearly the same rates, exceeding those given by the Arrhenius law. Taylor and Salley followed their reaction up to 530°C where the activation energy has already increased to 25,000 cal./mole. For higher temperatures the thermal reaction obscures the photochemical reaction.

The latter authors interpret this agreement between the two types of the photochemical reaction (starting from either H or O atoms) by the assumption that in the "direct" photochemical reaction O atoms produce H atoms by $O+H_2 \rightarrow OH+H$ and so cause the same sequence of reactions started in the "sensitized" photochemical reaction by H atoms. Furthermore, the authors assume that below 490° the OH radicals are inactive, but that above this limit the length

[11] O. Oldenberg and A. A. Frost, Chem. Rev. **20**, 99 (1937).

[12] C. N. Hinshelwood and A. T. Williamson, *The Reaction between Hydrogen and Oxygen* (Oxford, Clarendon Press, 1934, p. 32.

* See reference 18.

[13] The low temperature range has recently been discussed by H. A. Smith and A. Napravnik, J. Am. Chem. Soc. **62**, 382 (1940). In similar investigations, H and O atoms were generated by brief duration electric discharges before the mixture $2H_2+O_2$ was admitted (F. Dubowizky, A. Nalbandjan and N. Semenoff, Trans. Faraday Soc. **29**, 606 (1933); but for our purpose, such experiments are less conclusive, since the effects observed may be due to free atoms *adsorbed at the walls* as well as free atoms *in the gas phase*.

[14] G. B. Kistiakowsky, Proc. Nat. Acad. Sci. **15**, 194 (1929).

[15] H. S. Taylor and D. J. Salley, J. Am. Chem. Soc. **55**, 96 (1933).

of the chain increases very rapidly with increasing temperature, possibly by the activity of the radical OH.[16] The authors do not specify the following steps of the reaction.

A more complete scheme of the sensitized photochemical reaction, that is the reaction started by H atoms, including its temperature coefficient and induction period, has recently been given by Lewis and von Elbe.[17] They assume that H atoms are attached to O_2 in triple collision and that, below 500°, the radicals HO_2 so formed react at the wall by

$$HO_2+HO_2 \text{ adsorbed}\rightarrow O_2+H_2O_2.$$

This would only lead to the quantum yield of unity, independent of the temperature. In order to explain the fact that above room temperature the quantum yield is slowly increasing, they assume additional surface reactions of HO_2 presumably with H_2 in analogy with the thermal slow catalytic surface reaction below 500°C, identified by Hinshelwood.[12] Above 500° they assume that HO_2 leads to a gas phase chain by

$$HO_2+H_2\rightarrow H+H_2O_2, \qquad \text{XI}$$

which is responsible for the observed rapid increase of the yield.

This photochemical gas phase reaction suggested by Lewis and von Elbe is closely related to the Bonhoeffer-Haber scheme; it differs from it by the intermediate formation of the radical HO_2. Furthermore it favors the production of H_2O_2 which actually is observed in the photochemical reaction.

This scheme of Lewis and von Elbe explains the induction period by the time required to build up the surface concentration of HO_2. Such an interpretation is satisfactory as far as the surface reaction goes; but it is incomplete in that it fails to explain the fact, described by Taylor and Salley that the induction period was also observed at higher temperatures where the gas phase reaction should be predominant. More specific assumptions permit a description of the rather complicated dependence of the yield on the light intensity.

III. Reconciliation of the Various Schemes

The main problem is how to unify the various schemes, in particular how to reach a compromise between the conflicting theories of the thermal reaction. Recent measurements of its temperature coefficient[18] seem to give a decision. A change of the temperature has different effects on the thermal and the photochemical rate: for the thermal reaction, the energy of activation is *far greater*, and, furthermore, this energy remains *constant* into a much higher temperature range, following the Arrhenius law; in a vessel of 5-cm diameter, this range reaches up to 543°, in a vessel of larger ratio surface/volume even up to 565°C. Below 490° the rate is too slow for measurement and above the limits just mentioned the steady reaction rapidly changes to the explosion. A constant energy of activation was also observed by Prettre[10] in a KCl-covered vessel over a narrower temperature range (540–560°C).

The *higher value* of the activation energy has nothing to do with the present problem; it is to be expected for the thermal reaction, since here thermal energy is needed for the creation of chain carriers, while in the photochemical reaction this share of the energy is supplied by light. Hence the comparatively low activation energy of the photochemical reaction is only due to the steps by which the chain continues or branches.

In the following argument we are concerned with the various ranges in which the two reactions *follow the Arrhenius law*. According to Semenoff,[19] a *nonbranched* chain follows the Arrhenius law with a constant activation energy while the rate of a *branched* chain, when formally represented by this law, shows an activation energy increasing with the temperature. The fact that the thermal reaction follows the Arrhenius law with constant activation energy gives preference to the Bonhoeffer-Haber scheme which does not involve branched chains while the Lewis-von Elbe scheme involves branching in two consecutive steps II and III. We tried

[16] G. von Elbe (J. Am. Chem. Soc. **55**, 62 (1933)) found a reaction between OH and H_2 even at room temperature; he points out, however, that in his experiment the OH radicals, produced by the photochemical decomposition of H_2O_2, may have been endowed with some excess kinetic energy.

[17] B. Lewis and G. von Elbe, J. Chem. Phys. **7**, 712 (1939).

[18] O. Oldenberg and H. S. Sommers, J. Chem. Phys. **9**, 432 (1941).

[19] N. Semenoff, reference 5, p. 48.

to preserve this latter scheme, because it describes certain features of the second explosion limit so well, but we failed to find a modification which would reconcile it to the Arrhenius law with a constant activation energy.

It seems a less important question whether the reaction starts at the wall or in the gas phase. For the starting at the wall, a wide range of special assumptions, presumably connecting this starting process with the surface reaction, remains open. The starting by reaction XIII (thermal dissociation of H_2) seems questionable. The reason is that the energy of activation of the thermal reaction in a Pyrex vessel, although it is not well reproducible, is consistently below 100,000 cal./mole; it may be as low as 74,000. The dissociation of H_2 molecules would require 103,000 cal./mole. One can hardly expect other processes of the chain to reduce this energy requirement to the lower value observed.

For the *photochemical* reaction at high temperature started by H atoms, the recent theory of Lewis and von Elbe discussed above is in harmony with the Bonhoeffer-Haber theory of the *thermal* reaction just advocated. It is not a great difference, whether the H atoms first form HO_2 in triple collisions followed by $HO_2+H_2 \rightarrow H_2O_2+H$, or whether $H+O_2+H_2$ form H_2O_2 in one process. (The intermediate formation of HO_2 may be preferable because it gives a chance for inert molecules to act as third bodies and so promote the rate.) In particular, this theory describes the rapid increase of the activation energy of the photochemical reaction above 500°C by the gradually increasing importance of the gas phase reaction XI.

This theory, applied by its authors to the photochemical reaction *started by* H *atoms*, lends itself very well to the interpretation of the photochemical reaction started by O atoms. Following Taylor and Salley[15] one assumes

$$O+H_2 \rightarrow OH+H.$$

By this step each O atom leads to the formation of just the two particles which alternate in the Bonhoeffer-Haber chain. Therefore it causes the formation of two chains of the Bonhoeffer-Haber type. (The reaction started by O atoms should have twice the yield of the reaction started by H atoms; but it will hardly be possible to test this theoretical prediction.)

The striking experimental contrast between the thermal and the photochemical reaction was discussed in the preceding section; in the same temperature range (above 500°C) the thermal reaction follows the Arrhenius law while the photochemical reaction violates it. This contrast must be reconciled with the present theory which gives the same interpretation to both reactions, a nonbranched gas chain which gradually vanishes with decreasing temperature, until at low temperature only a surface reaction remains. In the theory the contrast comes in by the starting process. In the *photochemical* investigation, *the number of chains started per second by light is constant.* This explains the persistence with decreasing temperature of a well measurable rate. Here the deviation from the Arrhenius law is attributed to the transition from a fast reaction (gas phase, predominant above 540°) to a slow reaction (surface, although started by light in the gas phase, predominant below 500°). The curvature is pronounced because the activation energy changes by the factor 6. The *thermal* reaction, however, is dominated by the fact that the *number of chains started per second by heat goes rapidly down with decreasing temperature.* This feature is responsible for the steep slope of the thermal curve. It is so steep that it is not noticeably affected by a small change of activation energy (by some weak surface reaction coming into play) in particular at the bottom where the rates are low and the measurements inaccurate. A curvature is actually evident in Hinshelwood and Thompson's[20] diagram representing experiments in quartz; in our experiments it failed to show up. But such a surface reaction may well be as erratic as many other surface properties.

When accepting this scheme of Lewis and von Elbe for the *photochemical* reaction, the very different scheme suggested by the same authors for the *thermal* reaction leads to the following two additional difficulties.[21] (1) Why, at high temperatures, is the fate of H atoms in the photochemical reaction different from their fate in the thermal reaction where the continuation by

[20] C. N. Hinshelwood and H. W. Thompson, Proc. Roy. Soc. **A118**, 180 (1928).

[21] A more comprehensive discussion of the second explosion limit leads us to attribute it to the surface rather than to the gas phase reaction (reference 4). In a letter to the editor (J. Chem. Phys. **9**, 194 (1941)) von Elbe and Lewis announced that they are continuing their investigation of this topic.

$H+O_2 \rightarrow OH+O$ competes with the formation of HO_2 in triple collisions? (2) Is it admissible in the theory of the thermal reaction to explain the second (or "upper") explosion limit by a gas phase reaction (Lewis and von Elbe,[2] reactions I, II, III, VI, XII) although in the photochemical scheme below 500°C, the gas phase reactions (except combination reactions) are supposed gradually to vanish and the general rule is stated that, toward lower temperatures, reactions of radicals in H_2-O_2 mixtures are heterogeneous rather than homogeneous? This statement contrasts with the fact that the upper explosion limit was measured by Hinshelwood down to a temperature of nearly 450°C; recently Lewis and von Elbe succeeded in tracing it even to 400°C. Its occurrence at such low temperatures seems to link the upper explosion to a surface reaction. If this attribution is accepted for low temperatures, it is hardly reasonable to assume a different mechanism for higher temperatures, considering the smoothness of Hinshelwood's curve representing this limit between 450 and 580°C. These two difficulties add weight to the arguments given above in favor of the Bonhoeffer-Haber scheme.

The present discussion leads to a unification of the theories of the photochemical and thermal reaction. Therefore it opens up the way to a more detailed analysis of the chains, even for the thermal reaction. In the photochemical reaction, the yield per quantum is measured and so the total rate is analyzed into number of chains times chain length. Once we accept that the same chains occur in both types of reaction, we are allowed to apply the photochemical evidence to the thermal reaction.

Thus a preliminary estimate can be made of how the energies of activation are distributed over the steps of the thermal reaction, particularly in Pyrex where the results are rather consistent. We assume 80,000 cal./mole as over-all value.[18] This must be distributed over the starting of the chain and its continuation. The continuation is the same as for the photochemical chain at high temperatures. According to Taylor and Salley its activation energy goes up to 25,000 cal./mole; but this is only the limit of the observation, possibly not the final value. Consequently, for the starting of the thermal chain, 55,000, or perhaps less, would be available.

A deficiency of the theory is that it fails to give a complete account of the inhibition period. This period has been attributed to surface phenomena by Lewis and von Elbe for the low temperature range of the photochemical reaction. For the thermal reaction, too, it may be explained by surface phenomena, provided that we attribute the starting of the chains to a surface reaction.[18] This period must have a different explanation in the high temperature photochemical reaction which certainly starts, and presumably continues, in the gas phase. The inhibition period needs more experimental investigation.

In making a quantitative comparison of the two reactions, thermal and photochemical, it must be borne in mind that there exists a possible source of trouble, arising not from the photochemical or thermal nature of the reaction, but from the use of the continuous flow method in the photochemical investigation in which free H atoms start the reaction. The difficulty is as follows. Suppose that a reaction performed with the *quiescent* method manifests a certain inhibition period, that is a period after which the rate becomes reasonably uniform over some length of time. The same reaction when performed with the streaming method is sure to show an inhibition period, too. But it is not sure whether the final rate observed is identical with the final rate of the quiescent method. This would depend on the velocity of streaming if, for example, the inhibition period would represent the time required until some water vapor is formed. A true comparison of the thermal and the photochemical reaction could only be obtained on the basis of a comprehensive investigation of both reactions; both should be investigated with quiescent rather than with flowing gases, with the purest possible gases prepared by the same methods, and, finally, both should be observed in the same vessel, aged with the same treatment.

The principal conclusion is that the Bonhoeffer-Haber scheme, possibly modified by introducing the radical HO_2 as intermediate carrier, is applicable over a wider range of reactions than originally considered by its authors.

Deviations from Ohm's Law in Soda Lime Glass*

R. J. MAURER
Massachusetts Institute of Technology, Cambridge, Massachusetts
(Received April 10, 1941)

The conductivity of soda lime glass has been measured as a function of field strength between 0°C and 110°C. The data are compared with a recent theory of electrolytic conductivity of solids. The form of the deviation from Ohm's law is correctly represented by this theory up to field strengths of 7×10^5 volts/cm. Reasonable values for the physical constants result from the measurements.

INTRODUCTION

THE electrical conductivity of solids has been the subject of extensive investigation.[1,2] Most of the work upon the deviations from Ohm's law, which occur at high field strengths, has been concerned with the verification of the empirical relation known as Poole's law

$$i=aVe^{bV} \tag{1}$$

or with attempts to show that if the resistance is properly measured, no deviations exist.[3]

Recent theories[4–6] of electrolytic conduction in solids predict a real deviation from Ohm's law and the present paper is an attempt to check the theoretical form of the deviation.

THEORY

The electrolytic conductivity of crystals arises because a fraction of the ions have left normal lattice sites either for interstitial positions[7] or to migrate to the surface.[8] If we consider only the case of interstitial ions their density is given approximately by

$$n=Ne^{-W/2kT}, \tag{2}$$

where N is the density of ions in "normal" positions and W is the work to move an ion from a "normal" to an interstitial site. The creation of an interstitial ion leaves a "hole" in the lattice.

The possible equilibrium positions of an ion in the interstitial space are separated by potential barriers which are due to the repulsive forces between the "normal" ions and an interstitial ion. The probability that a fluctuation in the thermal energy of an interstitial ion will supply the energy necessary for crossing the barrier depends upon the Boltzmann factor. The number of jumps per ion per unit time may be written approximately

$$z=\nu e^{-U/kT}, \tag{3}$$

where ν is the vibration frequency of the interstitial ion and U is the height of the potential barrier. U will increase with the size and valence of an ion.

When an electric field, E, is applied to the crystal, the height of the potential barriers in the direction of the field is

$$U-eEd/2 \tag{4}$$

and in the opposite direction

$$U+eEd/2, \tag{5}$$

where e is the charge of the ion and d is the distance between the interstitial positions of equilibrium. Consequently, the number of jumps per second in the direction of the field is greater than in the opposite direction. The difference in the rate of jumps in these two directions is given by

$$\Delta z=\frac{\nu e^{-U/kT}}{\gamma}\left[e^{eEd/2kT}-e^{-eEd/2kT}\right] \tag{6}$$

* Publication No. 7 of the Solar Energy Conversion Research Program.
[1] H. H. Poole, Phil. Mag. **42**, 488 (1921).
[2] H. Schiller, Zeits. f. tech. Physik **6**, 588 (1925).
[3] A. Joffe, *The Physics of Crystals* (McGraw-Hill Book Company, Inc., New York, 1928).
[4] H. Eyring, J. Chem. Phys. **4**, 283 (1936).
[5] F. Seitz, *The Modern Theory of Solids* (McGraw-Hill Book Company, Inc., New York, 1940).
[6] N. Mott and R. Gurney, *Electronic Processes in Ionic Crystals* (Oxford University Press, 1940).
[7] J. Frenkel, Zeits. f. Physik **35**, 657 (1926).
[8] C. Wagner and W. Schottky, Zeits. f. physik. Chemie **B11**, 163 (1930).

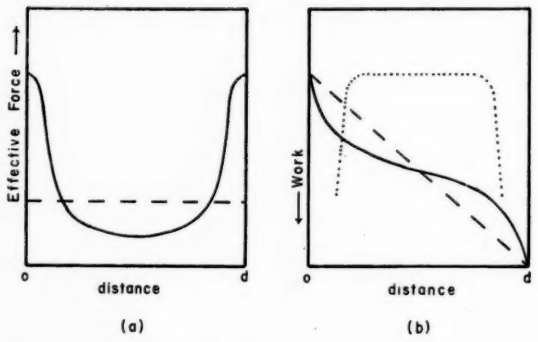

FIG. 1. (a) The effective force on an ion as a function of position. Dashed line is average force, eE. (b) Work performed by effective force. Dashed line gives work done by average force. Dotted line is potential barrier in absence of field.

and the associated current density may be written

$$=ned\Delta z=\frac{2Ned\nu}{\gamma}$$
$$\times\exp\left[-\left(\frac{W/2+U}{kT}\right)\right]\sinh\left(\frac{eEd}{2kT}\right), \quad (7)$$

in which γ is the number of possible jump directions of the ion. When the argument of the hyperbolic sine is small, this function is approximately equal to its argument. Under this condition Ohm's law is valid, with a conductivity

$$\sigma=\sigma_0\exp\left[-\left(\frac{W/2+U}{kT}\right)\right]$$
$$=\frac{Ne^2d^2\nu}{\gamma kT}\exp\left[-\left(\frac{W/2+U}{kT}\right)\right]. \quad (8)$$

A more rigorous analysis would take into account the temperature dependence of W and U and would lead to a slightly different form for the coefficient σ_0.

To a first approximation, n will be independent of the field, as we have assumed. The distortion of the potential barriers by the field changes the rate of formation and the rate of disappearance of the interstitial ions by the same term

$$\cosh(eEd'/2kT)-1. \quad (9)$$

A fraction of the interstitial ions will be in the neighborhood of "holes." These "pairs" may be thought of as associated in the sense of Bjerrum.[9] If the density of these "pairs" is field dependent, n will vary with the field.[10] This possibility is neglected in deriving.[7]

The lattice structure of a solid eliminates electrophoretic forces, and, where only ions of one sign are mobile, prevents the formation of a Debye-Hückel "atmosphere." Usually the number of interstitial ions and "holes" is so small that the magnitude of the two last mentioned effects would be negligible in any case.

The assumption that the effective force on an ion is eE deserves some discussion.[11] Consider a dielectric medium in which non-overlapping dipoles are produced by a field E. The force on a charge e, attached to one of the dipoles is

$$eF_0=e[E+4\pi P/3]=[(\epsilon+2)/3)]eE, \quad (10)$$

if the arrangement is cubic or random. If the charge and dipole are moved about the force will change, subject always to the restriction that

$$\int_0^d F_{\text{eff}}dl=Ed \quad (11)$$

between two equivalent positions. Figure 1 shows qualitatively how the effective force and work will depend upon the position of an interstitial ion as it is moved from one equilibrium site to another. In the case of a broad flat potential barrier such as shown in Fig. 1(b) (dotted curve) only the field near 0 is effective in lowering the barrier. As a result, the effective field may be

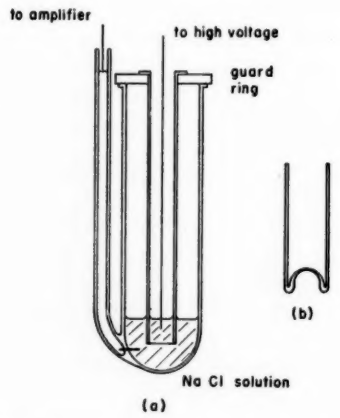

FIG. 2(a), (b). Glass samples.

[9] R. Fuoss, Chem. Rev. **17**, 27 (1935).
[10] L. Onsager, J. Chem. Phys. **2**, 599 (1934).
[11] H. Mueller, Phys. Rev. **47**, 948 (1935).

greater than E. The quantity d must then be interpreted as the width of the potential hole. We mention this case because the experimental data indicate that the effective field is greater than E and that it is given approximately by F_0. However, we have no information about the actual shape of the potential barrier. If the barrier is bell shaped, as we should expect, the effective field will be E.

For comparison with experimental data it is convenient to write (7) in the form

$$i = s' \sinh (a'V), \tag{12}$$

where i is the measured current, V is the applied voltage. Ohm's law takes the form

$$i = (s'a')V = sV. \tag{13}$$

Thus, if s is determined from the initial slope of the current-voltage curve, a' can be found by fitting the theoretical curve to the experimental at high field strengths. From a', d can be calculated and compared with the expected value.

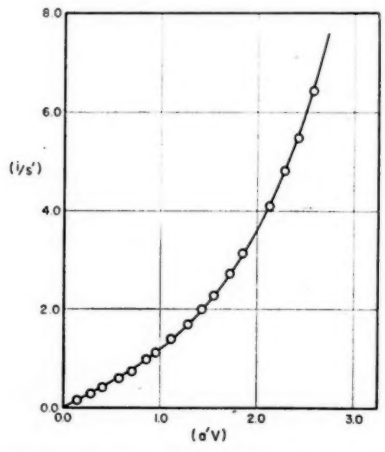

FIG. 3. Soda lime glass 23.1°C. NaCl solution electrodes. $a' = 5.65 \times 10^{-4}$ volt^{-1}. $s' = 1.81 \times 10^{-7}$ amp.$^{-1}$.

SODA LIME GLASS

A soda lime glass was chosen for the experimental material. This glass may be thought of as a random network of silicon and oxygen with the calcium and sodium ions in interstitial positions.[12,13] The interstitial sodium ions are not produced as the result of "holes" in the "normal"

[12] W. H. Zachariasen, J. Am. Chem. Soc. **54**, 3841 (1932).
[13] B. E. Warren, J. App. Phys. **8**, 645 (1937).

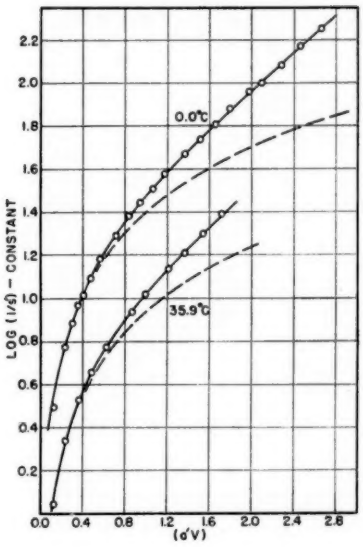

FIG. 4. Soda lime glass. NaCl solution electrodes. (a) 0.0°C. $a' = 4.75 \times 10^{-4}$ volt^{-1}. (b) 35.9°C. $a' = 5.15 \times 10^{-4}$ volt^{-1}. Ohm's law is represented by the dashed curves.

network and their number is independent of both temperature and field strength. The activation energy U may vary from one interstitial position to another, however, because of the irregular nature of the glass structure. As a result, all of the sodium ions need not contribute equally to the current. Actually, the measurements of Robinson[14] give a constant value of $U = 0.79$ ev, from 50°C to 350°C.

The work of Quittner[15] has shown that, under the proper conditions, the sodium ion is the sole charge carrier. His check of Faraday's law extended to 6×10^5 volts/cm. While sodium ions are always discharged at the cathode, the anode material must be properly chosen to avoid the introduction of foreign ions or the development of an anode layer which has been depleted of sodium ions. A concentrated solution of a sodium salt fulfills these requirements. A uniform field E has been assumed in the derivation of Eq. 7, but no information is available as to the potential distribution in a glass at high field strengths. Wenderowitch and Lapkin[16] using low fields of 100 volts/cm found it necessary to go to temperatures of about 400°C before the linear potential

[14] D. Robinson, Physics **2**, 52 (1932).
[15] F. Quittner, Akad. Wiss. Wien **136**, 151 (1927).
[16] A. Wenderowitch and B. Lapkin, J. Exp. Theor. Phys. U. S. S. R. **9.1**, 46 (1939).

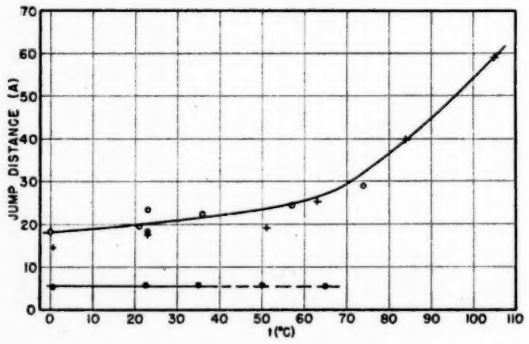

FIG. 5. Jump distance *vs.* temperature. ○ NaCl solution electrodes. + Silver electrodes. The lower curve results if the effective force on an ion is assumed to be given by Eq. (10).

distribution was disturbed by the formation of a high resistance anode layer. They used silver electrodes and the introduction of silver into the glass from the anode was responsible probably for at least a part of the potential distortion which was observed.

EXPERIMENTAL

The measurements were made on two types of glass samples. The most favorable arrangement is sketched in Fig. 2(a). A sheet of the glass,* 8.2×10^{-3} cm thick and 1.33 sq. cm in area, closed the end of a thick-walled cylinder. Concentrated sodium chloride solution ($3.5N$) served as electrodes. The electrical connection to the anode solution was a platinum wire and to the cathode solution was a nickel wire.

Thin bubble windows,† having evaporated silver electrodes were also used (Fig. 2(b)). With this arrangement the test sample is not of uniform thickness; the effective area is unknown, and silver enters the glass during an experiment.

The high voltage power source and instruments have been described.[17,18] In obtaining a current-voltage curve, the voltage was raised in steps, sufficient time elapsing between voltage increments for the current to become constant. The current-voltage characteristic of a sample was usually quite reproducible.

RESULTS

Figures 3 and 4 show typical comparisons of the data with the theoretical curve. The hyperbolic sine relation represents the measurements within the experimental error. a' has been treated as a parameter and chosen in each case to give the best fit of the experimental to the theoretical curve. The logarithmic plot of Fig. 4 emphasizes the exponential behavior of the hyperbolic sine for large values of the argument. Except at low field strengths, Poole's equation can be fitted to such data quite satisfactorily.

Figure 5 shows the jump distance d calculated from a' as a function of temperature. The value of d, obtained from the bubble window data, tends to be slightly low, because the thickness of these windows was measured at their thinnest point. When d is calculated from a' with the assumption that E is the effective field, it is about three times larger than expected at room temperature and the discrepancy increases with the temperature. The expected value of d can be estimated from the average distance between silicon atoms in the glass, which is three to four angstroms.

As was previously mentioned, the disagreement can be removed by assuming that the effective field is given by (10) rather than by E. In order to calculate the Lorentz force F_0, the dielectric

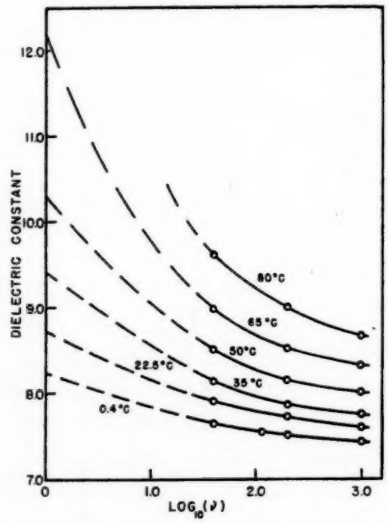

FIG. 6. Dielectric constant *vs.* log frequency.

* This glass contained 5.54 percent CaO and 16.80 percent Na_2O.

† These were the samples used in reference 18 for the measurement of the breakdown strength. The composition was probably very similar to that of the analyzed lot.

[17] R. C. Buehl and A. von Hippel, Phys. Rev. **56**, 941 (1939).

[18] A. von Hippel and R. J. Maurer, Phys. Rev. **59**, 820 (1941).

constant of the glass was measured with a modified Schering bridge.[19] The condenser was a wafer of the glass, 1.2×10^{-2} cm thick, with graphite (Aquadag) electrodes.

Figure 6 gives the dielectric constant as a function of the frequency for several temperatures. 40 hertz was the lowest frequency available, and, because of the strong dispersion, it is impossible to extrapolate to the static field (1 hertz) at the higher temperatures. By using the plausible extrapolations of Fig. 6, which are without theoretical significance, the lower curve of Fig. 5 was obtained. At room temperature, the substitution of F_0 for E in the calculation of the jump distance leads to a very satisfactory value between 5 and 6A. The apparent dependence of d on the temperature is then due to the temperature dependence of the dielectric constant.

It is possible, of course, that the true jump distance is a multiple of the average distance between interstitial cells. This would occur if a large fraction of the interstitial cells cannot provide equilibrium positions for the sodium ion since their value of U is of magnitude kT or less. Such a situation might arise if the cells were distributed into two sharply defined groups—those of quite small volume and those of sufficient volume to accommodate a sodium ion.

A third possible explanation of the large apparent jump distance is that the barrier cannot be adequately represented by an electrostatic potential. The barrier is distorted as the ion moves over it and the term $4\pi P/3$ in Eq. (10) is then to be interpreted as a crude method of evaluating the effect of the polarization of the barrier in terms of the dielectric constant, and the average velocity of the sodium ion.

At room temperature, with fields greater than 7×10^5 volts/cm there is a systematic deviation from Eq. (12) and the measured currents become larger than the predicted. The measurements of Fig. 7(a) were carried to the breakdown point of the glass. It is probable that the onset of the deviation (which is usually less abrupt than for the data shown in Fig. 7(a) is connected with the approach to the breakdown point. In soda lime glass, the breakdown is of the thermal type for the range of temperatures used in this work.

[19] J. Balsbaugh, A. Howell and J. Dotson, Trans. A.I.E.E. 59, 1 (1940).

A few current-voltage curves were taken with Pyrex glass at room temperature. The agreement with the theoretical curve is as satisfactory as in the case of the soda lime glass (Fig. 7(b)). But, though the deviation of the experimental from the theoretical curve begins at about the same field strength, the measured currents become smaller than predicted. This discrepancy increases in systematic fashion until the breakdown point is reached.

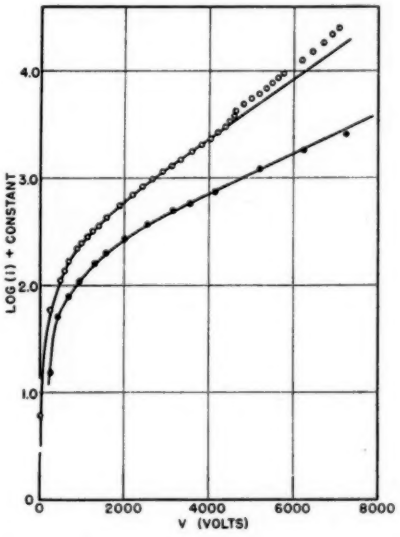

FIG. 7. (a) Soda lime glass. 5.8×10^{-3} cm thick. NaCl solution electrodes. 23.0°C. $d=19.2$A. (b) Pyrex glass. 9.5×10^{-3} cm thick. NaCl solution electrodes. 23.5°C. $d=20.3$A. (Lorentz-Lorenz correction neglected.)

Over the short range of temperature used, σ, the ohmic conductivity of the soda lime glass, can be represented by Eq. (8) with $U=0.75$ ev. σ_0 is obtained from the intercept of the log (σT) *vs.* $1/T$ plot, and, with an appropriate assumption as to the value of γ, ν can be calculated. If γ is taken as 10, then $\nu=8\times10^{13}$ sec.$^{-1}$

CONCLUSION

This brief discussion of the mechanism of electrolytic conduction in solids should emphasize the approximate nature of Ohm's law. With respect to their ionic conductivity, solids are frequently classed as weak electrolytes. However, this classification may be misleading. A mobility, independent of field strength, can be conveniently defined for the ions of a solution of a weak

electrolyte but for a solid such a definition is an approximation limited to a much narrower range of field strengths.

Soda lime glass provides an opportunity to test the theoretical form of the field dependence of the ionic mobility in solids because the field effects which are characteristic of solutions are absent. The data can be represented by the proposed hyperbolic sine relation over a wide range of field strengths. In addition the measurements yield reasonable values for the three physical constants (ν, U, and d) which determine the absolute magnitude of the current density and its field and temperature dependence.

ACKNOWLEDGMENTS

The author is deeply indebted to Professor A. R. von Hippel for his interest in this work and for the benefit of many illuminating discussions. The measurements of the dielectric constant of the glass were made by Mr. W. W. Pendleton of the Oil Research Laboratory, whose cooperation is gratefully acknowledged.

AUGUST, 1941 JOURNAL OF CHEMICAL PHYSICS VOLUME 9

The Reaction Between Hydrogen and Oxygen: Kinetics of the Third Explosion Limit[1]

HAROLD R. HEIPLE[2] AND BERNARD LEWIS[3]
Physical Chemistry Section, Central Experiment Station, Bureau of Mines, Pittsburgh, Pennsylvania

(Received May 16, 1941)

The third explosion limit of hydrogen and oxygen has been investigated in spherical Pyrex vessels of different sizes, covered with an almost invisible layer of KCl, at temperatures from 530° to 570°C, using different ratios of hydrogen and oxygen, and inert gases, nitrogen, helium, and argon. The results are described rather well by the mechanism developed by Lewis and von Elbe from experiments at the second explosion limit and the reaction above it. The explosion is preceded by an induction period, which decreases to zero at higher pressures. It is shown that such third limit explosion pressures of zero induction period are representative of the isothermal branched chain explosion, whereas lower third limit explosion pressures with induction periods have a thermal disturbance superimposed, the difference between the two values providing a measure of the magnitude of the thermal effect. From the energy of activation of k_2 for reaction $H+O_2=OH+O$ determined at the second explosion limit, and the slope of the third explosion limit curve with temperature determined by Oldenberg and Sommers in a heavily KCl-coated vessel for zero induction period, an energy of activation of k_{10} for reaction the $HO_2+H_2=H_2O_2+H$ was calculated to be 33.5 kcal. This agrees with the value 32.9 kcal. found by calculating k_{10} directly from the experimental data. This sets an upper limiting value of the bond energy of H and O_2 in HO_2 as 65.3 kcal. The energy of H and HO_2 in H_2O_2 then has a lower limiting value of 69.5 kcal. It is pointed out that the third explosion limit *per se* does not lend itself well to a study of the reaction mechanism. This must be provided by studies of the second explosion limit and the reaction above it which are in progress. The third explosion limit can, however, provide support for any mechanism so developed.

THE knowledge that an explosion limit is of the isothermal branched chain type is of considerable value in the qualitative and quantitative study of the reaction mechanism. This has been demonstrated for the second explosion limit of the hydrogen-oxygen reaction, but the character of the third explosion limit has remained unsettled. The theory of the reaction mechanism[4] formally accounts for an isothermal branched chain third explosion limit; but, as was pointed out,[4] the actual limit is probably at least partly thermal in character. A rigorous quantitative treatment of the thermal explosion in the case of a complex reaction of the chain type is hopelessly difficult. One can, however, compare third explosion limit data with results to be expected

[1] Published by permission of the Director, Bureau of Mines, U. S. Department of the Interior. The material of this paper represents part of a dissertation submitted to the University of Pittsburgh by H. R. H. in partial fulfillment of the requirements for the Ph.D. degree, February, 1941.

[2] Bureau of Mines-University of Pittsburgh Research Fellow. Present address: Shell Oil Co., Wood River, Ill.

[3] Senior Physical Chemist, Physical Chemistry Section, Central Experiment Station, Bureau of Mines, Pittsburgh, Pennsylvania.

[4] B. Lewis and G. von Elbe, *Combustion, Flames and Explosions of Gases* (Cambridge Press, 1938), Chapter II.

from the equation developed on the basis of the isothermal branched chain explosion condition.

The general isothermal branched chain condition for explosion for the case of chain breaking at the surface can, with good approximation, be written[5] as

$$\frac{\pi^2 D}{r^2}\frac{1}{1+(2\lambda/\epsilon r)(1-\epsilon)}=\alpha, \qquad (1)$$

where α is the chain branching coefficient, ϵ the efficiency of chain breaking at the wall, λ the mean free path, D the diffusion coefficient, and r the radius of the vessel. It is seen that if $\epsilon \gg 2\lambda/r$, the explosion condition becomes independent of the nature of the surface of the vessel. If the surface can be treated in a way such that ϵ is successively increased, it should be possible, by keeping other conditions the same, to increase the explosion pressure to some maximum value that is not sensitive to further surface changes. Such a result appears to be possible by coating the vessel with KCl. In a clean quartz or Pyrex vessel the third explosion limits are low and very erratic, obviously strongly dependent on the nature of the surface. Rinsing the vessel with a weak solution of KCl increases the explosion pressure and decreases the erratic behavior. With a heavy layer of KCl the explosion pressure is increased still further and becomes quite reproducible.[6] If KCl is replaced by potassium metaborate ($K_2B_2O_4$) the same ultimate or limiting explosion pressure is obtained. Thus, there is strong evidence that the condition $\epsilon \gg 2\lambda/r$ is fulfilled with a sufficiently heavy coating. From this fact alone, however, no deductions can be made regarding the isothermal or thermal character of the explosion.

TABLE I. *Dependence of third explosion limit on diameter in heavily* KCl-*coated vessels.* $H_2/O_2=2$.

Temperature, °C	Explosion Pressure, mm Hg				
	3.9 cm Diam.	7.4 cm Diam.	P_1/P_2	d_2/d_1	d_2^2/d_1^2
560	1500	730	2.1	1.9	3.6
570	1250	544	2.3		
580	1060	370	2.9		

[5] L. S. Kassel and H. H. Storch, J. Am. Chem. Soc. **57**, 672 (1935); G. von Elbe and B. Lewis, *ibid.* **59**, 970 (1937); also reference 4, Chapter I.

[6] See also M. Prettre, J. de chem. physique **33**, 193 (1936); O. Oldenberg and H. S. Sommers, J. Chem. Phys. **7**, 279 (1939).

The first test of the above relationship concerns the diameter dependence, which is that α/D is inversely proportional to d^2. For this purpose α/D must be developed as a function of pressure. The reaction mechanism[4]

$$H+O_2=OH+O, \qquad II$$

$$O+H_2=OH+H, \qquad III$$

$$OH+H_2=H_2O+H, \qquad I$$

$$H+O_2+M=HO_2+M, \qquad VI$$

$$HO_2+H_2=H_2O_2+H_2, \qquad X$$

$$HO_2 \xrightarrow{\text{surface}} \text{destruction}, \qquad XII$$

where M is any molecule, leads to the explosion condition,

$$\frac{k_{12}}{(M)d^2}\left(1-\frac{2k_2}{k_6(M)}\right)=\frac{2k_2}{k_6(M)}k_{10}(H_2). \qquad (2)$$

This describes the second explosion limit if it is assumed that reaction (X) occurs there very infrequently compared with reaction (12), that is $(2k_2/k_6(M))k_{10}(H_2)\leqslant 0$; inasmuch as $2k_2/k_6(M)\ll 1$ at the third explosion limit, the approximate expression for the latter is

$$\frac{k_{12}}{(M)d^2}=\frac{2k_2}{k_6(M)}k_{10}(H_2). \qquad (2a)$$

Thus, the reaction mechanism furnishes an α independent of pressure, and, since D is inversely as the pressure, the explosion pressure is expected to be proportional to $1/d^2$.

Experiments[7] in spherical Pyrex vessels of different sizes, with a heavy coating of KCl, showed that this relation is not fulfilled. As Table I shows, the diameter dependence lies between the first and second power.

Two major disturbances may distort the experimental explosion pressures. One is convective mixing of the gases, which flattens the normal concentration gradient of the chain carriers and causes an increase of the explosion pressure above that for a quiescent mixture. The other is the self-acceleration of the reaction due to heat liberated, which may superimpose a thermal

[7] G. von Elbe and B. Lewis, unpublished.

explosion condition onto the branched chain condition, thus tending to decrease the explosion pressure.

It is clear that the less steep the chain carrier concentration gradient, the less the percentage change of the gradient by a given disturbance. The present experiments on the third explosion limit were therefore carried out in an intermediate range of chain breaking efficiency, where ϵ is neither very large nor very small, that is, $\epsilon \backsimeq 2\lambda/r$. The conditioning of the surface to give intermediate chain breaking efficiency was accomplished (see estimate of ϵ below) by rinsing the vessel with a 10-percent solution of KCl and removing visible crystals by a couple of rinsings with small amounts of distilled water. This left a practically invisible KCl coating that resulted in a reasonably stable surface and at the same time gave sufficiently low third limits[8] to allow investigation over a fairly large range of temperature, 530° to 570°C, and still preserve the vessel. The consistency of the results among themselves was assured by frequently checking the explosion limit at some reference point (560°C) for stoichiometric mixture. These rarely deviated by more than 10 to 15 mm Hg total pressure. All limits were determined to 10 mm Hg.

For the case of intermediate ϵ, the chain breaking term in Eq. (1) becomes $(\pi^2 D/r^2) \times (1/[1+2\lambda/\epsilon r])$, since ϵ is small compared with 1. Equation (2a) then becomes

$$\frac{1}{1+4\lambda/\epsilon d} = \frac{2k_2}{k_6}\frac{k_{10}}{k_{12}}(\mathrm{H_2})d^2, \tag{3}$$

$$\frac{\lambda}{d} = \frac{0.677}{\pi\sigma^2(M)}\frac{1}{d} = 0.2\times 10^{15}/(M)d, \tag{4}$$

where the average $\sigma^2 \backsimeq 10^{-15}$ cm^2. For $T=560$°C, $(M)=0.9\times 10^{19}\times p/760$ molecules per cc, where p is in mm Hg, and for $d=7.4$ cm Eq. (3) becomes

$$1\Big/\left[1+\frac{1.2\times 10^{-5}}{\epsilon}\frac{760}{p}\right] = \text{const.}\times\frac{p}{760}, \tag{5}$$

where const. $=2k_2k_{10}/k_6k_{12}$ times the mole fraction of H_2 times d^2. Const. can be determined from the third limit explosion pressure in a heavily KCl-coated vessel, that is $\epsilon \gg 2\lambda/r$, which is 730 mm for a stoichiometric mixture at 560°C.[7] Equation (5) then becomes

$$\text{const.}\ 730/760 = 1, \tag{6}$$

$$\text{const.} = 1.04.$$

The third explosion limit in the thinly KCl-coated vessel, that is, intermediate ϵ, was found to be 360 mm for stoichiometric mixture. Then

$$1/1+2.5\times 10^{-5}/\epsilon = 1.04\times 360/760, \tag{7}$$

$$\epsilon = 2.4\times 10^{-5};$$

$2\lambda/r = 2.5\times 10^{-5}$, and thus the desired experimental surface condition (namely, $\epsilon \backsimeq 2\lambda/r$) has been realized. It is of interest to note that the third limit pressure is approximately halved by decreasing ϵ from $\gg 2\lambda/r$ to $\backsimeq 2\lambda/r$.

For this surface condition the third limit pressure should be inversely proportional to the diameter raised to a power between 1 and 2. Table II, containing some of the results obtained at a few temperatures, shows that this is fulfilled.

The above treatment of thinly coating the vessel should not disturb the temperature dependence of α, and one should find a rather large increase of the third limit pressure with decreasing temperature, consistent with the presumably large energies of activation of reactions II and X (that is $2k_2/k_6$ and k_{10}); that is, the const. in Eq. (5) should increase strongly with temperature. At $T=560°$ and 540°C, the third limit pressures were found to be 360 and 556 mm ($H_2/O_2=2$) for $d=7.4$ cm; $\epsilon=2.4\times 10^{-5}$, and, from Eq. (5), one calculates $\text{const.}_{560°}=1.04$ and $\text{const.}_{540°}=0.81$. From this a combined energy of activation for reactions 2 and 10 is found to be $E^{560}_{540}=16.9$ kcal. Inasmuch as a value of E of

TABLE II. *Dependence of third explosion limit on diameter in thinly* KCl-*coated vessels.* $H_2/O_2=2$.

Temperature, °C	Explosion Pressure, mm Hg Vessel Diameter, cm 4.0	5.8	7.4	8.4	9.9	P_1/P_2	d_2/d_1	d_2^2/d_1^2
531			620		429	1.5	1.4	1.8
540		699*			350	2.0	1.7	2.9
550		560			240	2.3	1.7	2.9
560	710			275		2.6	2.1	4.4

* Vessel diameter =5.9 cm.

[8] The fact that the third limits were much lower in a vessel so treated than in a heavily KCl-coated vessel indicates a marked shift in the range of ϵ.

about 22.5 kcal. is found for $2k_2/k_6$ from second limit experiments,[7] this would ascribe to reaction 10 a negative value of E.

Now, the third limit pressures referred to above were determined as the lowest pressures at which explosion occurs at all. A period of time may elapse between admission of the gas to the vessel and ignition. These times are vanishingly small toward high temperatures at the juncture of the second and third explosion limits, and increase with decreasing temperature. If, at lower temperatures, the gases are admitted at pressures exceeding the above-described lowest third limit explosion pressure, the induction periods become progressively shorter. It is feasible to extrapolate the observations to zero induction period as has been done by Oldenberg and Sommers.[9] Working in a heavily KCl-coated vessel of 5-cm diameter their extrapolated values of the third limit pressures for $H_2/O_2=2$ are 730, 640, and 533 mm for $T=569°$, 572°, and 577°C, which give a value of $E_{569}^{577}=56$ kcal. for $2k_2k_{10}/k_6$. This leaves a value of E for k_{10} equal to 33.5 kcal.

A value of E for k_{10} can also be calculated directly from the data using the relation

$$k_{10}=f\frac{Z}{N_1N_2}e^{-E/RT}, \tag{8}$$

assuming the steric factor f to be not far from unity. Z is the collision frequency of HO_2 and H_2, and N_1 and N_2 are concentrations of these gases in molecules per cc. k_{10} is calculated from the equation for large chain breaking efficiency.

$$\frac{\pi^2D}{r^2}\left(1-\frac{2k_2}{k_6(M)}\right)=\frac{2k_2}{k_6(M)}k_{10}(H_2). \tag{9}$$

The diffusion coefficient is approximately given by[4]

$$D=\frac{14{,}500\left[T\left(\frac{1}{m_{HO_2}}+\frac{1}{\bar{m}}\right)\right]^{\frac{1}{2}}}{\frac{3}{4}\pi(\sigma_{HO_2}+\bar{\sigma})^2(M)}, \tag{10}$$

where $\bar{m}$ is the average mass of the mixture through which the HO_2 diffuses and $\bar{\sigma}$ the average molecular diameter of the gas molecules. They are given by

$$\bar{m}=f_{H_2}m_{H_2}+f_{O_2}m_{O_2}, \tag{11}$$

$$\bar{\sigma}=f_{H_2}\sigma_{H_2}+f_{O_2}\sigma_{O_2}, \tag{12}$$

where f_{H_2} and f_{O_2} are the mole fractions of H_2 and O_2 in the mixture. The value $2k_2/k_6$ is obtained from the second explosion limit. Using Oldenberg and Sommers' data of the third limit pressure equal to 640 mm at $T=572°$C, $d=5$ cm, $H_2/O_2=2$, and $\sigma_{H_2}=2.36\times10^{-8}$ [10] cm, $\sigma_{O_2}=2.93\times10^{-8}$ cm, σ_{HO_2} (assumed) $=2.93\times10^{-8}$ cm, and $2k_2/k_6=187$[11] mm $=2.295\times10^{18}$ cm^{-3},

$$k_{10}=2.13\times10^{-18}\ \text{cm}^3\times\text{sec.}^{-1},$$

and

$$E=32.9\ \text{kcal.}$$

The agreement of this value of E for k_{10} with the value of E determined from the slope of the third explosion limit curve is only apparent since f is probably less than unity. A value between 20 and 30 kcal. is indicated from the analysis of new second explosion limit data.[7] This raises the question of interpretation of the third explosion limit pressures. It is known that explosions at or near the second limit have no appreciable induction period; that is, if an explosion condition is established by the equality of the chain branching and chain breaking rates, explosion follows immediately. This would be the case immediately after the gases are admitted to the vessel at the proper concentrations, irrespective of the development of the rate-determining chain initiating reaction. In this way it is understandable that third limit pressures for zero induction period are more nearly representative of the isothermal branched chain explosion condition. Lowest third limit pressures, accompanied by an induction period, would then correspond to a condition where the chain breaking rate still exceeds the chain branching rate and the explosion is forced only by gradual acceleration of the chain initiating reaction and the rise in temperature. Upon the basis of a modified mechanism of the reaction to be developed in a subsequent paper, this may be understood as the

[9] O. Oldenberg and H. S. Sommers, J. Chem. Phys. **9**, 114 (1941).

[10] All σ's are from R. C. Tolman, *Statistical Mechanics*, (Chemical Catalog Company, 1927).

[11] Calculated from unpublished data of Lewis and von Elbe from value of $2k_2/k_6=154$ at 560°C, and $E=22.5$ kcal.

TABLE III. *Effect of mixture composition of hydrogen and oxygen on the lowest third explosion limit pressure. Diameter of vessel = 7.4 cm.*

Temp. °C	Ratio H_2/O_2	$P_{expl.}$ mm Hg	P_{H_2}	P_{O_2}
530	1.5	661	395.8	265.3
	2	700	466.5	233.2
535	1.5	590	353.9	236.0
	2	670	447.0	222.7
540	1.5	520	312.2	208.0
	2	556	370.0	186.5
	3	631	472.1	158.5
	4	699	560.0	139.0
545	1.5	479	288.3	190.7
	2	520	346.9	173.3
	3	601	450.1	150.4
	4	680	544.1	135.9
550	1.5	415	249.2	166.0
	2	469	313.1	156.2
	3	535	401.5	133.7
	4	610	488.0	122.1
555	1.5	370	221.8	148.3
	2	410	273.6	136.1
	3	490	367.4	122.1
	4	550	439.4	110.1
560	1.5	320	192.2	127.8
	2	360	240.1	119.9
	3	429	322.1	106.6
	4	491	392.2	98.3
565	2	299	200.1	98.5
	3	375	281.0	93.9
	4	430	344.0	86.2
570	4	320	256.2	63.9

gradual accumulation of an intermediate chain carrier-producing product, and, perhaps, to a lesser extent, as temperature rise. The difference between zero induction period third limit pressures and lowest third limit pressures gives a measure of the magnitude of the thermal disturbance.

Using the above value of E, the energy of reaction X is

$$HO_2+H_2=H_2O_2+H-(\leqq 33)\text{ kcal.}$$

From the heat of dissociation, $H_2=2H-102.5$ kcal.

$$H_2O_2=HO_2+H-(\leqq 69.5)\text{ kcal.},$$

and, from the heat of reaction $H_2O_2=O_2+2H-134.8$ kcal., a maximum value of the bond energy of H and O_2 in HO_2 is found to be $\leqq 65.3$ kcal.

TABLE IV. *Effect of inert gases on the lowest third explosion limit pressures. $T=560°C$, $H_2/O_2=2$, $d=7.4$ cm.*

Ratio X : H_2 : O_2	$P_{expl.}$ mm Hg	P_{H_2}	P_{O_2}	Ratio X : H_2 : O_2	$P_{expl.}$ mm Hg	P_{H_2}	P_{O_2}
N_2				He			
1 : 2 : 1	360	180.0	90.0	1 : 2 : 1	431	215.4	108.4
2 : 2 : 1	395	157.9	78.9	2 : 2 : 1	551	220.1	110.3
3 : 2 : 1	416	138.5	69.8	3 : 2 : 1	636	211.3	107.6
4 : 2 : 1	445	127.0	64.9				
5 : 2 : 1	480	120.6	59.1	Argon*			
6 : 2 : 1	521	115.5	58.6	1 : 2 : 1	310	155.8	76.8
8 : 2 : 1	590	107.2	54.1	2 : 2 : 1	339	136.1	67.2
				3 : 2 : 1	481	126.6	64.9
				5 : 2 : 1	460	115.0	57.8

* See appendix for remarks concerning these experiments.

Lowest third limit pressures were measured for different mixture ratios of hydrogen and oxygen (Table III) and with inert gases (Table IV), and it is of interest to see to what extent the trends can be represented by the simplified theory of isothermal branched chain explosion.

As the treatment cannot claim to be exact it will be given for the case of quiescent gases and large chain breaking efficiency, $\epsilon \gg 2\lambda/r$, which is more easily handled and which will not be significantly different from the case of intermediate chain breaking efficiency as far as the effect of mixture composition is concerned. Since[4]

$$k_6(M)=k_{6,H_2}(H_2)+k_{6,O_2}(O_2)+k_{6,x}(X), \quad (13)$$

Eq. (9) transforms to

$$\frac{\pi^2 D}{r^2}\left(1-\frac{2k_2}{k_6(M)}\right)=\frac{2k_2k_{10}H_2}{k_{6,H_2}(H_2)+k_{6,O_2}(O_2)+k_{6,x}(X)}=\frac{2k_2k_{10}}{k_{6,H_2}+k_{6,O_2}f_{O_2}/f_{H_2}+k_{6,x}f_x/f_{H_2}}, \quad (14)$$

$$D=\frac{14{,}500\left[T\left(\frac{1}{33}+\frac{1}{2f_{H_2}+32f_{O_2}+m_xf_x}\right)\right]^{\frac{1}{2}}}{\frac{3}{4}\pi(2.93+2.36f_{H_2}+2.93f_{O_2}+\sigma_xf_x)^2\times 10^{-16}(M)}, \quad (15)$$

where f_{H_2}, f_{O_2}, f_x are the mole fractions of H_2, O_2 and inert gas. The value of $k_{6,O_2}/k_{6,H_2}$ is 0.35 from

second limit determinations.[7]

$$\frac{2k_2}{k_{6,H_2}}\frac{1}{0.667+0.35\times0.333}=(M)_{\text{2nd expl. limit for } f_{H_2}=0.667} \quad (16)$$

or

$$\frac{2k_2}{k_{6,H_2}}=0.784(M)_{\text{2nd limit for } f_{H_2}=0.667}. \quad (17)$$

For constant T and d the expression for the third explosion limit becomes

$$\frac{\left(1+0.35\frac{f_{O_2}}{f_{H_2}}+\frac{k_{6,x}}{k_{6,H_2}}\frac{f_x}{f_{H_2}}\right)\left(1+\frac{1}{\frac{1}{16}f_{H_2}+f_{O_2}+m_xf_x/33}\right)^{\frac{1}{2}}}{(1+f_{O_2}+0.81f_{H_2}+\sigma_xf_x/2.93)^2}=\frac{\text{const. }(M)}{\frac{1}{0.784(M)_{\text{2nd limit } f_{H_2}=0.667}}-\frac{1}{f_{H_2}+0.35f_{O_2}+k_{6,x}f_x/k_{6,H_2}}\frac{1}{(M)}}, \quad (18)$$

where (M) is the third explosion limit pressure and const. $\sim k_{10}$.

For inert gas mixtures containing hydrogen and oxygen at a ratio $H_2/O_2=2$, Eq. (18) reduces to

$$\frac{\left(1.175+\frac{k_{6,x}}{k_{6,H_2}}\frac{f_x}{0.667(1-f_x)}\right)\left(1+\frac{1}{0.375+(m_x/33-0.375)f_x}\right)^{\frac{1}{2}}}{(1.874+(\sigma_x/2.93-0.874)f_x)^2}=\frac{\text{const. }(M)}{\frac{1}{(M)_{\text{2nd limit}}}-\frac{1}{1+(1.275k_{6,x}/k_{6,H_2}-1)f_x}\frac{1}{(M)}}. \quad (19)$$

The results are given in the Tables V and VI.

It is noted that the function represents the effect of mixture composition on the third explosion limit rather well, and, although it is of uncertain theoretical significance, it constitutes at least a satisfactory empirical relationship. It is conceivable that the relationship would describe the third limit pressures for zero induction period equally well, although this has not been investigated.

According to the theory an inert gas should

TABLE V. *Effect of ratio of hydrogen and oxygen on third explosion limit. Comparison of theory and experiment. Diameter = 7.4 cm.*

Temp. °C	(M) 2nd Limit for $(f_{H_2}=0.667)$[7] mm Hg	f_{H_2}	Const. (M) $\times10^2$	$(M)_{exp.}$ mm Hg	$(M)f_{H_2}=.6/(M)f_{H_2}=.8$ Theor.	Exp.
540	104	0.6	0.61	520	0.85	0.74
		.8	.75	699		
545	114	.6	.53	479	.78	.70
		.8	.68	680		
550	126	.6	.43	415	.74	.68
		.8	.58	610		
555	138	.6	.35	370	.69	.67
		.8	.51	550		
560	154	.6	.26	320	.62	.65
		.8	.42	491		

TABLE VI. *Effect of inert gases on third explosion limit. Comparison of theory and experiment $T=560°C$, $H_2/O_2=2$, diameter = 7.4 cm, (M) 2nd limit $(f_{H_2}=0.667)=154$ mm.*

Inert Gas	f_x	Const. (M) $\times10^2$	$(M)_{exp.}$ mm Hg	$(M)_1/(M)_2$ Theor.	Exp.
Nitrogen	$k_{6,N_2}/k_{6,H_2}=0.43$;[7] $\sigma_{N_2}=3.10\times10^{-8}$ cm.				
	0.25	0.22	360	0.76	0.81
	.571	.29	445	.66	.75
	.727	.44	590		
Helium	$k_{6,He}/k_{6,H_2}=0.36$;[7] $\sigma_{He}=1.89\times10^{-8}$ cm				
	.25	.32	431	.73	.78
	.40	.44	551	.83	.87
	.50	.53	636		
Argon	$k_{6,A}/k_{6,H_2}=0.20$;[7] $\sigma_A=2.84\times10^{-8}$ cm				
	.25	.14	310	1.0	.81
	.50	.14	381	.88	.83
	.625	.16	460		

have two opposing functions. It impedes diffusion of chain carriers to the wall, which is an aid to chain branching, and it fixes H atoms as HO_2 by virtue of reaction VI (as it does also at the second explosion limit), which is an impediment to chain branching. The results bring out well these two opposing tendencies. The fact that the hydrogen and oxygen pressures in the helium experiments go up with respect to those in the argon experiments would indicate that helium is a more efficient third body than argon in reaction VI, a fact that is found experimentally,[7] and that helium allows HO_2 to diffuse more readily than argon.

The results are therefore considered to be a corroboration of the third explosion limit mechanism. Equation (18) is insensitive to the calculation of $(M)_1/(M)_2$, and this is another manifestation of the opposing functions.

It is obvious from these experiments that the third explosion limit *per se* does not lend itself well to a study of the reaction mechanism. The latter must be investigated from studies of the second explosion limit and the reaction rate above it. Such studies are in progress and the results will be reported soon. The third explosion limit can, however, provide support for any mechanism so developed.

Appendix

Experimental procedure and other observations

The furnace temperature was maintained constant, manually, to 0.25°C although a temperature gradient of 1° to 2°C existed over the reaction vessels. A chrome-alumel thermocouple was placed near the vessel at its center. The gases were measured with a mercury manometer to 0.1 mm Hg. Gold foil was placed between manometer and vessel to prevent diffusion of mercury, although it was shown that this amount of mercury had no effect on the results. The gases were admitted to the spherical Pyrex vessels in the order: inert gas, H_2, O_2. The oxygen was admitted rapidly from a reservoir containing such a pressure of oxygen that, on opening the latter to the reaction vessel, the desired mixture composition was obtained. The final mixture was therefore made up in 2 to 3 seconds. Electrolytic O_2 and H_2 were used. The O_2 was passed over heated Pt-asbestos and dried over magnesium perchlorate; the H_2 and He were purified by passage through a charcoal trap cooled to liquid-air temperature; tank N_2 and A, which were about 99.5 percent pure, were dried. The gases were admitted to the reaction vessel through special brass needle valves with sylphon bellows and having no packing. A standard procedure was followed in all experiments, namely, during the night the furnace was kept at a somewhat lower temperature than that to be used; the day's work was started by 30 minutes' evacuation with mercury vapor pump and oil pump; between runs the vessel was evacuated for 15 minutes, flushed with H_2, and pumped 5 minutes. Only the second and subsequent experiments were considered reliable in any day's measurements. Determinations were made by approaching the explosion limit from above and below. Many experiments went to make up a single determination.

An explosion is accompanied by a sharp click and emission of light. Both were observed. In the argon experiments the temperature at which the experiments were carried out was higher than the temperature at the juncture of the second and third limits. These explosion pressures were taken as the lowest pressures at which there was an induction period and an audible click; at lower pressures the gases inflamed as the O_2 entered—obviously a manifestation of the influence of the second limit.

After a vessel had been used for some time it became colored deep brown, a fact already noted by others.[12] The depth of color depended on the number of experiments performed. It is likely that reduction of some compound in the glass had occurred.

In an uncoated vessel a pronounced lowering of the third explosion limit was observed with use. Moreover, the limit was lower if the determination was preceded by several experiments at pressures well above the limit. If a vessel is etched with HF a particularly low third limit is found, and the vessel shows an erratic behavior with use. After considerable use, a vessel that had been coated in the manner described earlier in this paper gave consistently lower limits. On removing the vessel it was found that a relatively heavy coating of KCl surrounded the inlet tube, indicating a slow distillation of KCl. This was confirmed directly by observing the distillation of KCl from the wall of a glass tube onto a glass rod mounted in its axis. The amount of KCl was not visibly different when H_2, O_2, a mixture of them, or N_2 was passed through the tube. The concentration of KCl in the gas is considered to be too low at the temperature of the experiments to affect appreciably determination of the third explosion limit.

It is a pleasure to acknowledge fruitful discussion with Guenther von Elbe.

[12] Reference 6; G. A. Williams and J. B. Ferguson, "Studies of diffusion of H_2 and He through glass," J. Am. Chem. Soc. **44**, 2162 (1922).

High Frequency Energy Losses in Solutions Containing Macromolecules

WILLARD P. CONNER*
Laboratory of Physical Chemistry, University of Wisconsin, Madison, Wisconsin
(Received April 22, 1941)

There is described a quantitative thermal method for measuring the loss factor of solutions containing polar molecules. By making use of the Debye dipole theory for both parts of the complex dielectric constant, it is found that normal lignin is fairly homogeneous and has a molecular weight of approximately 3900 and a shape factor of 8. The ω-hydroxydecanoic acid polymers show internal rotation of the polar groups in solution, whereas methyl methacrylate linear polymers appear to have less, but still appreciable, internal group motions.

THE frequency variation of the dielectric constant of solutions of macromolecules has been applied in the study of the size and shape of such molecules by numerous investigators.[1–4] Since the energy absorbed in the dielectric medium resulting from the rotation of polar molecules is a function of the same variables which describe the frequency variation of the real part of the dielectric constant, an investigation of the frequency dependence of the energy absorbed in macromolecular solutions can be used for studies of the size, shape and rigidity of the dissolved units.

Two advantages of such a method of investigation are at once evident. Energy absorption measurements may be performed without the precision equipment necessary for accurate dielectric constant determinations, especially in the region of short waves. Further, no precise conclusions concerning molecular size can be arrived at from ordinary dielectric constant measurements in a frequency region remote from the central frequency. However, even in this low frequency region, the energy absorbed, if detectable, can give considerable information. Thus the method has been applied in the study of the sizes of small polar molecules.[5] Work of this type is the subject of a recent review by Müller.

The object of the present report is to describe an apparatus capable of giving accurate energy absorption measurements and to compare the results of such measurements with those obtainable from ordinary dielectric constant measurements over essentially the same frequency range: that is, 0.5 to 15 megacycles/sec. The results of both types of measurements will be drawn upon to determine the size and shape of the molecular kinetic unit of several lignins. Less complete and less satisfactory studies have also been made with solutions of methyl methacrylate, and ω-hydroxydecanoic acid ester macromolecules. The selection of the solute molecules was governed by the requirement that they be soluble in nonpolar solvents in order to minimize energy losses resulting from ion conduction; and by the fact that other investigations in this laboratory have already obtained information concerning their molecular properties.

The symbols chosen for the expression of the results will be those which are related closely to molecular properties rather than to the electrical circuits involved. As Debye[6] has suggested, the generalized dielectric constant ϵ of a medium may be resolved into a real ϵ' and an imaginary component ϵ''. Thus,

$$\epsilon=\epsilon'-i\epsilon'', \tag{1}$$

in which ϵ' is the measured dielectric constant and ϵ'' determines the energy absorbed in the dielectric per cycle.

For a solution of polar molecules we write,

$$\epsilon'=\epsilon_\infty+(\epsilon_0-\epsilon_\infty)/(1+\omega^2\tau^2) \tag{2}$$

and

$$\epsilon''=(\epsilon_0-\epsilon_\infty)\omega\tau/(1+\omega^2\tau^2). \tag{3}$$

In these expressions ϵ_0 is the static dielectric constant of the solution and ϵ_∞ is the correspond-

* Procter and Gamble Fellow in Chemistry 1939–40. Present Address: Frick Chemical Laboratory, Princeton, New Jersey.

[1] Marinesco, J. chim. phys. **28**, 51 (1931).
[2] Errera, J. chim. phys. **29**, 577 (1932).
[3] Oncley, J. Am. Chem. Soc. **60**, 1115 (1938).
[4] Elliott and Williams, J. Am. Chem. Soc. **61**, 718 (1939).
[5] Müller, Ergeb. d. exakt. Naturwiss. **17**, 164–228 (1938).
[6] P. Debye, *Polar Molecules* (Chemical Catalog Company, New York, 1929).

ing optical value. It is assumed with Wyman[7] that the polarization is a linear function of the dielectric constant. The time of relaxation τ for a spherical particle is given by the formula,

$$\tau = 4\pi\eta a^3/kT, \qquad (4)$$

in which η is the viscosity of the solvent and a is the molecular radius. For a molecular model of the nature of an ellipsoid of revolution, the expressions for the time of relaxation about the long axis τ_2 and that about the short axis τ_1 as a function of the ratio of the major to minor axis of the ellipsoid have been developed by Perrin.[8]

Experimental

Purification and preparation of materials

The methods for the preparation of the larger molecular species used in this research have been previously reported. The lignin was extracted with methyl alcohol which had been acidified with hydrochloric acid.* The methyl methacrylate and ω-hydroxydecanoic acid ester polymers were prepared by following accepted procedures.[9,10]

The benzene, obtained from the Eastman Kodak Company, was shaken with concentrated sulfuric acid, washed with water, shaken with mercury, again washed with water, distilled over phosphorus pentoxide, and finally redistilled over sodium. The physical constants of the product used were $\epsilon_{25}=2.273$ (125 meters wavelength) $d_4^{25}=0.8735$, and $n_D^{25}=1.49749$.

The chloroform, a Merck product, was shaken with 10 percent sodium hydroxide solution,[11] thoroughly washed with water, shaken for ten hours with phosphorus pentoxide and afterwards distilled. Since phosgene always appeared in the chloroform within a few days, 2 percent ethyl alcohol was added to stabilize the solvent. For this mixture $\epsilon_{25}=4.810$ (125 meters).

The 1,4-dioxane, supplied by the Carbon and Carbide Chemical Company, was refluxed for six hours with 10 percent by volume of normal hydrochloric acid in a slow air stream to remove aldehydes, then refluxed with sodium hydroxide pellets for twenty-four hours, the aqueous layer being removed several times. Final distillation was carried out over metallic sodium. Since dioxane is strongly hygroscopic, only small amounts were purified as they were needed. The dielectric constant of the samples at 25° varied from 2.234 to 2.245 (125 meters).

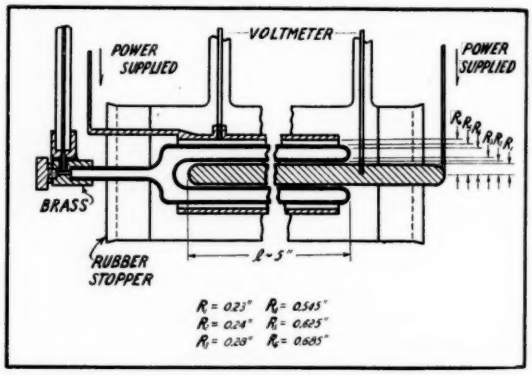
VOLTMETER
POWER SUPPLIED
POWER SUPPLIED
BRASS
RUBBER STOPPER
R_1 R_2 R_3 R_4 R_5 R_6
l - 5"
R_1 = 0.23" R_2 = 0.24" R_3 = 0.28" R_4 = 0.545" R_5 = 0.625" R_6 = 0.685"

FIG. 1. Cell for measurement of dielectric loss in liquids. $R_1=0.23''$, $R_2=0.24''$, $R_3=0.28''$, $R_4=0.545''$, $R_5=0.625''$, $R_6=0.685''$.

Apparatus

The experimental method was based upon the determination of the imaginary dielectric constant ϵ'', preferably called the loss factor, in the equation,

$$P = \tfrac{1}{2}\omega\epsilon'' C_0 V_0^2. \qquad (5)$$

Here P is the power loss in a condenser of air capacity C_0 under the alternating voltage of amplitude V_0 and of frequency $\omega/2\pi$ cycles per second. The thermal measurements were accomplished by use of a dilatometer which was built about the electrodes of a condenser.[12–15] The rate of evolution of heat in the liquid as a result of absorption of electrical energy was indicated by the rate of rise of the liquid in the capillary column of the dilatometer. Two types of cell were used. One cell was of the parallel-plate type, much like ones previously described by Martin and by Holtzmüller. The second assembly

[7] J. Wyman, Jr., Chem. Rev. **19**, 213 (1936).
[8] Perrin, J. de phys. **5**, 497 (1934).
* Samples of lignin were placed at our disposal through the kindness of Drs. E. E. Harris and A. J. Stamm of the U. S. Forest Products Laboratory of Madison, Wisconsin.
[9] Strain, Ind. Eng. Chem. **30**, 345 (1938).
[10] Bridgman, J. Am. Chem. Soc. **60**, 530 (1938).
[11] Weissberger and Proskauer, *Organic Solvents* (The Clarendon Press, Oxford, 1935).
[12] Harms, Ann. d. Physik **5**, 564 (1901).
[13] Malsch, Physik. Zeits. **33**, 19 (1932); Ann. d. Physik **12**, 865 (1932).
[14] Martin, Physik. Zeits. **37**, 665 (1936).
[15] Holtzmüller, Physik. Zeits. **38**, 576 (1937).

was constructed with concentric cylinder plates. It is illustrated in Fig. 1. The capillaries, with radii of 6.66×10^{-3} cm and 2.01×10^{-2} cm were interchangeable. Either cell was immersed in an oil thermostat during the performance of an experiment. The power was introduced through wires which passed through the oil of the thermostat. The leads to the voltmeter were passed through glass tubes, $\frac{1}{2}$ inch in diameter, in order to reduce errors in voltage reading due to power loss in the oil. In addition to the oil thermostat an air jacket was placed around the cylindrical cell to prevent too rapid heat exchange with the bath. The temperature of the bath was maintained at approximately 25°C, but was varied slightly in order to adjust the height of the liquid in the capillary at the beginning of the experiments. During an experiment the temperature of the bath did not vary by more than $\pm0.02°$.

The air capacity of the parallel plate cell was determined by calculation to be 7.04×10^{-13} $\mu\mu$f, and that of the concentric cylinder plates, 8.40×10^{-12} $\mu\mu$f. However, since the electrodes are outside of the cell in the concentric cylinder type of cell, the air capacity is not the important quantity. The generalized capacity C must be considered to be composed of a real part C' and an imaginary part C'', and

$$C=C'-iC''. \tag{6}$$

The power loss is then given by

$$P=\tfrac{1}{2}C''\omega V_0^2. \tag{7}$$

The capacity C of such a cell when filled with a liquid of dielectric constant ϵ_l may be expressed by means of the equation

$$C=C'-iC''=A\Big/\left(B+\frac{G}{\epsilon'_g-i\epsilon''_g}+\frac{H}{\epsilon'_l-i\epsilon''_l}\right). \tag{8}$$

In the formula the subscripts g refer to glass and l to the liquid. The constants A, B, G, H are independent of the materials of construction but dependent upon the geometrical dimensions of the cell. Simplification of the expression (with elimination of terms of the order of ϵ''/ϵ' in comparison with unity) shows that the explicit expressions for C' and C'' are:

$$C'=\frac{A}{B+G/\epsilon'_g+H/\epsilon'_l}, \tag{9}$$

$$C''=(C')^2\left[\frac{H}{A}\frac{\epsilon''_l}{(\epsilon'_l)^2}+\frac{G}{A}\frac{\epsilon''_g}{(\epsilon'_g)^2}\right]. \tag{10}$$

Thus the total power loss in the cell may be considered to be the sum of two parts, one resulting from the conductivity of the liquid, and the other from conductivity of the glass. After subtraction of the loss in the pure solvent from that in solution, only the first term of the expression for C'' remains.

The constants of the equations were determined empirically by measuring in an impedance bridge the variation of the capacity of the cell as the dielectric medium was changed. The translation of capacity in divisions on the scale of the precision condenser to absolute units was accomplished by comparison with an air condenser constructed of circular parallel plates for which the end effects are accurately known. Extraneous lead capacitance and inductance were eliminated by varying the distance between the parallel plates.

In both cells the leads to the voltmeter were attached directly to the condenser plates, and not to the leads through which power was introduced, in order to avoid a voltage drop along the leads carrying high frequency current.

Two losses peculiar to the cylindrical cell proved to be completely negligible by calculation. They are conduction by translational motion of the dipole molecules in the inhomogeneous field, and Maxwell interfacial polarization at the liquid-glass and glass-air interfaces.[16]

Transformation of the rate of rise of the liquid in the capillary tube into units of energy absorbed is made practical by the equation

$$W(\text{cal./sec.})=(c\rho/\alpha)\Delta l r^2\pi,$$

in which c is the specific heat of the liquid in cal. deg.$^{-1}$; ρ is the density in g cc^{-1}; α is the thermal coefficient expansion of the liquid in deg.$^{-1}$ and Δl is the rate of rise of the liquid column in cm sec.$^{-1}$. Thus the rate of liquid rise is proportional to the wattage input. The pro-

[16] Hartshorn, J. Inst. Elec. Eng. **64**, 1152 (1926).

portionality constant was determined for each pure solvent by measuring the rate of rise of the liquid in the capillary when a known amount of direct current was introduced into a similar cell by means of a helical Nichrome wire of resistance 39.86 ohms. This constant was reproducible to within 0.5 percent. Actual calculation of $\alpha/\rho c$ for benzene gave 2.98×10^{-3} cm^3 cal.$^{-1}$ as compared with 3.05×10^{-3} cm^3 cal.$^{-1}$ reported by Martin.[14]

Two oscillators were required for the generation of the alternating voltage. A tuned-grid tuned-plate oscillator employing an RCA 807 tube was found to be completely satisfactory as a frequency source at frequencies from 0.5 to 25 megacycles. For the 60-megacycle measurements a Kolster oscillator[17] was used. Both oscillators showed constancy of frequency and lack of modulation on investigation of the nature of the beat note between the oscillator in question and an independent electron coupled oscillator.

The low frequencies were determined by means of a General Radio Company precision wave meter of Type 224–6. The highest frequency was observed with a frequency meter of Type 458–S, manufactured by the same firm.

The vacuum tube voltmeter was an adaptation of one reported by Holtzmüller[15] for similar investigations. The null instrument was a Weston galvanometer, Model 699, of sensitivity of two microamperes per division. A Rawson variable milliammeter of sensitivity one microampere per division was converted into a direct reading voltmeter by adding in series a two-watt graphite radio resistor of 3.14×10^6 ohms. Its resistance was studied periodically and was found to be quite stable with the small currents involved.

If the coupling coil is center-tapped exactly, the voltage read is one-half of the maximum voltage across the plates of the condenser. Switches were inserted in the filament circuits so that each tube might be used independently without the removal of the other. Thus the electrical center of the coil could be located as the point for which each tube gave identical voltage readings.

Because of the sinusoidal nature of the voltage impressed upon the anode of the tubes, the current through the tube in the voltage cut-off region approaches zero so slowly that measurement of the cut-off voltage is slow and tedious. To alleviate this difficulty, the current was plotted against the voltage difference between the anode and the cathode. Thus the small current flowing through the tube could be read in the null indicator and along with it the voltage of the cathode could be recorded. The additional voltage necessary for cut-off could be read directly from the graph. The plots so constructed were essentially independent of the frequency employed.

There are two errors inherent in a diode voltmeter of this type. The error in voltage measurement will be small provided that the inductive reactance of the leads from the cell is small as compared with the capacitative reactance of the tube. Upon substitution of reasonable values for the inductive reactance of the straight, round wire leads (20 cm in length) and the capacitative reactance of the tube, this error is found to be negligible for the lower frequencies and approximately 1 percent for the measurements at 60 megacycles. Moreover, calculation indicates that the error in the diode voltmeter due to electron transit time is negligible[18] for all but the highest frequency and in that case it amounts to about 3 percent. This voltage error is partially compensated by the fact that the actual voltage cut-off was not measured, but instead the current-voltage difference was extrapolated to the cut-off value. Inasmuch as these two errors act in opposite directions, no correction was applied to the data.

To eliminate harmonics from the fundamental frequency a coupled circuit of inductance and capacitance was always used. The power in the cell circuit could be varied by changing the distance between the link coupling coil from the oscillator to the coupling circuit. All energy loss measurements were proportional to the square of the voltage across the cell. The lack of deviation indicates that at no time was the coupling sufficiently close to change appreciably the frequency of the oscillator.

The rate of rise of the liquid in the capillary due to the high frequency current alone was

[17] Kolster, Proc. I. R. E. **22**, 1335 (1934).

[18] Nergaard, Proc. I. R. E. **24**, 1207 (1936).

considered to be the difference between the rate of rise while the power was applied and the rate of rise immediately before the application of the high frequency power, the cell circuit being short circuited at this time. The cell was allowed to come to thermal equilibrium with the thermostat bath so as to insure that the rate of rise of the column of liquid in the capillary during the rest period was less than 10 percent of the total rate of rise after the high frequency voltage had been applied. It was usually much less than this. The reproducibility in rate of liquid rise at one voltage was usually within 1 percent and at different voltages the rate of rise per unit voltage squared was within 2 percent. If the reproducibility was less satisfactory more observations were made and the average was taken as the correct value. Time measurements were made with a stopwatch. However, access was had to a chronograph capable of reading to one one-hundredth of a second if more accurate measurements were essential. Time measurements extended from 6 to 90 sec. depending upon the magnitude of the power loss.

The difficulty in reproducibility similar to that encountered by Holtzmüller[15] was met in the investigation of low power losses with the parallel plate cell. Analysis of the rate of rise of the liquid in the capillary with the chronograph showed that there occurred considerable lag in the motion of the column of liquid at both the application and suspension of power. The rate of rise of the liquid column at intermediate times was fairly reproducible (5 percent) and would appear to offer a better choice for investigation as compared to reference to extrapolation to the time of suspension of high frequency power as was done by Holtzmüller. However, in general for measurements with macromolecular solutions, the power loss was sufficiently large to obliterate the induction period, and hence the rate of rise appeared to be linear at the start.

The direct capacitance measurements were carried out with a standard heterodyne beat assembly or with an impedance bridge apparatus.[19]

[19] Daniels, Mathews and Williams, *Experimental Physical Chemistry* (McGraw-Hill Book Company, New York, 1941), third edition.

Results

An abnormal rise in ϵ'' in the region of low frequencies was apparent to some extent for all liquids and more especially for the solutions. Inasmuch as all solutions contained slight traces of inorganic salts (as a result of the methods of preparation and purification), this abnormal rise is undoubtedly due to electrolyte conductivity even though the solvent is nonpolar in character. In general, the magnitude of the ion conductance was not subject to independent measurement because an adequate impedance bridge apparatus was not available. For this reason an empirical evaluation was necessary. The power loss due to ion conductance is independent of frequency in this frequency region. Therefore, the difference between the power loss for solution and for solvent was plotted as a function of the applied frequency and then extrapolated to zero frequency. The loss at zero frequency was attributed to ion conductivity. Since ϵ'' is a hyperbolic function of the specific ionic conductivity, the corrected values of ϵ'' in the low frequency region are very sensitive to slight changes in conductance. However, in the higher frequency region, ϵ'' is almost independent of conductance so that little error is made in the frequency region important in this investigation. In the case of the 0.965 percent solution of maple lignin in chloroform-alcohol solvent, the conductivity was sufficiently high to be measurable with an ordinary laboratory 1000-cycle resistance bridge. The specific conductance determined was $5.0\pm2 \times10^{-8}$ ohm^{-1} cm^{-1}, a value in good agreement with that found by extrapolation to zero frequency.

Power Loss in Solvents

When either cell is filled with pure benzene and pure dioxane a finite value of ϵ'' independent of frequency is noted. Moreover, after correcting the energy loss in chloroform for ionic conductivity and dipole loss, there still remains a value of ϵ'' for the cell which is independent of frequency. This loss must be identified with loss in the glass itself. A fairly quantitative estimate of ϵ'' for glass can be made for the cylindrical plate cell by assuming sufficient heat transfer from the interior of the glass to the liquid and

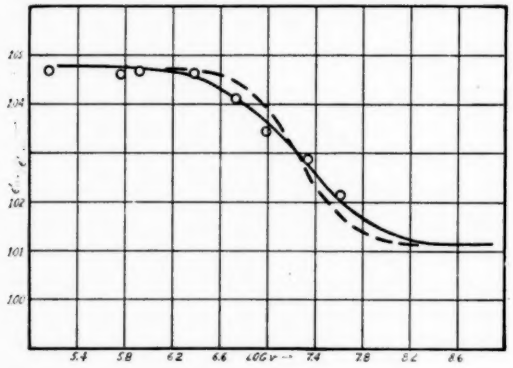

FIG. 2. Dispersion of dielectric constant ratio. Aspen lignin in chloroform (4.4 percent). Abscissa—log ν, ordinate—dielectric constant ratio. Calculated curves drawn for critical frequency of 1.80×10^7 cycles per sec. with a variation in the distribution coefficient of relaxation time constants b.

reasonable value for the dielectric constant of the glass. (For Pyrex glass $\epsilon'=4.8$.) The data given in Table I[20] are obtained. The value of the loss factor tan ϕ computed in this way is only one-tenth of its normal value.[21]

In a frequency region very much lower than that in which maximum dispersion takes place,

$$d\epsilon''/d\omega=\tau(\epsilon'_0-\epsilon'_\infty). \qquad (11)$$

By inserting the slope of the (ϵ'' *vs.* ω) straight line and the value of 2.3 for ϵ'_∞, found by assuming the atomic polarization to be 10 percent of the electronic polarization, the value of τ for chloroform is determined to be 5×10^{-12} sec. and a, the molecular radius, is equal to 1.5×10^{-8} cm. This value is considerably smaller than the geometrical value of 2.5×10^{-8} cm. Such a discrepancy, usually found in observations of the type in question, is undoubtedly due to the strong intermolecular interactions in the pure solvent.

LIGNIN

Diffusion, osmotic pressure, and viscosity investigations[22] have indicated that lignin has a molecular weight of 3900 ± 300 and a shape factor of 7.5 or 8.0. In order to further confirm these results, extensive dielectric constant measurements have been performed in this laboratory.[23] Such data for aspen, maple and spruce lignin are recorded in Table II.

Since all three kinds of lignin gave essentially the same type of curve, the data for aspen lignin only will be discussed. The dielectric constant ratio-frequency data for aspen lignin are plotted to form Fig. 2. The heavy (full line) curve is the simplest symmetrical dispersion curve which can be drawn through the experimental points. The critical frequency determined as the frequency of half-dispersion, $\frac{1}{2}(\epsilon'_0-\epsilon'_\infty)$, is 1.80×10^7 cycles/sec. Making the assumption that the molecular weight is 3900, the ratio of the relaxation time for rotation about the short axis of an ellipsoid of revolution to that for rotation as a spherical molecule of the same molecular weight, is 4.65. Solution of the Perrin equation[8] indicates that the shape factor for the molecule, that is, the ratio of the long axis to either of the short axes, is 8. The result is in excellent agreement with that reported by Loughborough and Stamm.[22]

Moreover, upon closer analysis it is seen that the curve so drawn does not correspond to a single relaxation time, but is considerably broader. If we assume that we have a distribution of relaxation times about a central time constant, we may apply the treatment of Yager.[24] It is found that the heavy line originally drawn fits exactly a curve for which the Yager distribution constant b is equal to 0.8. For comparison, the dotted line describes the dispersion for a monodisperse system. In addition it is noted that the dielectric constant in the high frequency range is unusually large in magnitude. One might conclude that in this region, inaccessible to the resonance apparatus, an additional dispersion

TABLE I. *Energy absorption data for glass.*

LIQUID IN CELL	ϵ''	TAN ϕ
C_6H_6	0.0023	0.000478
$CHCl_3$	0.0012	0.000250
$C_2H_4O_2$	0.0020	0.000416

[20] Wulff and Schmidt [Zeits. f. physik. Chemie **B39**, 290 (1938)] report a loss factor in pure benzene of order of magnitude 10^{-4}. This loss factor is independent of frequency.

[21] Morey, *The Properties of Glass* (Reinhold Publishing Corp., New York, 1938).

[22] Loughborough and Stamm, J. Phys. Chem. **40**, 1113 (1936).

[23] Myron Elliott, Dissertation, University of Wisconsin (1938). Dr. Elliott has been generous enough to allow us to present his data at this point.

[24] Yager, Physics **7**, 434 (1936).

would occur due to rotation of the ellipsoid particle about the long axis.

Energy absorption experiments were carried out with a similar sample of maple lignin dissolved in the more viscous dioxane in order to shift the second dispersion toward lower frequencies. The data are illustrated in Fig. 3. The heavy line drawn through the experimental points is the sum of two absorption curves, each of distribution constant, $b=0.8$. The critical frequencies are of such magnitude as to give a shape factor of 8 and a molecular weight of 3900. Only very minor deviations in the critical frequencies can be permitted if it is assumed that both curves are to have the same distribution constant and that the heights of the two curves are to be widely different and yet have the sum of their maximal values less than $\frac{1}{2}(\epsilon'_0-\epsilon'_\infty)$. Thus the molecular weight and shape factor have been determined independently of other data.

It is important to note that these lignin preparations are not completely monodisperse, but consist of molecules whose relaxation times are distributed somewhat sharply about a mean value. In addition, a lignin molecule with different characteristic constants was also studied. This was indicated by experiments performed with the most soluble lignin fraction—i.e., that which precipitated last in the fractionation process. As can be seen from Fig. 4 the real and imaginary components of the dielectric constants are completely consistent when the critical frequency of 3.5×10^7 cycles per sec. and a distribution coefficient of $b=0.6$ are used in the theoretical equations. However, this critical frequency indicates either a much smaller molecule of the same shape (mol. wt. 2200) or a more spherical molecule of the same weight ($a/b=1.5$). Unfortunately, the high polydispersity and small relaxation time prevented any measurement of the second critical frequency.

TABLE II. *Dielectric constant ratio data for aspen, maple and spruce lignins. Solvent: chloroform; $\epsilon=4.761$; $\eta=0.00540$. Concentration of solutions: aspen lignin—4.41% (wt.), maple lignin—4.61% (wt.), spruce lignin—4.60% (wt.).*

Wave-length	log ν	$\frac{\epsilon'\ (\text{Solution})}{\epsilon'\ (\text{Solvent})}=R$ Aspen	Maple	Spruce
		Bridge apparatus		
2136	5.147	1.046	1.054	1.051
534	5.749	1.046	1.054	1.050
356	5.925	1.046	1.051	1.047
267	6.050		1.052	1.046
		Resonance apparatus		
126	6.377	1.046	1.042	1.046
56.1	6.728	1.041		1.038
31.3	6.988	1.034	1.035	1.033
14.17	7.325	1.029	1.031	1.031
7.50	7.622	1.022		1.013

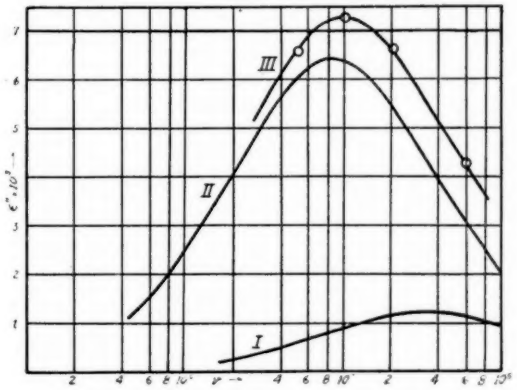

FIG. 3. Variation of ϵ'' with frequency. Maple lignin in dioxane. Abscissa—log ν, ordinate—ϵ''. Curve I—Calculated curve for rotation about the long axis; $\nu_c=3.32\times10^7$, $b=0.8$. Curve II—Calculated curve for rotation about the short axis; $\nu_c=8.8\times10^6$; $b=0.8$. Curve III—Sum of curves I and II. Molecular weight = 3900; shape factor = 8.

ω-Hydroxydecanoic Acid Ester Polymer

As a result of extensive dielectric constant measurements with solutions of samples of this polymer, Bridgman[10] concluded that the ester groups within the molecule rotated freely. In Fig. 5 is plotted the variation of imaginary dielectric constant with the frequency for a 4.50 percent by weight solution of ω-hydroxydecanoic acid ester polymer of molecular weight 8570 dissolved in benzene. The dotted line is drawn through the points after correction for a specific conductivity of 8.53×10^{-10} ohm^{-1} cm^{-1} has been made. The expected curve for a rigid and spherical particle of that molecular weight is also indicated. The value of ϵ'' is obviously independent of frequency. However, a limiting relaxation time can be estimated. The quantity ϵ'_∞ was taken to be equal to the square of the refractive index, 1.49674, plus 0.031, the contribution due to atomic polarization. The value of ϵ'_0 is independent of frequency and was found

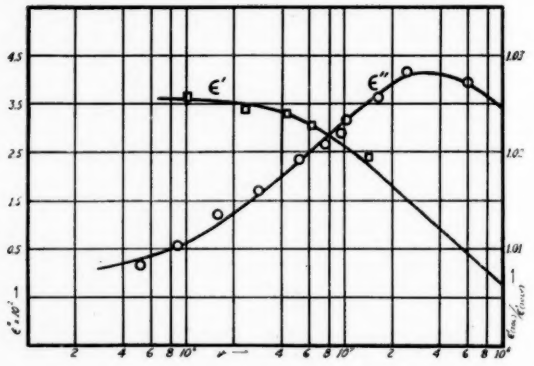

FIG. 4. Frequency variation of ϵ' and ϵ''. Maple lignin in chloroform. Abscissa—log frequency, ordinates—dielectric constant ratio and ϵ''. Specific conductance of solution 4.7×10^{-8} ohm^{-1} cm^{-1}.

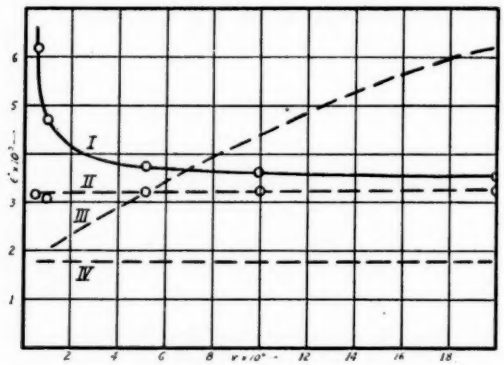

FIG. 5. Frequency variation of ϵ'' in ω-hydroxydecanoic acid. Polymer molecular weight 8570. Abscissa—frequency, ordinate—ϵ''. Curve I—Solution in benzene. Curve II—Benzene solution corrected for specific conductance of 8.5×10^{-10} ohm^{-1} cm^{-1}. Curve III—Calculated curve for equivalent spherical molecule. Curve IV—Pure benzene.

to be equal to 2.372. Upon substitution of these values into Eq. (11), a limiting relaxation time of 5×10^{-12} sec. is obtained. Such a value is of the proper order for the rotation of ester groups. The insolubility of the material prevented a more accurate determination of this limiting time constant. It is readily seen from the data that the molecule does not act as a rigid unit in any sense of the term.

METHYL METHACRYLATE POLYMERS

Flow double refraction measurements[25] with a series of polymers have indicated length to width ratios up to 100 to 1 for samples having molecular weights of 30,000 to 80,000. Data for measurements of real dielectric constant are plotted to form Fig. 6. The dotted line shows the expected dispersion curve for a unit of molecular weight 50,000 dissolved in dioxane when spherical shape is assumed. The height of the dispersion is, of course, arbitrary.

It is noted that dispersion has not occurred, suggesting that these are long flexible molecules. The data show that the shape factor is at least greater than 40 ($\tau_1/\tau_0=90$). Unfortunately, apparatus was not available with which to study possible dielectric dispersion in the region expected for a long narrow particle of the same weight and with ratio of major to minor axis equal to 100.

With carefully dried samples of one polymer, the polarization data given in Table III were

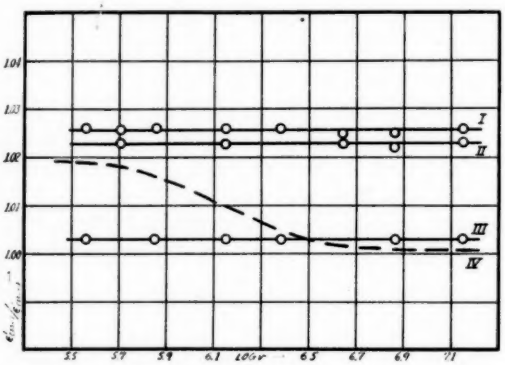

FIG. 6. Frequency variation of dielectric constant ratio methyl methacrylate solutions. Abscissa—log ν, ordinate—dielectric constant ratio. Curve I—3 percent solution in benzene. Curve II—0.5 percent solution in dioxane. Curve III—1 percent solution in benzene. Curve IV—Calculated curve for 0.5 percent solution in dioxane assuming rigid spherical solute molecule.

obtained. In these calculations, the molecular weight was chosen arbitrarily as 50,000. The molar refraction, 11,800 cc, obtained from refractive index measurements agrees well with that determined by the sum of the atomic refractivities, 11,400. The later value was assumed in the calculations.

With completely free rotation about every bond in the linear molecule, a polymer of this molecular weight should show a dipole moment[26] of 40.2×10^{-18}. The agreement between the observed and calculated moments indicates a high degree of flexibility in the molecule. Such agree-

[25] de Rosset, Dissertation, University of Wisconsin (1939).

[26] H. Eyring, Phys. Rev. **39**, 746 (1932).

ment cannot be due solely to a fortuitous choice of molecular weight, for the ratio of the two values remains constant as long as the mole fraction f_2 of the solute is very much less than unity. That there may be some steric hinderance[27] to free rotation is shown by molecular models of the polymeric chain.

Energy absorption measurements were performed at two frequencies with a 1.0 percent solution of the polymer of average molecular weight 50,000. The ratio of energy absorbed in solution to that in the solvent at frequency 17.3 megacycles is 5.40, whereas the same ratio at 80 megacycles is 5.00. Inasmuch as the difference between the ratios is not significant, it may be concluded that these solutions show no dispersion at frequencies of this order. The magnitude of the ratio may be explained by the fact that the solutions were rather viscous, and after the first filling of the capillary with solution, the effective radii of the tube were undoubtedly smaller because of the liquid adhering to the glass walls. Thus the energy absorption measurements confirm the failure to find dielectric constant dispersion for these polymers.

TABLE III. *Polarization of methyl methacrylate polymer.*

f_2	P_{12}	P_2	$\mu\times10^{+18}$
5.64×10^{-5}	28.42	31,400	31.2
1.33×10^{-5}	27.06	30,100	30.2
5.73×10^{-5}	28.45	31,200	31.0

The author wishes to thank Professor J. W. Williams for his generous aid and advice during the course of this research.

[27] Gross, Ott and Arnold [Trans. Electrochem. Soc. **74**, 193 (1938)] report dispersion measurements for methacrylate resins in solution.

AUGUST, 1941 JOURNAL OF CHEMICAL PHYSICS VOLUME 9

Vibration-Rotation Energies of the Planar XY_3 Molecular Model

SAMUEL SILVER AND WAVE H. SHAFFER
Mendenhall Laboratory of Physics, Ohio State University, Columbus, Ohio

(Received April 2, 1941)

The vibration-rotation energies of the planar XY_3 molecular model are investigated to the second order of approximation, including the cubic and quartic anharmonic terms of the potential energy, the Coriolis interactions between the degenerate oscillations and the total angular momentum, the dependence of the moments of inertia upon the vibrational state, and the centrifugal expansion terms. The contact transformation developed by Shaffer, Nielsen, and Thomas is applied to the Wilson-Howard Hamiltonian, and it is found that the energies are simply the diagonal elements of the transformed Hamiltonian. The energies are expressed in term value form, $E/hc=G_{\text{vib}}+F_{\text{rot}}-\zeta h/4\pi^2 c\overset{0}{I}_{zz}(l_2-l_1)K$, G_{vib}, F_{rot}, and ζ being given in terms of the constants appearing in the Hamiltonian. The dependence of the moments of inertia, I_{xx} and I_{zz}, upon the vibrational states is determined, and it is found that the quantity $\Delta=I_{zz}-2I_{xx}$ is independent of the anharmonic constants, depending only on the dimensions of the molecule, the normal frequencies, and the vibrational state.

1. INTRODUCTION

THE planar XY_3 molecular model is of interest in connection with several molecular systems, notably the BF_3 molecule and the carbonate ions, and as a limiting case of the pyramidal XY_3 model. The latter is treated in detail in the preceding paper, but, in view of the complexity of the material, we thought it would be desirable to discuss the planar model separately, so as to give the results in a form directly applicable to molecules of this type, and also as a verification of the more general treatment.

2. THE VIBRATIONAL COORDINATES

The vibrational frequencies have been developed for special force systems by Menzies[1] and

[1] A. C. Menzies, Proc. Roy. Soc. **A134**, 265 (1931).

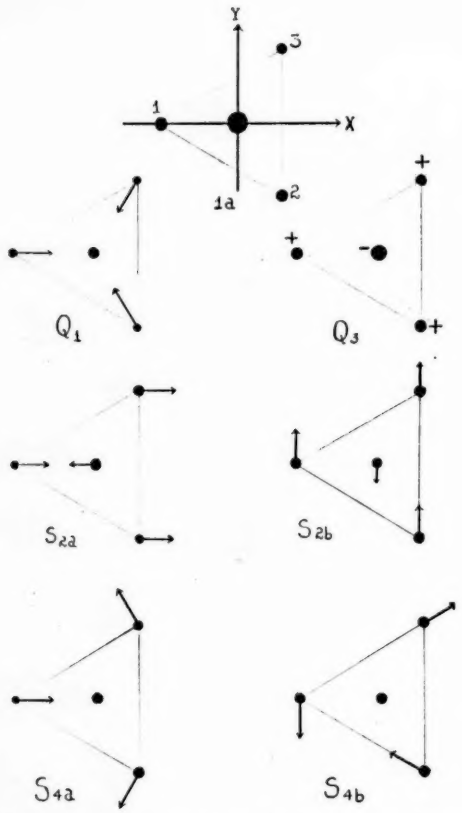

FIG. 1. The equilibrium configuration and symmetry coordinates. Q_1 and Q_3 are the nondegenerate normal modes; + indicates a displacement out of the plane of the figure. S_{2a}, S_{2b} and S_{4a}, S_{4b} are the two pairs of doubly degenerate coordinates.

by Lassettre, Anderson, and Yost,[2] and for a general force system by Rosenthal.[3] Since none of these papers develops the normal coordinates, which are required for the present work, we shall first give a brief treatment of this phase of the problem. The method we have used is the group theory analysis of Wigner[4] and Wilson,[5] and in the following we shall simply quote the essential results, referring to their papers for the details.

The coordinate system is a set of rotating axes whose origin lies at the center of gravity of the molecule. The equilibrium configuration is shown in Fig. 1(a). The equilibrium coordinates of the kth atom are denoted by $x_{k\alpha}^0$, the components of its displacement from the equilibrium position by $x_{k\alpha}$. The masses of the Y atoms and the X atom are m and M, respectively.

The group theory analysis leads to the result that the secular equation for the normal frequencies can be factored, on symmetry considerations alone, into two first-order equations and two identical second-order equations, corresponding to two nondegenerate and two doubly degenerate frequencies. Accordingly, we develop two nondegenerate symmetry coordinates, one totally symmetric to the symmetry elements of the molecule, and the other antisymmetric to the reflection in the plane of the molecule; and two pairs of doubly degenerate coordinates which transform, under the symmetry operations, in the same manner as a pair of rigid translations along the X and Y axes. The complete set of coordinates is shown in Fig. 1. The analytical expressions are:

$$
\begin{aligned}
Q_1 &= 1/(12)^{\frac{1}{2}}[2\xi_1-\xi_2-\xi_3+\sqrt{3}(\eta_2-\eta_3)],\\
Q_3 &= \frac{1}{[3(3m+M)]^{\frac{1}{2}}}[M^{\frac{1}{2}}(\zeta_1+\zeta_2+\zeta_3)-3m^{\frac{1}{2}}\zeta_4],\\
S_{2a} &= \frac{1}{[3(3m+M)]^{\frac{1}{2}}}[M^{\frac{1}{2}}(\xi_1+\xi_2+\xi_3)-3m^{\frac{1}{2}}\xi_4],\\
S_{2b} &= \frac{1}{[3(3m+M)]^{\frac{1}{2}}}[M^{\frac{1}{2}}(\eta_1+\eta_2+\eta_3)-3m^{\frac{1}{2}}\eta_4],\\
S_{4a} &= 1/(12)^{\frac{1}{2}}[2\xi_1-\xi_2-\xi_3-\sqrt{3}(\eta_2-\eta_3)],\\
S_{4b} &= -1/(12)^{\frac{1}{2}}[\sqrt{3}(\xi_2-\xi_3)+2\eta_1-\eta_2-\eta_3]
\end{aligned}
\qquad (1)
$$

into which we have introduced mass-reduced coordinates,

$$\xi_k = M_k^{\frac{1}{2}}x_k; \quad \eta_k = M_k^{\frac{1}{2}}y_k; \quad \zeta_k = M_k^{\frac{1}{2}}z_k. \qquad (2)$$

The symmetry coordinates are orthogonal and are normalized to unity. The inverse transformation is obtained by interchanging rows and columns, and, having this, it may be readily verified that the coordinates satisfy Eckart's conditions for defining the rotating axis:[6]

$$\sum_k M_k x_{k\alpha} = 0; \quad \sum_k M_k(x_{k\alpha}^0 x_{k\beta} - x_{k\beta}^0 x_{k\alpha}) = 0. \qquad (3)$$

The most general quadratic form for the potential energy, expressed in terms of the sym-

[2] T. F. Anderson, E. N. Lassettre and D. M. Yost, J. Chem. Phys. **4**, 703 (1936).
[3] J. Rosenthal, Phys. Rev. **47**, 235 (1935).
[4] E. Wigner, Göttingen Nachrichten, p. 133 (1930).
[5] E. B. Wilson, Jr., Phys. Rev. **45**, 706 (1934); J. Chem. Phys. **2**, 432 (1934).
[6] C. Eckart, Phys. Rev. **47**, 552 (1935).

metry coordinates, is

$$2U_0=\frac{k_1}{m}Q_1^2+\frac{k_3}{\mu}Q_3^2+\frac{k_2}{\mu}S_{2a}^2+\frac{k_4}{m}S_{4a}^2+\frac{2k_{24}}{(\mu m)^{\frac{1}{2}}}S_{2a}S_{4a}$$
$$+\frac{k_2}{\mu}S_{2b}^2+\frac{k_4}{m}S_{4b}^2+\frac{2k_{24}}{(\mu m)^{\frac{1}{2}}}S_{2b}S_{4b}, \quad (4)$$

where $\mu=3mM/(3m+M)$. By means of the inverse transformation, giving the $x_{k\alpha}$ in terms of the symmetry coordinates, any potential function can be expressed in terms of the latter, and the relations between the constants of a particular force model and the generalized constants $k_1, \cdots, k_{24}$ can be found directly. The kinetic energy is simply a sum of square terms,

$$2T=\dot{Q}_1^2+\dot{Q}_3^2+\dot{S}_{2a}^2+\dot{S}_{4a}^2+\dot{S}_{2b}^2+\dot{S}_{4b}^2. \quad (5)$$

It is immediately evident that Q_1 and Q_3 are the non-degenerate normal coordinates corresponding to the frequencies

$$\nu_1=\frac{1}{2\pi c}\left(\frac{k_1}{m}\right)^{\frac{1}{2}} \quad \text{and} \quad \nu_3=\frac{1}{2\pi c}\left(\frac{k_3}{\mu}\right)^{\frac{1}{2}}, \quad (6)$$

the frequencies being expressed in cm^{-1}. The doubly degenerate frequencies are the roots of the quadratic equation

$$\lambda^2-\left(\frac{k_2}{\mu}+\frac{k_4}{m}\right)\lambda+\frac{k_2k_4-k_{24}^2}{\mu m}=0, \quad (7)$$

where $\lambda=\omega^2=4\pi^2c^2\nu^2$; or, explicitly,

$$\nu_{2,4}=\frac{1}{2\pi c}\left\{\frac{k_1}{2\mu}+\frac{k_4}{2m}\pm\left[\left(\frac{k_1}{2\mu}-\frac{k_4}{2m}\right)^2+\frac{k_{24}^2}{\mu m}\right]^{\frac{1}{2}}\right\}^{\frac{1}{2}}. \quad (7a)$$

TABLE I. *Basic transformation functions S_i required to remove the types of terms occurring in H_1' together with the corresponding values of $i(H_0S_i-S_iH_0)$.*

i	S_i	$i(H_0S_i-S_iH_0)$
1	$-a_1p_k/\hbar^2\omega_k$	a_1q_k
2	a_2q_k/ω_k	a_2p_k
3	$-2a_3(p_k^3/3\hbar^2+\frac{1}{2}q_kp_kq_k)/\hbar^2\omega_k$	$a_3q_k^3$
4	$-a_4(\omega_lq_kq_l+\omega_kp_kp_l/\hbar^2)/(\omega_k^2-\omega_l^2)$	$a_4q_kp_l$
5	$-a_5\{(2\omega_k^2-\omega_l^2)q_kp_l+\omega_k\omega_l(p_kq_k+q_kp_k)q_l+2\omega_k^2p_kp_l/\hbar^2\}/\hbar^2\omega_l(4\omega_k^2-\omega_l^2)$	$a_5q_kq_l^2$
6	$-a_6(q_kq_l+p_kp_l/\hbar^2)/(\omega_k-\omega_l)$	$a_6(q_kp_l-q_lp_k)$
7	$-a_7\dfrac{\{(\omega_k^2+\omega_l^2)q_kq_l+2\omega_k\omega_lp_kp_l/\hbar^2\}}{(\omega_k\omega_l)^{\frac{1}{2}}(\omega_k^2-\omega_l^2)}$	$a_7[(\omega_l/\omega_k)^{\frac{1}{2}}q_kp_l-(\omega_k/\omega_l)^{\frac{1}{2}}q_lp_k]$

Corresponding to these, we have two pairs of doubly degenerate normal coordinates, Q_2, R_2 and Q_4, R_4, given by

$$\begin{cases} S_{2a}=\gamma Q_2+\delta Q_4 \\ S_{4a}=-\delta Q_2+\gamma Q_4, \end{cases} \qquad \begin{cases} S_{2b}=\gamma R_2+\delta R_4 \\ S_{4b}=-\delta R_2+\gamma R_4 \end{cases} \quad (8)$$

where

$$\gamma=\frac{k_{24}/(\mu m)^{\frac{1}{2}}}{[(k_2/\mu-\lambda_2)^2+k_{24}^2/\mu m]^{\frac{1}{2}}};$$
$$\delta=\frac{k_2/\mu-\lambda_2}{[(k_2/\mu-\lambda_2)^2+k_{24}^2/\mu m]^{\frac{1}{2}}}. \quad (9)$$

3. THE QUANTUM-MECHANICAL HAMILTONIAN

The general Hamiltonian for the vibration-rotation states of a polyatomic molecule has been developed by Wilson and Howard.[7] For the present case it reduces to

$$H=\tfrac{1}{2}\sum_{\alpha,\beta}\mu_{\alpha\beta}(P_\alpha-p_\alpha)(P_\beta-p_\beta)+\tfrac{1}{2}\sum_k\mu^{\frac{1}{2}}p_k\mu^{-1}p_k+U, \quad (10)$$

where the P_α are the operators associated with the components of the total angular momentum in the rotating axes; the p_k are the momenta conjugate to the normal coordinates; the $p_\alpha=\sum_k X_{k\alpha}p_k$ are the components of the vibrational angular momentum:

$$\left.\begin{aligned} p_x&=(\gamma R_2+\delta R_4)p_{Q_3}-\gamma Q_3p_{R_2}-\delta Q_3p_{R_4} \\ p_y&=-(\gamma Q_2+\delta Q_4)p_{Q_3}+\gamma Q_3p_{Q_2}+\delta Q_3p_{Q_4} \\ p_z&=-[(\gamma^2-\delta^2)R_2+2\gamma\delta R_4]p_{Q_2}+[(\gamma^2-\delta^2)Q_2+2\gamma\delta Q_4]p_{R_2} \\ &\quad +[(\gamma^2-\delta^2)R_4-2\gamma\delta R_2]p_{Q_4}-[(\gamma^2-\delta^2)Q_4-2\gamma\delta Q_2]p_{R_4} \end{aligned}\right\} \quad (11)$$

[7] E. B. Wilson, Jr., and J. B. Howard, J. Chem. Phys. **4**, 262 (1936).

The $\mu_{\alpha\beta}$ are given by

$$\mu_{xx}=\frac{I'_{yy}}{I'_{xx}I'_{yy}-I'^2_{xy}};\quad \mu_{yy}=\frac{I'_{xx}}{I'_{xx}I'_{yy}-I'^2_{xy}};\quad \mu_{zz}=\frac{1}{I'_{zz}};\quad \mu_{xy}=\mu_{yx}=\frac{I'_{xy}}{I'_{xx}I'_{yy}-I'^2_{xy}};\quad \mu_{xz}=\mu_{zx}=\mu_{yz}=\mu_{zy}=0, \tag{12}$$

in which $I'_{\alpha\beta}=I_{\alpha\beta}\mp\sum_k X_{k\alpha}X_{k\beta}$ (the upper sign for $\alpha=\beta$), $I_{\alpha\beta}$ being the instantaneous moments and products of inertia. μ is the determinant of the elements $\mu_{\alpha\beta}$.

We are interested in obtaining the energies to the second-order approximation, to include the cubic and quartic anharmonic terms in the potential energy, the Coriolis interactions between the degenerate vibrations and the total angular momentum, and the centrifugal expansion terms. We expand the Hamiltonian, taking the $\mu_{\alpha\beta}$ to the second degree in the normal coordinates. It is convenient to replace the latter by dimensionless coordinates, $q_k=(\omega_k/\hbar)^{\frac{1}{2}}Q_k$. The q_k have the same symmetry properties as the Q_k, and from the analysis of these it can be seen that the cubic and quartic anharmonic terms must have the form:

$$U_1=hc\{\beta_{111}q_1^3+\beta_{122}q_1(q_2^2+r_2^2)+\beta_{133}q_1q_3^2+\beta_{144}q_1(q_4^2+r_4^2)\}, \tag{13a}$$

$$U_2=hc\{\gamma_{1111}q_1^4+\gamma_{2222}(q_2^2+r_2^2)^2+\gamma_{3333}q_3^4+\gamma_{4444}(q_4^2+r_4^2)^2+\gamma_{1122}q_1^2(q_2^2+r_2^2)+\gamma_{1133}q_1^2q_3^2+\gamma_{1144}q_1^2(q_4^2+r_4^2)$$
$$+\gamma_{2233}(q_2^2+r_2^2)q_3^2+\gamma_{2244}(q_2^2+r_2^2)(q_4^2+r_4^2)+\gamma_{3344}q_3^2(q_4^2+r_4^2)\}. \tag{13b}$$

The expanded Hamiltonian arranged in terms according to orders of magnitude is then,

$$H_0=\tfrac{1}{2}\left(\frac{P_x^2+P_y^2}{I^0_{xx}}+\frac{P_z^2}{I^0_{zz}}\right)+\tfrac{1}{2}\sum_k\hbar\omega_k\left(\frac{p_{q_k}^2}{\hbar^2}+q_k^2\right), \tag{14a}$$

$I^0_{\alpha\alpha}$ being the moments of inertia of the molecule in its rotationless equilibrium configuration;

$$H_1=\frac{3i}{2}\left(\frac{\hbar\omega_1}{I^0_{zz}}\right)p_{q_1}+2\left(\frac{\hbar}{\omega_1(I^0_{zz})^3}\right)^{\frac{1}{2}}\left(P_x^2+P_y^2+\frac{P_z^2}{2}\right)q_1-2\left(\frac{\hbar}{(I^0_{zz})^3}\right)^{\frac{1}{2}}(P_y^2-P_x^2)\left(\frac{\delta}{\omega_2^{\frac{1}{2}}}q_2-\frac{\gamma}{\omega_4^{\frac{1}{2}}}q_4\right)$$
$$-2\left(\frac{\hbar}{(I^0_{zz})^3}\right)^{\frac{1}{2}}\left(\frac{\delta}{\omega_2^{\frac{1}{2}}}r_2-\frac{\gamma}{\omega_4^{\frac{1}{2}}}r_4\right)(P_xP_y+P_yP_x)-\frac{\gamma P_x}{I^0_{xx}}\left[\left(\frac{\omega_3}{\omega_2}\right)^{\frac{1}{2}}r_2p_{q_3}-\left(\frac{\omega_2}{\omega_3}\right)^{\frac{1}{2}}q_3p_{r_2}\right]$$
$$-\frac{\delta P_x}{I^0_{xx}}\left[\left(\frac{\omega_3}{\omega_4}\right)^{\frac{1}{2}}r_4p_{q_3}-\left(\frac{\omega_4}{\omega_3}\right)^{\frac{1}{2}}q_3p_{r_4}\right]+\frac{\gamma P_y}{I^0_{xx}}\left[\left(\frac{\omega_3}{\omega_2}\right)^{\frac{1}{2}}q_2p_{q_3}-\left(\frac{\omega_2}{\omega_3}\right)^{\frac{1}{2}}q_3p_{q_2}\right]$$
$$+\frac{\delta P_y}{I^0_{xx}}\left[\left(\frac{\omega_3}{\omega_4}\right)^{\frac{1}{2}}q_4p_{q_3}-\left(\frac{\omega_4}{\omega_3}\right)^{\frac{1}{2}}q_3p_{q_4}\right]-\frac{(\gamma^2-\delta^2)}{I^0_{zz}}[(q_2p_{r_2}-r_2p_{q_2})-(q_4p_{r_4}-r_4p_{q_4})]P_z$$
$$-\frac{\gamma\delta}{I^0_{xx}}\left[\left(\frac{\omega_2}{\omega_4}\right)^{\frac{1}{2}}(q_4p_{r_2}-r_4p_{q_2})+\left(\frac{\omega_4}{\omega_2}\right)^{\frac{1}{2}}(q_2p_{r_4}-r_2p_{q_4})\right]P_z+U_1, \tag{14b}$$

$$H_2=\frac{3i\hbar}{2I^0_{zz}}q_1p_{q_1}+\frac{i\hbar}{I^0_{zz}}[\delta^2(q_2p_{q_2}+r_2p_{r_2})+\gamma^2(q_4p_{q_4}+r_4p_{r_4})]+\frac{3\hbar}{(I^0_{zz})^2}\left\{\frac{q_1^2}{\omega_1}+\frac{\delta^2}{\omega_2}(q_2^2+r_2^2)\right.$$
$$\left.+\frac{\gamma^2}{\omega_4}(q_4^2+r_4^2)\right\}(P_x^2+P_y^2)+\frac{3\hbar}{2I^0_{zz}\omega_1}q_1^2P_z^2+\frac{1}{2}\left[\frac{(p_x^2+p_y^2)}{I^0_{xx}}+\frac{p_z^2}{I^0_{zz}}\right]+U_2. \tag{14c}$$

plus terms which have no diagonal matrix elements, and, therefore, as we shall see below, need not be considered. The constants γ and δ are those defined by Eq. (9) above.

4. The Contact Transformation

It was shown by Van Vleck and Jordahl[8] that the Hamiltonian can be transformed by a contact transformation, $H'=THT^{-1}$, which takes terms of first order in H into second-order terms in H'. The form of T is $T=e^{i\lambda S}$, where λ is the "smallness" parameter according to which H is separated into its orders of magnitude. The appropriate form of S for the vibration-rotation problem has been developed by Shaffer, Nielsen and Thomas.[9] It is a sum of basic functions (given in Table I) which have been chosen to remove from H_1 all terms except the Coriolis interaction terms between the degenerate modes and P_z. The new Hamiltonian H' is given by

$$H'_0=H_0=\frac{P^2}{2I^0_{xx}}+\frac{P_z^2}{2}\left(\frac{1}{I^0_{zz}}-\frac{1}{I^0_{xx}}\right)+\tfrac{1}{2}\sum_k \hbar\omega_k\left(\frac{p_{q_k}^2}{\hbar^2}+q_k^2\right), \tag{15a}$$

$$H'_1=H_1+i(SH_0-H_0S)=-\frac{(\gamma^2-\delta^2)}{I^0_{zz}}[(q_2p_{r_2}-r_2p_{q_2})-(q_4p_{r_4}-r_4p_{q_4})]P_z, \tag{15b}$$

$$\begin{aligned}
H'_2&=H_2+\frac{i}{2}[S(H_1+H'_1)-(H_1+H'_1)S]\\
&=-\frac{2}{(I^0_{zz})^3}\left\{\frac{1}{\omega_1^2}+\frac{\delta^2}{\omega_2^2}+\frac{\gamma^2}{\omega_4^2}\right\}(P_x^4+P_y^4)-\frac{2}{(I^0_{zz})^3}\left\{\frac{1}{\omega_1^2}-\frac{\delta^2}{\omega_2^2}-\frac{\gamma^2}{\omega_4^2}\right\}(P_x^2P_y^2+P_y^2P_x^2)-\frac{1}{2(I^0_{zz})^3\omega_1^2}P_z^4\\
&\quad-\frac{2}{(I^0_{zz})^3}\left(\frac{\delta^2}{\omega_2^2}+\frac{\gamma^2}{\omega_4^2}\right)(P_xP_y+P_yP_x)^2-\frac{1}{(I^0_{zz})^3\omega_1^2}[(P_x^2+P_y^2)P_z^2+P_z^2(P_x^2+P_y^2)]\\
&\quad+\frac{1}{I^0_{zz}}\{a_{11}q_1^2+a_{33}q_3^2+a_{22}(q_2^2+r_2^2)+a_{44}(q_4^2+r_4^2)\}(P_x^2+P_y^2)+\frac{1}{I^0_{zz}}\{b_{22}(r_2^2P_x^2+q_2^2P_y^2)+b_{44}(r_4^2P_x^2+q_4^2P_y^2)\}\\
&\quad+\frac{1}{2I^0_{zz}}\{c_{11}q_1^2+c_{33}q_3^2+c_{22}(q_2^2+r_2^2)+c_{44}(q_4^2+r_4^2)\}P_z^2+\frac{9\hbar^2}{I^0_{zz}}\\
&\quad+\frac{3i\hbar}{I^0_{zz}}\left\{\frac{q_1p_{q_1}}{2}+\delta^2(q_2p_{q_2}+r_2p_{r_2})+\gamma^2(q_4p_{q_4}+r_4p_{r_4})\right\}+\frac{1}{I^0_{zz}}\left\{p_x^2+p_y^2+\frac{p_z^2}{2}\right\}\\
&\quad-\frac{hc\beta_{111}^2}{\nu_1}\left[3\frac{p_{q_1}^2q_1^2}{\hbar^2}+1+\frac{3}{2}q_1^4\right]-\frac{hc\beta_{133}^2}{2\nu_1[4\nu_3^2-\nu_1^2]}\left\{(2\nu_3^2-\nu_1^2)q_3^4+4\nu_1\nu_3q_1^2q_3^2+\frac{2\nu_3^2}{\hbar^2}q_3^2p_{q_3}^2\right\}\\
&\quad-\frac{hc}{2\nu_1}\sum_{k=2,4}\frac{\beta_{1kk}^2}{(4\nu_k^2-\nu_1^2)}\left[(2\nu_k^2-\nu_1^2)(q_k^2+r_k^2)^2+4\nu_1\nu_kq_1^2(q_k^2+r_k^2)\right.\\
&\quad\left.+\frac{\nu_k^2}{\hbar^2}\{(p_{q_k}^2+p_{r_k}^2)(q_k^2+r_k^2)+(q_k^2+r_k^2)(p_{q_k}^2+p_{r_k}^2)\}\right]-3\frac{hc}{\nu_1}\beta_{111}q_1^2[\beta_{133}q_3^2+\beta_{122}(q_2^2+r_2^2)+\beta_{144}(q_4^2+r_4^2)]\\
&\quad-\frac{hc}{\nu_1}[\beta_{133}\beta_{122}q_3^2(q_2^2+r_2^2)+\beta_{133}\beta_{144}q_3^2(q_4^2+r_4^2)+\beta_{122}\beta_{144}(q_2^2+r_2^2)(q_4^2+r_4^2)]\\
&\quad+hc\{\gamma_{1111}q_1^4+\gamma_{3333}q_3^4+\gamma_{2222}(q_2^2+r_2^2)^2+\gamma_{4444}(q_4^2+r_4^2)^2+\gamma_{1122}q_1^2(q_2^2+r_2^2)+\gamma_{1133}q_1^2q_3^2\\
&\qquad+\gamma_{1144}q_1^2(q_4^2+r_4^2)+\gamma_{2233}(q_2^2+r_2^2)q_3^2+\gamma_{2244}(q_2^2+r_2^2)(q_4^2+r_4^2)+\gamma_{3344}q_3^2(q_4^2+r_4^2)\},
\end{aligned} \tag{15c}$$

[8] J. H. Van Vleck, Phys. Rev. **33**, 467 (1929); O. M. Jordahl, Phys. Rev. **45**, 87 (1934). See also E. C. Kemble, *Fundamental Principles of Quantum Mechanics* (McGraw-Hill Book Company, Inc., New York, 1937), Chapter XI, Section 48(c).

[9] W. H. Shaffer, H. H. Nielsen and L. H. Thomas, Phys. Rev. **56**, 895 (1939).

where

$$\left.\begin{aligned}
a_{11}&=\frac{3\hbar}{I^0_{zz}\omega_1}-\frac{6hc\beta_{111}}{(\hbar\omega_1^3 I^0_{zz})^{\frac{1}{2}}};\quad a_{22}=\frac{3\hbar\delta^2}{I^0_{zz}\omega_2}-\frac{2hc\beta_{122}}{(\hbar\omega_1^3 I^0_{zz})^{\frac{1}{2}}}\\
a_{33}&=-\frac{\hbar}{\omega_3}\left[\frac{(3\omega_3^2+\omega_2^2)\gamma^2}{I^0_{xx}(\omega_2^2-\omega_3^2)}+\frac{(3\omega_3^2+\omega_4^2)\delta^2}{I^0_{xx}(\omega_4^2-\omega_3^2)}\right]-\frac{2hc\beta_{133}}{(\hbar\omega_1^3 I^0_{zz})^{\frac{1}{2}}}\\
a_{44}&=\frac{3\hbar^2\gamma^2}{I^0_{zz}\omega_4}-\frac{2hc\beta_{144}}{(\hbar\omega_1^3 I^0_{zz})^{\frac{1}{2}}}\\
b_{22}&=\frac{(3\omega_2^2+\omega_3^2)\gamma^2\hbar}{I^0_{xx}\omega_2(\omega_2^2-\omega_3^2)};\quad b_{44}=\frac{(3\omega_4^2+\omega_3^2)\delta^2\hbar}{I^0_{xx}\omega_4(\omega_4^2-\omega_3^2)}\\
c_{11}&=\frac{3\hbar}{I^0_{zz}\omega_1}-\frac{6hc\beta_{111}}{(\hbar\omega_1^3 I^0_{zz})^{\frac{1}{2}}};\quad c_{33}=-\frac{2hc\beta_{133}}{(\hbar\omega_1^3 I^0_{zz})^{\frac{1}{2}}}\\
c_{22}&=-\frac{2\hbar^2\gamma^2\delta^2(3\omega_2^2+\omega_4^2)}{I^0_{xx}\omega_2(\omega_4^2-\omega_2^2)}-\frac{2hc\beta_{122}}{(\hbar\omega_1^3 I^0_{zz})^{\frac{1}{2}}}\\
c_{44}&=\frac{2\hbar^2\gamma^2\delta^2(3\omega_4^2+\omega_2^2)}{I^0_{xx}\omega_4(\omega_4^2-\omega_2^2)}-\frac{2hc\beta_{144}}{(\hbar\omega_1^3 I^0_{zz})^{\frac{1}{2}}}.
\end{aligned}\right\}\tag{15d}$$

The two pairs of degenerate normal modes can be regarded as two isotropic two-dimensional oscillators, and as such it is best to express them in polar coordinates,

$$q_k=\rho_k\cos\varphi_k;\quad r_k=\rho_k\sin\varphi_k.\tag{16}$$

We then obtain

$$(H_0')_{\text{vib}}=\frac{\hbar\omega_j}{2}\left(\frac{p_{qj}^2}{\hbar^2}+q_j^2\right)+\frac{\hbar\omega_k}{2}\left[-\frac{1}{\rho_k}\frac{\partial}{\partial\rho_k}\left(\rho_k\frac{\partial}{\partial\rho_k}\right)-\frac{1}{\rho_k^2}\frac{\partial^2}{\partial\varphi_k^2}+\rho_k^2\right],\quad (j=1,3;\ k=2,4)\tag{17a}$$

$$H_1'=+i\hbar\frac{\zeta}{I^0_{zz}}\left[\frac{\partial}{\partial\varphi_2}-\frac{\partial}{\partial\varphi_4}\right]P_z,\tag{17b}$$

where $\zeta=\gamma^2-\delta^2$. Similar transformations occur in H_2', which we shall not rewrite.

5. The Wave Functions and Energies

The basic wave functions, solutions of H_0', are

$$\Psi^{0'}(JKMV_1\cdots_4)V=R(JKM)\prod_{k=1}^{4}\psi'(V_k),\tag{18}$$

where $R(JKM)$ are the symmetrical rigid top functions, and the $\psi'(V_k)$ are the harmonic oscillator functions[10]

$$\psi'(V_k)=NV_k\exp(-q_k^2/2)HV_k(q_k),\quad k=1\text{ and }3,\tag{18a}$$

$$\psi'(V_k)=\frac{N'V_k}{(2\pi)^{\frac{1}{2}}}\exp(-\rho_k^2/2)FV_{k,|l_k|}(\rho_k)\exp(il_k\varphi_k);\quad k=2\text{ and }4.\tag{18b}$$

The zeroth-order energy level,

$$E^{(0)}=J(J+1)\frac{h^2}{8\pi^2 I^0_{xx}}+\frac{K^2h^2}{8\pi^2}\left(\frac{1}{I^0_{zz}}-\frac{1}{I^0_{xx}}\right)+\sum_i\left(V_i+\frac{d_i}{2}\right)hc\nu_i\tag{19}$$

($d_i=1$ if $i=1$, 3, and $d_i=2$ if $i=2$, 4), is

[10] See, for example, D. M. Dennison, Rev. Mod. Phys. **3**, 280 (1931).

$2(V_2+1)(V_4+1)$-fold degenerate since $K=\pm\sqrt{K^2}$ and $l_i=V_i,\ V_i-2,\ V_i-4,\ \cdots,\ -V_i+2,\ -V_i$. To obtain the first-order energy corrections we must set up the secular equation corresponding to the complete set of wave functions of the level $E^0(J,\ K,\ M,\ V_1,\ \cdots,\ V_4)$. This is very simple in the present case, since H_1' does not possess off-diagonal elements for either the vibrational factor or the rotational factor, and the first-order corrections to the energy are just the diagonal elements of H_1':

$$E^{(1)}=-\frac{\zeta h^2}{4\pi^2 I^0_{zz}}(l_2-l_4)K. \tag{20}$$

There is no first-order correction to the wave functions,* but we have removed the degeneracy in the quantum numbers l_i. The second-order correction due to H_2' is obtained by the usual perturbation methods. As is well known, the second-order corrections consist of the diagonal elements of H_2' and contributions from the nondiagonal elements of H_1'. The latter do not arise in our case.† The diagonal matrix elements of terms such as $P_\alpha P_\beta$ and $P_\alpha P_\beta P_\gamma P_\delta$ have been listed by Shaffer and Nielsen.[11] The diagonal elements for the two-dimensional oscillator terms ρ^2 and ρ^4 are:

$$\begin{aligned}&(Vl|\,\rho^2\,|Vl)=V+1\,;\\ &(Vl|\,\rho^4\,|Vl)=\tfrac{3}{2}(V+1)^2-\tfrac{1}{2}(l^2-1).\end{aligned} \tag{21}$$

The second-order energy can be written down directly. Collecting terms, the complete energy in term-value form is

$$E=hc\left\{[G_{\rm vib}+F_{\rm rot}]-\frac{\zeta h}{4\pi^2 cI^0_{zz}}(l_2-l_4)K\right\}, \tag{22}$$

where

$$G_{\rm vib}=G_0+\sum_{i=1}^{4}\nu_i\left(V_i+\frac{d_i}{2}\right)+\sum_{i=1}^{4}G_{ii}\left(V_i+\frac{d_i}{2}\right)^2+\sum_{i<k}G_{ik}\left(V_i+\frac{d_i}{2}\right)\left(V_k+\frac{d_k}{2}\right)+g_{22}(1-l_2^2)+g_{44}(1-l_4^2)+g_{24}l_2l_4. \tag{22a}$$

with

$$G_0=-\frac{5h}{64\pi^2cI^0_{xx}}-\frac{3\gamma^2\delta^2h}{4\pi^2cI^0_{xx}}-\frac{7\beta_{111}^2}{16\nu_1}+\frac{3}{16}\frac{\beta_{133}^2\nu_1}{(4\nu_3^2-\nu_1^2)}+\tfrac{3}{8}(\gamma_{1111}+\gamma_{3333}),$$

$$G_{11}=-\frac{15}{4\nu_1}\beta_{111}^2+\tfrac{3}{2}\gamma_{1111},$$

$$G_{kk}=-\frac{\beta_{1kk}^2(8\nu_k^2-3\nu_1^2)}{4\nu_1(4\nu_k^2-\nu_1^2)}+\tfrac{3}{2}\gamma_{kkkk},\quad k=2,\ 3,\ 4$$

$$G_{1k}=-\frac{2\beta_{1kk}^2\nu_k}{4\nu_k^2-\nu_1^2}-\frac{3\beta_{111}\beta_{1kk}}{\nu_1}+\gamma_{11kk},\quad k=2,\ 3,\ 4$$

$$G_{23}=\frac{\gamma^2h}{8\pi^2cI^0_{xx}}\left(\frac{\nu_3}{\nu_2}+\frac{\nu_2}{\nu_3}\right)-\frac{\beta_{122}\beta_{133}}{\nu_1}+\gamma_{2233},$$

$$G_{24}=\frac{\gamma^2\delta^2h}{8\pi^2cI^0_{xx}}\left(\frac{\nu_4}{\nu_2}+\frac{\nu_2}{\nu_4}\right)-\frac{\beta_{122}\beta_{144}}{\nu_1}+\gamma_{2244},$$

$$G_{34}=\frac{\delta^2h}{8\pi^2cI^0_{xx}}\left(\frac{\nu_3}{\nu_4}+\frac{\nu_4}{\nu_3}\right)-\frac{\beta_{133}\beta_{144}}{\nu_1}+\gamma_{3344},$$

$$g_{kk}=-\frac{(\gamma^2-\delta^2)^2h}{16\pi^2cI^0_{xx}}+\frac{\beta_{1kk}^2\nu_1}{4(4\nu_k^2-\nu_1^2)}+\frac{\gamma_{11kk}}{2},\quad k=2,\ 4$$

$$g_{24}=-\frac{(\gamma^2-\delta^2)^2h}{8\pi^2cI^0_{xx}}$$

and

$$F_{\rm rot}=B_vJ(J+1)-C_vK^2-D_JJ^2(J+1)^2-D_KK^4-D_{JK}J(J+1)K^2 \tag{22b}$$

with

$$B_v=B_e-\alpha_0-\sum_{i=1}^{4}(V_i+d_i/2)\alpha_i,$$

$$C_v=C_e-\beta_0-\sum_{i=1}^{4}(V_i+d_i/2)\beta_i,$$

* This, of course, applies only to the wave functions of H'. The corresponding wave functions of H can be obtained by the inverse transformation $\Psi=T^{-1}\Psi'$.

† There are terms in H' in addition to those given in Eq. (15b). They arise from the contact transformation because of the non-commutability of P_z with the rotational operators. They are of third degree in the quantum numbers J and K, and possess no diagonal elements. Therefore, they can enter into the energy only as squared terms; that is, terms of sixth degree in J and K, which is far beyond the order of approximation in which we are interested.

[11] W. H. Shaffer and H. H. Nielsen, Phys. Rev. **56**, 188 1939).

where

$$B_e=h/8\pi^2cI^0_{xx},\quad \alpha_0=-4B_e^3(\delta^2/\nu_2^2+\gamma^2/\nu_4^2),$$

$$\alpha_1=-B_ea_{11},\quad \alpha_3=-B_ea_{33},$$

$$\alpha_2=-B_e(a_{22}+b_{22}/2),\quad \alpha_4=-B_e(a_{44}+b_{44}/2),$$

$$C_e=-\frac{h}{8\pi^2c}\left(\frac{1}{I^0_{zz}}-\frac{1}{I^0_{xx}}\right)=\frac{B_e}{2},$$

$$\beta_0=-10B_e^3(\delta^2/\nu_2^2+\gamma^2/\nu_4^2),$$

$$\beta_1=-B_e(a_{11}-c_{11}/2),$$

$$\beta_2=-B_e(a_{22}+b_{22}/2-c_{22}/2),$$

$$\beta_3=-B_e(a_{33}-c_{33}/2),$$

$$\beta_4=-B_e(a_{44}+b_{44}/2-c_{44}/2),$$

$$D_J=2B_e^3(1/\nu_1^2+\delta^2/\nu_2^2+\gamma^2/\nu_4^2),$$

$$D_K=2B_e^3(1/4\nu_1^2+\delta^2/\nu_2^2+\gamma^2/\nu_4^2),$$

$$D_{JK}=-\tfrac{2}{3}(D_J+2D_K),$$

the constants a_{11}, $\cdots$, c_{44} being given by (15d).

The quantities B_v and C_v may be regarded as reciprocals of effective moments of inertia. By analogy with the zeroth-order rotational energy, we define

$$(I_{xx})_{\text{effective}}=h^2/8\pi^2cB_v;$$

$$(I_{zz})_{\text{effective}}=h^2/8\pi^2c(B_v-C_v).$$

Expanding $(B_v)^{-1}$ and $(B_v-C_v)^{-1}$ to the first order in the α_i and β_i, we obtain explicitly the dependence of the moments of inertia upon the vibrational state V_1, $\cdots$, V_4. Darling and Dennison[12] have shown that for the water vapor molecule there exists a relation between the effective moments of inertia which is independent of the anharmonic constants. Similar relations probably exist for molecules in which there is a simple linear relation between the equilibrium moments of inertia, and we have, in fact, found such a relation for the present case. Using Darling and Dennison's notation, we have

$$\Delta=(I_{zz})_{\text{effective}}-2(I_{xx})_{\text{effective}}$$

$$=\frac{2}{I^0_{xx}}\left[\frac{16}{B_e^2}\left(\frac{\delta^2}{\nu_2^2}+\frac{\gamma^2}{\nu_4^2}\right)+(V_1+\tfrac{1}{2})(a_{11}-c_{11})\right.$$
$$+(V_3+\tfrac{1}{2})(a_{33}-c_{33})+(V_2+1)(a_{22}+b_{22}/2-c_{22})$$
$$\left.+(V_4+1)(a_{44}+b_{44}/2-c_{44})\right].$$

Referring to (15d) it is evident that Δ depends only on the dimensions of the molecule, the normal frequencies, and the vibrational quantum numbers.

Acknowledgments

The authors take pleasure in expressing their appreciation to Dean Alpheus W. Smith for his interest and encouragement, and to Professor Harald H. Nielsen and Professor L. H. Thomas for helpful discussions during the course of this work.

[12] B. T. Darling and D. M. Dennison, Phys. Rev. 57, 128 (1940).

Rotation-Vibration Energies of the Pyramidal XY_3 Molecular Model

WAVE HENRY SHAFFER
Mendenhall Laboratory of Physics, Ohio State University, Columbus, Ohio

(Received April 2, 1941)

Complete expressions have been derived for the rotation-vibration energies of the pyramidal XY_3 molecular model in such a way as to include, through second order of approximation, all contributions to the energies arising from Coriolis interactions, anharmonicities, etc.

I. INTRODUCTION

THE band spectra of many polyatomic molecules, which can now be studied by improved experimental methods, exhibit details which require fairly complete analytical energy expressions for their interpretation. This is true especially in the case of the infra-red vibration-rotation spectra of these molecules and also in connection with the fine structure of their electronic bands to which experimentalists are giving increasing attention. This paper deals with the rotation-vibration energies of the pyramidal XY_3 molecular model and should be applicable to such molecules as phosphine, arsine, phosphorous trifluoride, etc., and some states of NH_3. Complete energy expressions have been derived which include the energies associated with the harmonic oscillator and rigid top approximations, and, in addition, first- and second-order corrections to these arising from the following: cubic and quartic anharmonic terms in the potential energy, Coriolis interactions between rotation and vibration, changes in the rotational constants arising from vibration and centrifugal stretching.

The normal vibrations of the XY_3 model have been studied by several workers[1-3] using various types of potential functions and by Wilson[4] and Wilson and Howard[5] from the standpoint of symmetry properties. Certain of the effects of Coriolis interactions on the energies have been studied by Teller and Tisza,[6] Teller,[7] and Johnston and Dennison.[8] The effects of centrifugal stretching on the rotational energies have been considered by Dennison and Slawsky.[9] None of these papers gives a complete treatment of the entire rotation-vibration problem of the XY_3 model and it is the purpose of this paper to present a unified comprehensive treatment of that problem.

II. THE NORMAL COORDINATES

The model assumed has, in its equilibrium configuration, the form of a pyramid with an equilateral triangle as base and with equal slant heights. The distance from center of the base to a base corner is denoted by a_0, the height of the apex above the center of the base by h_0, and the slant height by $s_0=(a_0^2+h_0^2)^{\frac{1}{2}}$. The X particle of mass M is situated at the apex and a Y particle of mass m at each base corner. In order to describe the positions of the particles a body-fixed right-handed rectangular coordinate system, xyz, is adopted whose origin lies at the center of gravity of the molecule and whose positive z axis points along the symmetry axis toward the X particle. The three Y particles lie in a plane which is parallel to the xy coordinate plane and intercepts the negative z axis. In this

[1] D. M. Dennison, Phil. Mag. **1**, 195 (1926).
[2] F. Lechner, Wien. Ber. **141**, 291, 663 (1932).
[3] J. E. Rosenthal, Phys. Rev. **47**, 235 (1935).
[4] E. B. Wilson, J. Chem. Phys. **2**, 432 (1934).
[5] J. B. Howard and E. B. Wilson, J. Chem. Phys. **2**, 630 (1934).
[6] E. Teller and L. Tisza, Zeits. f. Physik **73**, 791 (1932).
[7] E. Teller, *Hand- und Jahrbuch der Chemischen Physik* (1934), Vol. 9.
[8] M. Johnston and D. M. Dennison, Phys. Rev. **48**, 868 (1935).
[9] D. M. Dennison and Z. I. Slawsky, J. Chem. Phys. **7**, 509 (1939).

coordinate system the particles have the following equilibrium coordinates $(\overset{0}{x}_i, \overset{0}{y}_i, \overset{0}{z}_i)$:

$$\begin{aligned} &\text{Y, 1:}\quad (-a_0, 0, -h_1); \qquad \text{Y, 2:}\quad (a_0/2, -a_0\sqrt{3}/2, -h_1);\\ &\text{Y, 3:}\quad (a_0/2, a_0\sqrt{3}/2, -h_1); \quad \text{X, 4:}\quad (0, 0, h_4)\cdots \end{aligned} \tag{1}$$

where $h_1=(\mu_1/3m)h_0$, $h_4=(\mu_1/M)h_0$ and $\mu_1=3mM/(3m+M)$. The position of the ith particle during a vibration is given by $(x_i, y_i, z_i)=(\overset{0}{x}_i+x_i', \overset{0}{y}_i+y_i', \overset{0}{z}_i+z_i')$, where the primed quantities denote components of displacement from the equilibrium position.

The body-fixed coordinate system is defined by the Eckart conditions:[10, 11] (a) The center of gravity remains at the origin, $\sum m_i x_i=0$, etc., and (b) the angular momentum of vibration vanishes in zeroth approximation, $\sum m_i(\overset{0}{x}_i\dot{y}_i'-\overset{0}{y}_i\dot{x}_i')=0$, etc. When one sets down in terms of the displacement coordinates, (x_i', y_i', z_i'), the six relations satisfying the Eckart conditions and the expressions giving the relative displacements for small oscillations of the particles, it is evident that the following is a suitable choice of symmetry coordinates:

$$\begin{aligned} &x=x_4'-(x_1'+x_2'+x_3')/3; \quad y=y_4'-(y_1'+y_2'+y_3')/3;\\ &z=z_4'-(z_1'+z_2'+z_3')/3; \quad \eta=x_3'-x_2'; \quad \xi=(1/2)[y_3'-y_2'+3^{-\frac{1}{2}}(2x_1'-x_2'-x_3')];\\ &\zeta=(1/2)[y_3'-y_2'-3^{-\frac{1}{2}}(2x_1'-x_2'-x_3')]. \end{aligned} \tag{2}$$

The expressions for the instantaneous coordinates of the particles are the following:

$$\begin{aligned} x_1&=-a_0-(\mu_1/3m)x+3^{-\frac{1}{2}}(\xi-\zeta)\\ x_2&=(a_0/2)-(\mu_1/3m)x-(1/2)[3^{-\frac{1}{2}}(\xi-\zeta)+\eta]\\ x_3&=(a_0/2)-(\mu_1/3m)x-(1/2)[3^{-\frac{1}{2}}(\xi-\zeta)-\eta]\\ x_4&=+(\mu_1/M)x \end{aligned}$$

$$\begin{aligned} y_1&=-(\mu_1/3m)y-3^{-\frac{1}{2}}\eta\\ y_2&=-(a_0 3^{\frac{1}{2}}/2)-(\mu_1/3m)y+(1/2)[3^{-\frac{1}{2}}\eta-(\xi+\zeta)]\\ y_3&=(a_0 3^{\frac{1}{2}}/2)-(\mu_1/3m)y+(1/2)[3^{-\frac{1}{2}}\eta+(\xi+\zeta)]\\ y_4&=+(\mu_1/M)y \end{aligned} \tag{3}$$

$$\begin{aligned} z_1&=(\mu_1/3m)[-h_0-z-2(h_0/a_0)x]\\ z_2&=(\mu_1/3m)[-h_0-z+(h_0/a_0)(x-3^{\frac{1}{2}}y)]\\ z_3&=(\mu_1/3m)[-h_0-z+(h_0/a_0)(x+3^{\frac{1}{2}}y)]\\ z_4&=(\mu_1/M)[h_0+z]. \end{aligned}$$

The expressions for the changes, δ_{ij}, in the distances, S_{ij}, between pairs of particles are obtained (under assumption of small oscillations) from the relation

$$S_{ij}=\overset{0}{S}_{ij}+\delta_{ij}=[(x_i-x_j)^2+(y_i-y_j)^2+(z_i-z_j)^2]^{\frac{1}{2}}$$

and can be shown to have the following form:

$$\begin{aligned} &\delta_{12}=\zeta-(1/2)(\xi+3^{\frac{1}{2}}\eta); \quad \delta_{13}=\zeta-(1/2)(\xi-3^{\frac{1}{2}}\eta); \quad \delta_{23}=\zeta+\xi;\\ &\delta_{14}=(h_0/s_0)z+(a_0/s_0)[(\mu_2/\mu_1)x-3^{-\frac{1}{2}}(\xi-\zeta)];\\ &\delta_{24}=(h_0/s_0)z+(a_0/s_0)[(\mu_2/2\mu_1)(3^{\frac{1}{2}}y-x)+3^{-\frac{1}{2}}(\xi+2\zeta)-\eta];\\ &\delta_{34}=(h_0/s_0)z+(a_0/s_0)[(\mu_2/2\mu_1)(-3^{\frac{1}{2}}y-x)+3^{-\frac{1}{2}}(\xi+2\zeta)+\eta] \end{aligned} \tag{4}$$

[10] C. Eckart, Phys. Rev. **47**, 552 (1935).
[11] E. B. Wilson and J. B. Howard, J. Chem. Phys. **4**, 260 (1936).

where $\mu_2=(2I_{0x}/I_{0z})\mu_1$ when the quantities I_{0z} and I_{0x} are the equilibrium values of the moments of inertia about the symmetry axis and about an axis perpendicular to that axis, respectively, and satisfy the relations

$$I_{0x}=I_{0y}=\mu_1 h_0^2+(3/2)ma_0^2=\mu_1 h_0^2+(1/2)I_{0z}. \tag{5}$$

The kinetic energy of the molecular vibration, $T_v=(1/2)\sum m_i(\dot{x}_i^2+\dot{y}_i^2+\dot{z}_i^2)$, is given by the expression

$$2T_v=\mu_1\dot{z}^2+\mu_2(\dot{x}^2+\dot{y}^2)+m(\dot{\xi}^2+\dot{\eta}^2+\dot{\zeta}^2). \tag{6}$$

The harmonic (quadratic) portion, U_0, of the potential energy is given by

$$2U_0=k_1z^2+2k_2z\zeta+k_3\zeta^2+n_1(x^2+y^2)+2n_2(\xi x+\eta y)+n_3(\xi^2+y^2). \tag{7}$$

The pyramidal XY_3 model belongs to the symmetry point group C_{3v}. It can readily be shown[4,12] by methods of group theory that it has the following normal modes of oscillation: two single parallel modes of class A and two doubly degenerate perpendicular modes of class E. In this paper the single modes are indicated by the symbols ν_1 and ν_3, and the double modes by ν_2 and ν_4, in agreement with Dennison's[1] notation. Diagrams illustrating these modes of oscillation are given by Sutherland[13] and Ta-You Wu.[14] By using (6) and (7) in Lagrange's determinantal equation, $|\lambda T_v-U_0|=0$, one can obtain the normal frequencies of oscillation ν_i (measured in cm^{-1}) which are related to the roots λ_i by $\lambda_i^{\frac{1}{2}}=2\pi c\nu_i=\omega_i$ (where c = velocity of light in cm/sec.). The angular frequencies ω_i are the following:

$$\left.\begin{matrix}\omega_1\\ \omega_3\end{matrix}\right\}=2^{-\frac{1}{2}}\{(k_1/\mu_1+k_3/m)\pm[(k_1/\mu_1-k_3/m)^2+4k_2^2/\mu_1 m]^{\frac{1}{2}}\}^{\frac{1}{2}},$$
$$\left.\begin{matrix}\omega_2\\ \omega_4\end{matrix}\right\}=2^{-\frac{1}{2}}\{(n_1/\mu_2+n_3/m)\pm[(n_1/\mu_2-n_3/m)^2+4n_2^2/\mu_2 m]^{\frac{1}{2}}\}^{\frac{1}{2}}. \tag{8}$$

If the normal coordinates associated with frequencies ω_i are denoted by S_1, Q_2, R_2, etc. then the transformations from the intermediate symmetry coordinates to the normal coordinates have the forms,

$$\begin{aligned} x&=\mu_2^{-\frac{1}{2}}(\gamma Q_2+\delta Q_4); \quad \xi=m^{-\frac{1}{2}}(-\delta Q_2+\gamma Q_4)\\ y&=\mu_2^{-\frac{1}{2}}(\gamma R_2+\delta R_4); \quad \eta=m^{-\frac{1}{2}}(-\delta R_2+\gamma R_4)\\ z&=\mu_1^{-\frac{1}{2}}(\alpha S_1+\beta S_3); \quad \zeta=m^{-\frac{1}{2}}(-\beta S_1+\alpha S_3), \end{aligned} \tag{9}$$

where

$$\left.\begin{matrix}\alpha\\ \beta\end{matrix}\right\}=\pm 2^{-\frac{1}{2}}\{1\pm[(k_1/\mu_1-k_3/m)^2/(4k_2^2/\mu_1 m+(k_1/\mu_1-k_3/m)^2)]^{\frac{1}{2}}\}^{\frac{1}{2}}$$
$$\left.\begin{matrix}\gamma\\ \delta\end{matrix}\right\}=\pm 2^{-\frac{1}{2}}\{1\pm[(n_1/\mu_2-n_3/m)^2/(4n_2^2/\mu_2 m+(n_1/\mu_2-n_3/m)^2)]^{\frac{1}{2}}\}^{\frac{1}{2}}. \tag{10}$$

In terms of the normal coordinates the quantities T_v and U_0 are

$$\begin{aligned} T_v&=(1/2)[\dot{S}_1^2+\dot{Q}_2^2+\dot{R}_2^2+\dot{S}_3^2+\dot{Q}_4^2+\dot{R}_4^2]\\ U_0&=(1/2)[\lambda_1 S_1^2+\lambda_2(Q_2^2+R_2^2)+\lambda_3 S_3^2+\lambda_4(Q_4^2+R_4^2)] \end{aligned} \tag{11}$$

or in the Hamiltonian form T_v becomes

$$T_v=(1/2)[p_{S_1}^2+p_{Q_2}^2+p_{R_2}^2+p_{S_3}^2+p_{Q_4}^2+p_{R_4}^2],$$

where $p_{S_1}=\partial T/\partial\dot{S}_1$ is the vibrational momentum conjugate to S_1, etc. It will be convenient at a later point in the discussion to introduce dimensionless coordinates s_1, q_2, r_2, etc., by the transforma-

[12] J. Rosenthal and G. M. Murphy, Rev. Mod. Phys. **8**, 317 (1936).
[13] G. B. B. M. Sutherland, *Infra-red and Raman Spectra* (Methuen, 1935).
[14] Ta-You Wu, *Vibrational Spectra and Structure of Polyatomic Molecules* (Prentice-Hall, 1941).

tions $S_1=(h/\omega_1)^{\frac{1}{2}}s_1$, $Q_2=(h/\omega_2)^{\frac{1}{2}}q_2$, etc., so that $H_v=T_v+U_0$ becomes

$$T_v+U_0=(hc/2)\{\sum_{i=1,3}\nu_i((p_{s_i}^2/h^2)+s_i^2)+\sum_{k=2,4}\nu_k((p_{q_k}^2+p_{r_k}^2)/h^2+q_k^2+r_k^2)\}. \quad (12)$$

The anharmonic portion of the potential energy contains the following cubic and quartic terms consistent with the symmetry of the molecular configuration:

$$U_1=hc\{\sum_{i=1,3}\beta_{iii}s_i^3+\sum_{i=1,3}\sum_{k=2,4}\beta_{ikk}s_i(q_k^2+r_k^2)+\beta_{133}s_1s_3^2+\beta_{311}s_3s_1^2\}, \quad (13)$$

$$U_2=hc\{\sum_{i=1,3}\gamma_{iiii}s_i^4+\sum_{k=2,3}\gamma_{kkkk}(q_k^2+r_k^2)^2+\sum_{i=1,3}\sum_{k=2,4}\gamma_{iikk}s_i^2(q_k^2+r_k^2)+\sum_{k=2,4}\gamma_{13kk}s_1s_3(q_k^2+r_k^2)$$
$$+\gamma_{1133}s_1^2s_3^2+\gamma_{1333}s_1s_3^2+\gamma_{1113}s_1^3s_3+\gamma_{2244}(q_2^2+r_2^2)(q_4^2+r_4^2)\}, \quad (14)$$

in which the coefficients β_{iii}, γ_{iiii}, etc., have the dimension cm^{-1}.

III. Internal Angular Momentum

The components p_x, p_y, p_z of internal angular momentum of vibration are of importance in connection with the Coriolis interaction between the total angular momentum and the internal angular momentum. These components are defined as

$$p_x=\sum m_i(y_i'\dot{z}_i'-z_i'\dot{y}_i'), \quad p_y=\sum m_i(z_i'\dot{x}_i'-x_i'\dot{z}_i') \quad \text{and} \quad p_z=\sum m_i(x_i'\dot{y}_i'-y_i'\dot{x}_i')$$

and are expressed in terms of the dimensionless coordinates as follows:

$$p_x=\xi_{24}[(\nu_2/\nu_4)^{\frac{1}{2}}(r_4p_{q_2}+q_4p_{r_2})-(\nu_4/\nu_2)^{\frac{1}{2}}(q_2p_{r_4}+r_2p_{q_4})]+\sum_{i=1,3}\sum_{k=2,4}\xi_{ik}[(\nu_i/\nu_k)^{\frac{1}{2}}r_kp_{si}-(\nu_k/\nu_i)^{\frac{1}{2}}s_ip_{r_k}]$$
$$p_y=\xi_{24}[(\nu_2/\nu_4)^{\frac{1}{2}}(q_4p_{q_2}-r_4p_{r_2})-(\nu_4/\nu_2)^{\frac{1}{2}}(q_2p_{q_4}-r_2p_{r_4})]-\sum_{i=1,3}\sum_{k=2,4}\xi_{ik}[(\nu_i/\nu_k)^{\frac{1}{2}}q_kp_{si}-(\nu_k/\nu_i)^{\frac{1}{2}}s_ip_{q_k}] \quad (15)$$
$$p_z=\zeta_2(q_2p_{r_2}-r_2p_{q_2})+\zeta_4(q_4p_{r_4}-r_4p_{q_4})+\zeta_{24}[(\nu_2/\nu_4)^{\frac{1}{2}}(q_4p_{r_2}-r_4p_{q_2})-(\nu_4/\nu_2)^{\frac{1}{2}}(r_2p_{q_4}-q_2p_{r_4})],$$

in which the Teller parameters are the following:

$$\zeta_2=\gamma^2(I_{0z}/2I_{0x})-\delta^2; \quad \zeta_4=\delta^2(I_{0z}/2I_{0x})-\gamma^2; \quad \zeta_{24}=\gamma\delta(1+I_{0z}/2I_{0x})=[\zeta_2\zeta_4+(I_{0z}/2I_{0x})]^{\frac{1}{2}}$$
$$\xi_{24}=2^{-\frac{1}{2}}b; \quad \xi_{12}=\gamma[\alpha(1-b^2)^{\frac{1}{2}}+2^{-\frac{1}{2}}\beta b]; \quad \xi_{14}=\delta[\alpha(1-b^2)^{\frac{1}{2}}+2^{-\frac{1}{2}}\beta b]; \quad \xi_{32}=\gamma[\beta(1-b^2)^{\frac{1}{2}}-2^{-\frac{1}{2}}\alpha b]; \quad (16)$$
$$\xi_{34}=\delta[\beta(1-b^2)^{\frac{1}{2}}-2^{-\frac{1}{2}}\alpha b], \quad \text{where} \quad 1-b^2=(I_{0z}/2I_{0x})=(\mu_1/\mu_2).$$

The above parameters satisfy the following simple relations:

$$\zeta_2+\zeta_4=(I_{0z}/2I_{0x})-1=-b^2; \quad \zeta_2^2+\zeta_4^2+\zeta_{24}^2=1+(I_{0z}/2I_{0x})^2;$$

$$\xi_{12}\xi_{14}+\xi_{32}\xi_{34}=\gamma\delta(1-b^2/2); \quad \xi_{12}^2+\xi_{14}^2+\xi_{32}^2+\xi_{34}^2=1-b^2/2; \quad \xi_{12}^2+\xi_{14}^2+\xi_{32}^2+\xi_{34}^2+\xi_{24}^2=1.$$

The parameters ζ_2 and ζ_4 are associated with the vibrational angular momentum about the symmetry axis arising separately from the twofold degenerate oscillations ν_2 and ν_4; it is these particular components which give rise to the type of Coriolis interaction to which most attention has been turned and which causes the rotational spacings to vary from band to band in symmetrical molecules. The other parameters ζ_{24}, ξ_{24}, ξ_{12}, etc., are associated with components of internal angular momentum arising from mixing of two different modes of oscillation, which may or may not belong to the same symmetry class as has been shown by Jahn[15] from the standpoint of group theory; these components

[15] H. A. Jahn, Phys. Rev. **56**, 680 (1939).

give rise to a type of Coriolis interaction which may cause the rotational spacings to converge or diverge away from the center of a vibration-rotation band as has been observed by Jahn and Childs[16] in the ν_4 band of CH_4, or, in cases where the two vibrational frequencies are very close together, the rotational fine structure may be greatly distorted, as has been shown by Nielsen[17] and applied to the case of bands ν_5 and ν_6 of H_2CO which were investigated by Ebers and Nielsen.[18] The calculation of the effect of this latter type of Coriolis interaction on the energies and band pattern is quite laborious and has been done for only a few special cases; it has been found possible to perform such a calculation in general for the axial model XY_3. The actual effects of the Coriolis interaction on the energies are discussed in Section V.

IV. The Quantum-Mechanical Hamiltonian

The appropriate quantum-mechanical Hamiltonian has been derived by the method of Wilson and Howard[11] and the details of the procedure are similar to those employed in papers on bent XY_2 molecules by Shaffer and Nielsen[19] (SN) and on XY_4 molecules by Shaffer, Nielsen and Thomas[20] (SNT). The form of the Hamiltonian given by Howard and Wilson[5] is

$$H=\tfrac{1}{2}\sum_{\alpha,\beta}\mu^{\frac{1}{2}}(P_\alpha-p_\alpha)\mu_{\alpha\beta}\mu^{-\frac{1}{2}}(P_\beta-p_\beta)+(1/2)\mu^{\frac{1}{2}}\sum_k p_k\mu^{-\frac{1}{2}}p_k+U_0+U_1+U_2+, \tag{17}$$

where the subscripts α and β refer to x, y, or z; the quantities $\mu_{\alpha\beta}$ are functions of the normal coordinates, which are related to the instantaneous moments and products of inertia; μ is the determinant of the $\mu_{\alpha\beta}$; the P_α are components of total angular momentum; the p_α are the components of internal angular momentum defined in (15); the p_k are the vibrational momenta conjugate to the normal coordinates; and the quantities U_0, U_1, U_2 are the zeroth-, first- and second-order parts of the potential energy and have been defined in Eqs. (13) and (14). For our purposes the expansions of the quantities $\mu_{\alpha\beta}$ and μ are broken off with terms quadratic in the vibrational coordinates. The Hamiltonian H is divided into its zeroth-, first- and second-order parts as $H=H_0+H_1+H_2$ where

$$H_0=(hc/2)\{\sum_{i=1,3}\nu_i(p_{si}^2/h^2+s_i^2)+\sum_{k=2,4}\nu_k(p_{qk}^2/h^2+p_{rk}^2/h^2+q_k^2+r_k^2)\}+(1/2)\{(P_x^2+P_y^2)/I_{0x}+(P_z^2/I_{0z})\} \tag{18}$$

with corresponding zeroth-order wave functions

$$\psi_0=\psi(V_1)\psi(V_2,l_2)\psi(V_3)\psi(V_4,l_4)R(J,K,M), \tag{19}$$

in which $\psi(V_i)$ stands for the normalized linear harmonic oscillator wave function

$$\psi(V_i)=N_{V_i}\quad\exp(-s_i^2/2)\quad H_{V_i}(s_i),$$

if $H_{V_i}(s_i)$ is the Hermitian polynomial; $\psi(V_k,l_k)$ stands for the wave function of the two-dimensional isotropic harmonic oscillator and is conveniently expressed in terms of ρ_k and ϕ_k, defined by $q_k=\rho_k\cos\phi_k$, $r_k=\rho_k\sin\phi_k$, so that

$$\psi(V_k,l_k)=N(V_k,l_k)\exp(\pm il_k\phi_k)\exp(-\rho_k^2/2)\rho_k^{l_k}L_{\sigma k}^{l_k}(\rho_k^2)$$

where $\sigma_k=(V_k+l_k)/2$, l_k may assume values $l_k=V_k$, V_k-2, $V_k-4\cdots0$ or 1, and $L_{\sigma k}^{l_k}(\rho_k^2)$ is the associated Laguerre polynomial; $R(J,K,M)$ is the symmetrical top wave function. The zeroth-order energy E_0 is given by

$$(E_0/hc)=\sum_{n=1}^{4}\nu_n(V_n+d_n/2)+B_eJ(J+1)+(C_e-B_e)K^2, \tag{20}$$

---

[16] H. A. Jahn and W. J. Childs, Proc. Roy. Soc. **A168**, 469 (1938); *ibid.* **A169**, 451 (1939); *ibid.* **A171**, 450 (1939).
[17] H. H. Nielsen, J. Chem. Phys. **5**, 818 (1937).
[18] E. S. Ebers and H. H. Nielsen, J. Chem. Phys. **5**, 822 (1937).
[19] W. H. Shaffer and H. H. Nielsen Phys. Rev. **56**, 188 (1939).
[20] W. H. Shaffer, H. H. Nielsen and L. H. Thomas, Phys. Rev. **56**, 895 (1939).

where d_n=degree of degeneracy of the frequency ν_n ($d_1=d_3=1$; $d_2=d_4=2$), where the rotational constants are defined for the equilibrium configuration as

$$B_e=(h/8\pi^2cI_{0x}),\quad C_e=(h/8\pi^2cI_{0z}).$$

The calculation of the contributions of the higher order parts of H requires for this case the use of degenerate perturbation theory and is very complicated if carried out in a straightforward manner. This calculation is shortened by the use of a contact transformation of H according to the procedure described by SNT. In this method a transformation function $T=e^{i\lambda S}$ is defined so that the transformed Hamiltonian H' is given by $H'=THT^{-1}=H_0'+H_1'+H_2'$ where $H_0'\equiv H_0$, $H_1'=H_1-i(H_0S-SH_0)$ and $H_2'=H_2+(i/2)[S(H_1+H_1')-(H_1+H_1')S]$. The function S is determined in such a way that as many terms as possible are eliminated from H_1', in this way the perturbation calculation is much simplified as pointed out by SNT. The details of this contact transformation are too lengthy to be included here and only the results are stated. Since $H_0'\equiv H_0$, the zeroth-order wave functions are the same as the ψ_0 defined in (19) and the zeroth-order energy E_0' is the same as E_0 defined in (20).

It can be shown that H_1' reduces to

$$H_1'=-(1/I_{0z})(\zeta_2p_{\phi_2}+\zeta_4p_{\phi_4})P_z, \tag{21}$$

where $p_{\phi 2}=-ih\partial/\partial\phi_2$, $p_{\phi 4}=-ih\partial/\partial\phi_4$. Now the only non-vanishing matrix elements of P_z and $p_{\phi k}$ are diagonal in all the quantum numbers, *viz.*, $(JKM|P_z|JKM)=Kh$ and $(V_k,\ \pm l_k|p_{\phi k}|V_k,\ \pm l_k)=\pm l_kh$, hence the eigenvalues, E_1' of H_1' are given by the equation

$$(E_1'/hc)=(2C_e)(\mp\rho_2l_2\mp\rho_4l_4)K. \tag{22}$$

It is to be noted that H_1' contains only the Coriolis interaction terms arising from the doubly degenerate modes of oscillations and that the vibrational degeneracy in $\pm l_k$ is removed by it. Furthermore, since H_1' has no non-vanishing off-diagonal matrix elements, the eigenfunctions, Ψ_0 of E_0 defined in (19) are also the eigenfunctions corresponding to $E_0'+E_1'$ and can be used as the basis for a perturbation calculation of the contribution of H_2' to the energy.

The second-order portion of H' contains the following terms;

$$\begin{aligned}
H_2'=&(h^2/8)(-5/I_{0x}+3I_{0z}/2I_{0x}^2+3/I_{0z})-(3\zeta_{24}^2h^2/2I_{0z})+(1/2I_{0x})(P_x^2+P_y^2)(\sum_{i=1,3}K_{ii}s_i^2\\
&+\sum_{k=2,4}K_{kk}\rho_k^2)+(1/2I_{0z})P_z^2(\sum_{i=1,3}N_{ii}s_i^2+\sum_{k=2,4}N_{kk}\rho_k^2)+(1/2I_{0x})\sum_{k=2,4}M_{kk}(r_k^2P_x^2+q_k^2P_y^2)\\
&+(b^2/4I_{0x})\{(\nu_2/\nu_4)(p_{q_2}^2+p_{r_2}^2)\rho_4^2+(p_{q_4}^2+p_{r_4}^2)\rho_2^2(\nu_4/\nu_2)\}+(1/2I_{0x})\sum_{i=1,3}\sum_{k=2,4}\xi_{ik}^2\{(\nu_i/\nu_k)\rho_k^2p_{s_i}^2\\
&+(\nu_k/\nu_i)s_i^2(p_{r_k}^2+p_{q_k}^2)\}+(1/2I_{0z})\{-h^2(\zeta_2^2+\zeta_4^2)+(\zeta_2p_{\phi 2}+\zeta_4p_{\phi 4})^2+\zeta_{24}^2[(\nu_2/\nu_4)(q_4^2p_{r_2}^2+r_4^2p_{q_2}^2)\\
&+(\nu_4/\nu_2)(r_2^2p_{q_4}^2+q_2^2p_{r_4}^2)]\}-(hc/h^4)\{\tau_{xxxx}(P_x^4+P_y^4)+\tau_{zzzz}P_z^4+\tau_{xyxy}(P_xP_y+P_yP_x)^2\\
&+\tau_{xxyy}(P_x^2P_y^2+P_y^2P_x^2)+\tau_{xzzz}[(P_xP_z+P_zP_x)^2+(P_yP_z+P_zP_y)^2]\\
&+\tau_{yyzz}[(P_y^2-P_x^2)(P_xP_z+P_zP_x)+(P_xP_z+P_zP_x)(P_y^2-P_x^2)]+\tau_{xzzz}[(P_x^2+P_y^2)P_z^2\\
&+P_z^2(P_x^2+P_y^2)]+\tau_{xyzz}[(P_xP_y+P_yP_x)(P_xP_z+P_zP_x)+(P_xP_z+P_zP_x)(P_xP_y+P_yP_x)]\}\\
&-hc\{\sum_{i=1,3}(\beta_{iii}^2/\nu_i)[1+(3/2)s_i^4+3(s_i^2p_{s_i}^2)/h^2]+3\sum_{i=1,3}\sum_{k=2,4}(\beta_{iik}\beta_{ikk}/\nu_i)s_i^2\rho_k^2+3(\beta_{111}\beta_{133}/\nu_1
\end{aligned}$$

$$+\beta_{333}\beta_{311}/\nu_3)s_1^2s_3^2+\sum_{i=1,3}(\beta_{i22}\beta_{i44}/\nu_i)\rho_2^2\rho_4^2+\sum_{k=2,4}(\beta_{133}\beta_{3kk}s_1^2/\nu_1+\beta_{311}\beta_{3kk}s_3^2/\nu_3)\rho_k^2$$

$$+\sum_{ij=13,31}\beta_{ijj}^2[(2\nu_j^2-\nu_i^2)s_j^4+4\nu_i\nu_j s_i^2s_j^2+2\nu_j^2s_j^2p_{s_j}^2/\hbar^2]/2\nu_i(4\nu_j^2-\nu_i^2)+\sum_{i=1,3}\sum_{k=2,4}\beta_{ikk}^2[(2\nu_k^2-\nu_i^2)\rho_k^4$$

$$+4\nu_i\nu_k\rho_k^2s_i^2+(2\nu_k^2/\hbar^2)((p_{r_k}^2+p_{q_k}^2)\rho_k^2+\rho_k^2(p_{r_k}^2+p_{q_k}^2)]/2\nu_i(4\nu_k^2-\nu_i^2)\}+U_2, \quad (23)$$

where

$$K_{11}=(h/\omega_1I_{0x})\{(3/2)(\alpha^2+1)+\sum_{k=2,4}(4\nu_k^2\xi_{1k}^2/(\nu_1^2-\nu_k^2))\}+(2\pi ch^{\frac{1}{2}})\{3a_1\beta_{111}/\omega_1^{3/2}+a_3\beta_{311}/\omega_3^{3/2}\}$$

$$K_{33}=(h/\omega_3I_{0x})\{(3/2)(\beta^2+1)+\sum_{k=2,4}(4\nu_k^2\xi_{3k}^2/(\nu_3^2-\nu_k^2))\}+(2\pi ch^{\frac{1}{2}})\{3a_3\beta_{333}/\omega_3^{3/2}+a_1\beta_{133}/\omega_1^{3/2}\}$$

$$K_{22}=(3h/2\omega_2I_{0x})\{\gamma^2+1-\gamma^2(2\mu_1/\mu_2)+(4b^2\nu_4^2/3(\nu_2^2-\nu_4^2))\}+(2\pi ch^{\frac{1}{2}})\{a_1\beta_{122}/\omega_1^{3/2}+a_3\beta_{322}/\omega_3^{3/2}\}$$

$$K_{44}=(3h/2\omega_4I_{0x})\{\delta^2+1-\delta^2(2\mu_1/\mu_2)+(4b^2\nu_2^2/3(\nu_4^2-\nu_2^2))\}+(2\pi ch^{\frac{1}{2}})\{a_1\beta_{144}/\omega_1^{3/2}+a_3\beta_{344}/\omega_3^{3/2}\}$$

$$M_{22}=(h/\omega_2I_{0x})\{(3\gamma^2\mu_1/\mu_2)+4\sum_{i=1,3}(\nu_i^2\xi_{i2}^2/(\nu_2^2-\nu_i^2))\}$$

$$M_{44}=(h/\omega_4I_{0x})\{(3\delta^2\mu_1/\mu_2)+4\sum_{i=1,3}(\nu_i^2\xi_{i4}^2/(\nu_4^2-\nu_i^2))\}$$

$$N_{11}=(3\beta^2h/\omega_1I_{0z})+(2\pi ch^{\frac{1}{2}})(3c_1\beta_{111}/\omega_1^{3/2}+c_3\beta_{311}/\omega_3^{\frac{1}{2}})$$

$$N_{33}=(3\alpha^2h/\omega_3I_{0z})+(2\pi ch^{\frac{1}{2}})(3c_3\beta_{333}/\omega_3^{3/2}+c_1\beta_{133}/\omega_1^{3/2})$$

$$N_{22}=(3\gamma^2h/2\omega_2I_{0x})b^2+(h/\omega_2I_{0z})\{6\gamma^2\delta^2(1+\mu_1/\mu_2)^2+(8\nu_4^2\zeta_{24}^2/(\nu_2^2-\nu_4^2))\}$$
$$+(2\pi ch^{\frac{1}{2}})(c_1\beta_{122}/\omega_1^{3/2}+c_3\beta_{322}/\omega_3^{3/2})$$

$$N_{44}=(3\delta^2h/2\omega_4I_{0x})b^2+(h/\omega_4I_{0z})\{6\gamma^2\delta^2(1+\mu_1/\mu_2)^2+(8\nu_2^2\zeta_{24}^2/(\nu_4^2-\nu_2^2))\}$$
$$+(2\pi ch^{\frac{1}{2}})(c_1\beta_{144}/\omega_1^{3/2}+c_3\beta_{344}/\omega_3^{3/2}),$$

in which

$$a_1=(2\alpha bI_{0x}^{\frac{1}{2}}-\beta I_{0z}^{\frac{1}{2}})I_{0x}^{-1};\quad c_1=-2\beta I_{0z}^{-\frac{1}{2}},$$

$$a_3=(2\beta bI_{0x}^{\frac{1}{2}}+\alpha I_{0z}^{\frac{1}{2}})I_{0x}^{-1};\quad c_3=+2\alpha I_{0z}^{-\frac{1}{2}}.$$

and where

$$\tau_{xxxx}=B_e^3\{4b^2(\alpha^2/\nu_1^2+\beta^2/\nu_3^2)+(2\mu_1/\mu_2)(\beta^2/\nu_1^2+\delta^2/\nu_2^2+\alpha^2/\nu_3^2+\gamma^2/\nu_4^2)+4\alpha\beta b(2\mu_1/\mu_2)^{\frac{1}{2}}(1/\nu_3^2-1/\nu_1^2)\}$$

$$\tau_{zzzz}=4C_e^3(\beta^2/\nu_1^2+\alpha^2/\nu_3^2)$$

$$\tau_{xyxy}=B_e^3\{4b^2(\alpha^2/\nu_1^2+\beta^2/\nu_3^2)+4\alpha\beta b(2\mu_1/\mu_2)^{\frac{1}{2}}(1/\nu_3^2-1/\nu_1^2)+(2\mu_1/\mu_2)(\beta^2/\nu_1^2+\alpha^2/\nu_3^2)\}$$

$$\tau_{xxyy}=\tau_{xxxx}-2\tau_{xyxy}$$

$$\tau_{xzxz}=2B_e^2C_eb^2(\gamma^2/\nu_2^2+\delta^2/\nu_4^2)$$

$$\tau_{yyxz}=\tau_{xyxz}=B_e^3(2)^{\frac{1}{2}}\gamma\delta b(1/\nu_4^2-1/\nu_2^2)$$

$$\tau_{xzzz}=B_e^2C_e\{(2\mu_1/\mu_2)^{\frac{1}{2}}4\alpha\beta b(1/\nu_3^2-1/\nu_1^2)+2(\beta^2/\nu_1^2+\alpha^2/\nu_3^2)\}.$$

V. The Energy Expression

The eigenvalues, E_0' and E_1', of H_0' and H_1' have already been given in (20) and (22). There remains the determination of the eigenvalues of H_2' which was defined in (23). This determination is effected by a perturbation calculation similar to that performed by SN for the XY_2 model. When this procedure is carried out and the contributions E_0', E_1', and E_2' are added together it is found that the total rotation-vibration energy, E, can be written in the simple form

$$E=hc\{G_{\text{vib}}+F_{\text{rot}}-2C_e(\pm l_2\zeta_2\pm l_4\zeta_4)K\}. \tag{24}$$

The quantities G_{vib} and F_{rot} are the vibrational and rotational term values, respectively, expressed in cm^{-1} and have the following values:

$$G_{\text{vib}}=G_0+\sum_{n=1}^{4}\nu_n(V_n+d_n/2)+\sum_{n=1}^{4}G_{nn}(V_n+d_n/2)^2+\sum_{m<n}G_{mn}(V_m+d_m/2)(V_n+d_n/2)$$
$$+g_{22}(l_2^2-1)+g_{44}(l_4^2-1)+g_{24}l_2l_4, \tag{25}$$

$$F_{\text{rot}}=B_vJ(J+1)+(C_v-B_v)K^2-D_JJ^2(J+1)^2-D_{JK}J(J+1)K^2-D_KK^4, \tag{26}$$

in which the rotational constants, B_v and C_v, effective in the various vibrational states have the forms,

$$B_v=B_e\{1-\alpha_0+\sum_{n=1}^{4}\alpha_n(V_n+d_n/2)\}, \tag{27}$$

$$C_v=C_e\{1-\beta_0+\sum_{n=1}^{4}\beta_n(V_n+d_n/2)\}, \tag{28}$$

and where

$$G_0=-(7/16)(\beta_{111}^2/\nu_1+\beta_{333}^2/\nu_3)-(3/16)[\nu_1\beta_{133}^2/(4\nu_3^2-\nu_1^2)+\nu_3\beta_{311}^2/(4\nu_1^2-\nu_3^2)]+(3/8)(\gamma_{1111}+\gamma_{3333})$$
$$+(1/4)(-5B_e+3C_e/2B_e^2+3C_e)-(3\zeta_{24}^2C_e)$$

$$G_{11}=(3/2)\gamma_{1111}-(15\beta_{111}^2/4\nu_1)-[(8\nu_1^2-3\nu_3^2)\beta_{311}^2/4\nu_3(4\nu_1^2-\nu_3^2)]$$

$$G_{33}=(3/2)\gamma_{3333}-(15\beta_{333}^2/4\nu_3)-[(8\nu_3^2-3\nu_1^2)\beta_{133}^2/4\nu_1(4\nu_3^2-\nu_1^2)]$$

$$G_{22}=(3/2)\gamma_{2222}-\sum_{i=1,3}[(8\nu_2^2-3\nu_i^2)\beta_{i22}^2/4\nu_i(4\nu_2^2-\nu_i^2)]$$

$$G_{44}=(3/2)\gamma_{4444}-\sum_{i=1,3}[(8\nu_4^2-3\nu_i^2)\beta_{i44}^2/4\nu_i(4\nu_4^2-\nu_i^2)]$$

$$G_{12}=\gamma_{1122}-(3\beta_{111}\beta_{122}/\nu_1)-(\beta_{311}\beta_{322}/\nu_3)-[2\nu_2\beta_{122}^2/(4\nu_2^2-\nu_1^2)]+[\xi_{12}^2B_e(\nu_1^2+\nu_2^2)/\nu_1\nu_2]$$

$$G_{14}=\gamma_{1144}-(3\beta_{111}\beta_{144}/\nu_1)-(\beta_{311}\beta_{344}/\nu_3)-[2\nu_4\beta_{144}^2/(4\nu_4^2-\nu_1^2)]+[\xi_{14}^2B_e(\nu_1^2+\nu_4^2)/\nu_1\nu_4]$$

$$G_{32}=\gamma_{3322}-(3\beta_{333}\beta_{322}/\nu_3)-(\beta_{133}\beta_{122}/\nu_1)-[2\nu_2\beta_{322}^2/(4\nu_2^2-\nu_3^2)]+[\xi_{32}^2B_e(\nu_3^2+\nu_2^2)/\nu_2\nu_3]$$

$$G_{34}=\gamma_{3344}-(3\beta_{333}\beta_{344}/\nu_3)-(\beta_{133}\beta_{144}/\nu_1)-[2\nu_4\beta_{344}^2/(4\nu_4^2-\nu_3^2)]+[\xi_{34}^2B_e(\nu_3^2+\nu_4^2)/\nu_3\nu_4]$$

$$G_{13}=\gamma_{1133}-(3\beta_{111}\beta_{133}/\nu_1)-(3\beta_{333}\beta_{311}/\nu_3)-[2\nu_3\beta_{133}^2/(4\nu_3^2-\nu_1^2)]-[2\nu_1\beta_{311}^2/(4\nu_1^2-\nu_3^2)]$$

$$G_{24}=\gamma_{2244}-(\beta_{122}\beta_{144}/\nu_1)-(\beta_{322}\beta_{344}/\nu_3)+[\zeta_{24}^2C_e+\xi_{24}^2B_e][(\nu_2^2+\nu_4^2)/\nu_2\nu_4]$$

$$g_{22}=-(1/2)\gamma_{2222}-[\nu_1\beta_{122}^2/4(4\nu_2^2-\nu_1^2)]-[\nu_3\beta_{322}^2/4(4\nu_2^2-\nu_3^2)]+\zeta_2^2C_e$$

$$g_{44}=-(1/2)\gamma_{4444}-[\nu_1\beta_{144}^2/4(4\nu_4^2-\nu_1^2)]-[\nu_3\beta_{344}^2/4(4\nu_4^2-\nu_3^2)]+\zeta_4^2C_e$$

$$g_{24}=2\zeta_2\zeta_4C_e;\quad B_e=(h/8\pi^2cI_{0x});\quad C_e=(h/8\pi^2cI_{0z})$$

$$D_J=(3/4)\tau_{xxxx}+(1/2)\tau_{xyxy}+(1/4)\tau_{xxyy}$$

$$D_{JK}=-(3/2)\tau_{xxxx}-\tau_{xyxy}-(1/2)\tau_{xxyy}+4\tau_{xxxz}+2\tau_{xxzz}$$

$$D_K=-D_J-D_{JK}+\tau_{zzzz}$$

$$\alpha_0=(1/2B_e)[\tau_{xxyy}+2\tau_{xxzz}-\tau_{xxxx}-2\tau_{xyxy}]$$

$$\beta_0=(1/4C_e)[-3\tau_{xxyy}-16\tau_{xxxz}+3\tau_{xxxx}+6\tau_{xyxy}]$$

$$\alpha_1=K_{11};\quad \alpha_3=K_{33};\quad \alpha_2=K_{22}+(M_{22}/2);\quad \alpha_4=K_{44}+(M_{44}/2)$$

$$\beta_1=N_{11};\quad \beta_3=N_{33};\quad \beta_2=N_{22};\quad \beta_4=N_{44}.$$

A few facts relative to the rotational term value F_{rot} of (26) should be pointed out. One can easily show the vanishing of all matrix elements of H_2' which are not diagonal in the rotational quantum members J, K and M; this is true both for the terms of H_2' which are quadratic in the angular momentum operators and for the centrifugal expansion terms which are quartic in those operators. This settles definitely the question raised by Dennison and Slawsky[9] regarding the approximation involved in neglecting such non-diagonal elements in their calculation of the centrifugal expansion contributions to the energy. This means that, to the order of approximation considered here, the rotational part of the energy of the axially symmetrical pyramidal XY_3 model retains essentially its symmetrical top form with the equilibrium values of the rotational constants, B_e and C_e, replaced by values, B_v and C_v, effective in the various vibrational states and with the addition of the terms quartic in J and K which arise from the centrifugal stretching. The quantities $-\alpha_0B_e$ and $-\beta_0C_e$ in the definitions of B_v and C_v in (27) and (28) represent small corrections to the equilibrium values of B_e and C_e which arise from centrifugal stretching. The parameters D_J, D_{JK} and D_K which occur in (26) are, to the order of approximation considered, constants independent of the vibrational quantum members. One might ask whether there is a relation for this model between the moments of inertia effective in the various vibrational states similar to the one pointed out by Darling and Dennison[21] for the bent XY_2 model. The analogous relation here would be $\Delta=I_{vz}-2I_{vx}$, where $I_{vz}=(h/8\pi^2cC_v)$ and $I_{vx}=(h/8\pi^2cB_v)$; an examination of the expressions for B_v and C_v reveals that Δ is not simple but is a rather complicated function of the anharmonic constants. However, for the case of the planar XY_3 model, as pointed out by Silver and Shaffer,[22] the corresponding Δ is independent of the anharmonic constants. This is to be expected since $I_{0z}-2I_{0x}=0$ for the planar model but $I_{0z}-2I_{0x}\neq 0$ for the pyramidal model.

In conclusion the writer wishes to express his appreciation to the National Research Council Fellowships Board for the fellowship which made possible the carrying out of this work. He also wishes to thank Professor R. S. Mulliken of Ryerson Laboratory for many helpful suggestions during the course of this work.

[21] B. T. Darling and D. M. Dennison, Phys. Rev. **57**, 128 (1940).
[22] S. Silver and W. H. Shaffer, J. Chem. Phys. **9**, 599 (1941).

The Photolysis of Acetone in Presence of Mercury[1]

KENNETH W. SAUNDERS AND H. AUSTIN TAYLOR
Department of Chemistry, New York University, New York, New York

(Received May 21, 1941)

The photolysis of acetone in the region 2600–2900A has been studied at temperatures from 100–275°C, alone, in presence of liquid mercury, mercury vapor and mercury dimethyl. From a comparison of the products formed in each case and the effect of temperature thereon a mechanism is suggested which indicates that mercury methyl, if not mercury dimethyl, is formed by reaction between methyl radicals and mercury atoms suggesting a greater stability of the mercury methyl radical than hitherto believed.

DESPITE the rapidly increasing amount of data being accumulated on the reactions between organic radicals and metals by the mirror method, relatively little is known concerning the reactions in the vapor phase. Leighton and Mortensen[2] reporting on a quantum yield for the photolysis of lead tetramethyl of 1.11 decreasing to unity in presence of oxygen conclude that the observed yield may represent a balance between a considerable chain length and a considerable recombination. A somewhat similar reduction of quantum yield was observed by Linnett and Thompson[3] for mercury dimethyl photolysis in presence of nitric oxide. The increased rate of decomposition of mercury dimethyl in presence of hydrogen was accounted for by Cunningham and Taylor[4] on the basis of a chain reaction involving hydrogen atoms formed by reaction between methyl radicals and hydrogen. Taylor[5] and Burton drew attention to the neglect of a consideration of any recombination between mercury and methyl radicals and indicated on this basis a possible alternative explanation. The observation by Heidt and Forbes[6] that the pyrolysis of azomethane was unaffected when 100 mm mercury vapor were intentionally introduced was not confirmed by analysis of the reaction products.

Since it is generally agreed that the photolysis of acetone proceeds through a primary step involving the production of methyl and acetyl radicals, if reaction can occur between methyl radicals and mercury atoms the products of acetone photolysis in presence and absence of mercury would be expected to be different. Furthermore, acetone photolysis in presence of mercury dimethyl would be expected to be similar to that of acetone and mercury. To simplify the interpretation of the results the radiation has been restricted to wave-lengths 2600–2900A since mercury dimethyl absorbs below 2600A while acetone gives its maximum radical concentration below 3000A. The temperatures used were restricted to the range 100–275°C since, above 100°, no diacetyl formation is observed in acetone while above 275°C mercury dimethyl pyrolysis becomes measurable.

EXPERIMENTAL

Materials

Acetone obtained from the sodium iodide complex compound was dried over calcium chloride and fractionally distilled. The middle fraction boiling at 55.8–56.0°C was further purified by distilling twice in vacuum from an ice-water mixture to dry-ice-toluene.

Mercury dimethyl was prepared by the method of Marvel and Gould[7] from mercuric chloride and Grignard reagent, dried over calcium chloride and fractionally distilled. A fraction boiling at 90.5–91.0°C was further distilled in vacuum from phosphorus pentoxide at room temperature and collected at dry-ice-toluene temperature.

[1] Abstract from a thesis presented in partial fulfillment of the requirements for the degree of Doctor of Philosophy at New York University, March, 1941.
[2] P. A. Leighton and R. A. Mortensen, J. Am. Chem. Soc. **58**, 448 (1936).
[3] J. W. Linnett and H. W. Thompson, Trans. Faraday Soc. **33**, 501, 874 (1937).
[4] J. P. Cunningham and H. S. Taylor, J. Chem. Phys. **6**, 359 (1938).
[5] H. A. Taylor and M. Burton, J. Chem. Phys. **7**, 675 (1939).
[6] L. J. Heidt and G. S. Forbes, J. Am. Chem. Soc. **57**, 2331 (1935).
[7] C. S. Marvel and V. L. Gould, J. Am. Chem. Soc. **44**, 153 (1922).

When not in use acetone and mercury dimethyl were protected from light and stored in dry ice.

Radiation

The light source was the General Electric Type H6 1000-watt, water-cooled, high pressure quartz mercury arc which emits relatively little resonance radiation. The lamp intensity varied considerably with use. Deposits of ferric oxide on the water cooler and quartz filter were removed daily. The quartz filter made according to the suggestion of Bowen[8] consisted of two compartments, the first 3 cm in depth contained chlorine at 1 atmos. pressure, the second, 1 cm in depth, through which an aqueous solution containing 45 g $HgCl_2$ per liter flowed continuously. The whole filter was water-cooled. Photographs of a low pressure mercury arc showed transmission by the filter from 2652 to 2967A.

Reaction system

A quartz reaction vessel of approximately 200-cc volume was connected by a graded seal to a Pyrex mercury manometer and to a Crist[9] valve, the latter eliminating contact between acetone and stopcock grease. In the experiments with acetone alone the reaction system was protected from mercury vapor by gold-leaf traps. The absence of change in the photolysis when these were removed eliminated the possibility of any mercury photo-sensitization having occurred, while at the same time showing that the low vapor pressure of mercury gave too small a concentration of mercury to show a measurable reaction with acetone decomposition products.

The reaction vessel was placed in an electric furnace carrying a two-inch aperture faced with a thin quartz plate at each end. The temperature was controlled manually and temperature gradients were minimized by having an air stirrer in the furnace. For the experiments with mercury present about 0.5 cc mercury was added to the reaction vessel. The mercury refluxed continuously into the vessel from the cooler connecting tube outside the furnace during the experiments. In the runs in presence of mercury vapor, the manometer was removed and the Crist valve replaced by a mercury U-tube cut-off filled from a reservoir below. The arm of the U connected to the reaction vessel was heated throughout its length with resistance wire and thermally insulated. A thermometer in the mercury in the U-tube indicated the temperature of the mercury and thus the partial pressure of mercury vapor in the reaction system. Particular care was taken during these latter runs to see that no liquid mercury could be present in the reaction vessel.

Procedure

The reaction cell was evacuated overnight before each run by a mercury vapor pump backed by an oil pump. Just prior to the run the cell was flushed out three times with acetone vapor and filled to a pressure of 90 mm. The Crist valve was then closed; the pressure on both sides of the valve being the same any leakage was minimized. Exposure to the arc was then made for the required period. At the conclusion of the run, the light was turned off, the pressure permitted to reach a steady value and the Crist valve was opened slightly to permit the gases to be drawn slowly through a trap in liquid nitrogen into a liter Toepler pump. From here the gas was pumped into the analyzer. To obtain complete fractionation it was sometimes necessary to remove the liquid nitrogen allowing the trap contents to melt and then refreeze and pump out residual noncondensible gas.

A second fraction containing residual methane and C_2 hydrocarbons was obtained by pumping the condensate in the trap cooled to $-131°C$ by melting sec-butyl chloride. As before the last fractions of the gas were recovered following vaporization and condensation. In a few tests a minute quantity of gas was obtained between $-131°$ and $-115°C$ and slightly above $-115°C$ acetone itself began to come through. Two fractions only were therefore collected and the volume of each was measured at low pressure in the gas analysis apparatus.

Micro gas analysis

Since, under the experimental conditions, an exposure of 30 minutes yielded seldom more than 0.6 cc gas for analysis a micro method

[8] E. J. Bowen, J. Chem. Soc. p. 76 (1935).
[9] R. H. Crist and F. B. Brown, Ind. Eng. Chem., Anal. Ed. 11, 396 (1939).

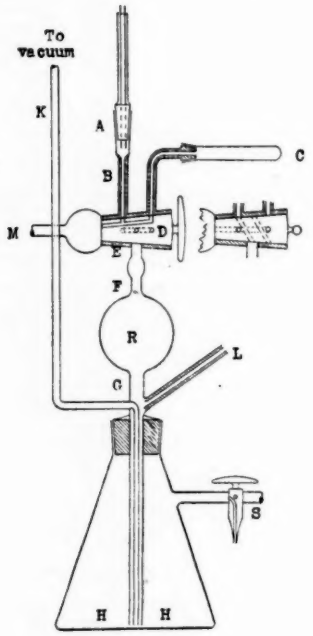

FIG. 1.

was essential. A technique was developed capable of analyzing for hydrogen, carbon monoxide, ethylene, methane and higher saturated hydrocarbons which was much less tedious than, yet at least as accurate as, the methods of Manning[10] and H. S. Taylor and his associates,[11] features from both of which were adopted. The method involved some modifications of that of Haden and Luttropp[12] and used a measurement of the pressure at constant volume, rather than the actual volume of the gas. Fig. 1 is a plan of the apparatus used.

A, the combustion chamber whose volume plus connecting capillary was 2.67 cc was equipped with a standard ground joint (size 14/29) carrying two tungsten lead-in wires 1 mm in diameter insulated in small glass tubing. A small platinum coil of six to eight turns was spot-welded to the tungsten electrodes. During operation the upper tube was filled with water and surrounding *A* was a water jacket (not shown) which prevented the trace of grease on the upper part of the joint from flowing.

B, this tube contained gold foil to prevent mercury vapor passing into *A*.

C, is a series of tubes to hold reagents for various tests carrying 7/15 interchangeable ground joints. The volume of one such tube plus the capillary tube was 2.83 cc.

D, is a stopcock designed so that both *A* and *C* may be evacuated simultaneously through *M* and that by proper manipulation either *A* or *C* may be connected to *R*. The volume of the capillary in *D* was 0.14 cc.

E, *F*, *G*, permanent markings. The volume from *E* to *D* was 0.48 cc, that from *F* to *D* was 2.95 cc. Any small error in these volumes is immaterial since all measurements are differences of two readings. The volume from *G* to *D* was 549 cc.

K, *R*, *H*, is essentially a Toepler pump so designed that when the mercury level is at *F* the pressure of gas in *F–D* can be read from the difference in levels in *K* and *F*. The reading is independent of atmospheric pressure. The distance *H–F* should be as short as possible. In this apparatus it was about 45 cm.

L, is the inlet tube for the gas to be analyzed; it was 2 mm bore capillary.

S, is a two-way stopcock connected to a pump and through a capillary leak to the atmosphere used to manipulate the mercury levels.

Before use the system is evacuated through *M* and *L* for about two days to remove gases from the grease around the stopcock. Picein was found suitable as a lubricant. The gas to be analyzed is brought into the evacuated system through *L*, the mercury level raised to *F* and the pressure of the gas is determined by reading the level in *K*. From the known volume of the system and the recorded pressure and temperature, the volume of the gas at S.T.P. may be calculated. It is assumed in all cases that the gases are ideal. The stopcock *D* is then opened to the proper chamber according to the test to be made and after due time for reaction to occur the mercury level is lowered to *G* and the stopcock closed. The pressure is again observed after the level is raised to *F*. The process is repeated until constant pressure readings are found. The difference before and after is the contraction when allowance is made for the residual gas left in the reaction chamber; the latter is easily calculable from the volume ratio of *A* or *C* and *R*.

Since the conclusions drawn from the work depend on the analyses of the products of acetone photolysis it has been thought advisable to outline the methods used in some detail and indicate the precision available.

[10] W. M. Manning, J. Am. Chem. Soc. **56**, 2589 (1934).
[11] Morikawa, Trenner and Taylor, J. Am. Chem. Soc. **59**, 1103 (1937); H. S. Taylor and C. Rosenblum, J. Chem. Phys., **6**, 119 (1938); H. S. Taylor and W. J. Moore, *ibid.*, **8**, 396, 466 (1940).
[12] W. L. Haden Jr. and E. S. Luttropp, J. Ind. Eng. Chem., Anal. Ed. In press.

Analysis of hydrogen

Pure hydrogen was prepared from tank hydrogen by passing it through a trap in liquid nitrogen, then over a platinum Grillo catalyst at 200–300° to remove oxygen and finally through a dry-ice trap to remove water. It was analyzed in three ways: (1) by direct combustion with oxygen on a heated platinum filament, (2) by combustion in oxygen on a platinum Grillo catalyst heated to 250–300°C, and (3) by oxidation on copper oxide at 300°C. For the latter, copper oxide wire as used in organic microcombustion methods was placed in *C* and separated from it by glass wool was some anhydrone. A small furnace raised the temperature of the copper oxide to 300° where it was evacuated for one hour. Oxidation of hydrogen at the pressures here used (50–200 mm) then occurs readily within two minutes. The shortness of this time is advantageous not only as a time saver but also in reducing the possibility of the liberation of CO_2 which was found to be adsorbed tenaciously by copper oxide even at 300°C. A summary of the results obtained is given in Table I where for convenience volumes are expressed as the pressures observed.

Analysis of carbon monoxide

Carbon monoxide was prepared from sodium formate and concentrated sulfuric acid and dried by passing through a trap in a dry-ice-toluene mixture. The silver oxide method used by Blacet[13] proved extremely slow, and gave inconsistent results and its use for carbon monoxide-methane mixtures rendered the remaining methane in some way passive to complete oxidation by the explosion method. Tests were therefore made using iodine pentoxide at 175° and copper oxide at 300°C. In each case solid potassium hydroxide was used in front of the oxidizing agent to absorb the carbon dioxide formed. The reproducibility of the methods is shown in Table II depicting analyses of a carbon monoxide-methane mixture.

TABLE I.

METHOD	mm H_2 TAKEN	mm H_2 FOUND	% H_2
Combustion	50.6	50.7	100.1
	48.2	48.5	100.6
	44.6	44.9	100.5
Grillo catalyst and anhydrone	125.1	124.8	100.2
	163.0	164.0	100.5
	81.8	82.8	100.2
	115.1	114.3	99.4
	93.1	92.9	99.8
	97.5	96.9	99.1
CuO and anhydrone	94.2	93.8	99.6
	80.4	79.9	99.5
	86.7	86.4	99.6

[13] F. E. Blacet and P. A. Leighton, Ind. Eng. Chem., Anal. Ed. **3**, 225 (1931); **5**, 272 (1933); **6**, 334 (1934); F. E. Blacet and D. H. Volman, *ibid.*, **9**, 44 (1937).

TABLE II.

METHOD	mm CO—CH_4 TAKEN	mm CO FOUND	% CO
I_2O_5	145.9	89.0	61.0
	133.3	81.3	61.0
	102.2	62.1	60.7
	154.2	94.1	61.0
CuO	126.9	79.7	62.8
	137.0	84.8	62.0
	139.9	87.7	62.8

The discrepancy between the two methods was not investigated further since the copper oxide was known to work well and could be used also for hydrogen.

Analysis of ethylene

The method used by Morikawa, Trenner and Taylor[11] of hydrogenation of ethylene on a nickel catalyst at 100°C was found adaptable. From 8–10 milligrams of catalyst prepared according to their specifications was used. It was found necessary even with this small amount of catalyst to use only a slight excess of hydrogen owing to its adsorption. After hydrogenation the excess hydrogen is determined over copper oxide at 300°C. Table III lists some analyses on two different samples of tank ethylene passed over KOH and dried. It is seen that the percentage ethylene based on the observed contraction is always high, due presumably to hydrogen adsorption.

Analysis of methane

The usual combustion method on a hot platinum filament was used. Anhydrone was placed in *C* to absorb the water produced. This was later replaced by KOH to absorb CO_2. Preliminary analyses always showed a greater absorption on KOH than expected. The answer is believed to

TABLE III.

mm C_2H_4 TAKEN	mm H_2 ADDED	CONTRACTION	H_2 BY CuO	TOTAL H_2 USED	mm C_2H_6 FORMED	% C_2H_4 CONTN.	% C_2H_6
49.2	65.9	50.7	15.4	66.1	49.6	101.8	100.4
33.8	53.8	34.5	18.9	53.4	34.1	102.2	100.9
32.8	47.6	32.4	15.1	47.5	32.3	98.8	98.5
30.2	49.0	30.6	18.0	48.6	30.4	101.2	100.8

be due to ozone formation while the oxygen is being passed over the hot platinum coil, for, although the low pressures would favor decomposition of ozone, the surrounding walls of *A* are cold and tend to stabilize it. Ozone reaets with KOH to form potassium tetraoxide K_2O_4. In one experiment pure oxygen passed successively over the hot filament and then KOH several times during four or five hours showed a total contraction of 32 percent. It was also observed that KOH can adsorb oxygen. This latter error is eliminated by using minimal amounts of recently pulverized KOH. The ozone error could not be eliminated and depends on the amount of oxygen remaining after combustion, the filament temperature and the number of passes over the filament or time of contact with the filament. These latter two factors can be kept reasonably constant and an empirical correction (0.5–1 mm) was subtracted from the apparent CO_2 contraction depending on the amount of residual oxygen. Examples of the effect of this correction are shown in Table IV on tank methane from two sources. Table V exemplifies the effect of the correction when a mixture consisting chiefly of methane, carbon monoxide and hydrogen was analyzed.

Analysis of ethane

Analysis of ethane by the combustion method was found to give contraction values in general higher than carbon dioxide values. The reason for this has not so far been traced. The observed hydrogen values have been arbitrarily reduced by four percent. The effect of this correction, in addition to the correction to the observed carbon dioxide based on the residual oxygen as mentioned previously in methane analysis is shown in Table VI. It is seen to be small and would in no way affect an interpretation of a mechanism based on such analyses. Table VI presents the results of several analyses of a mixture of ethylene and ethane.

Since attempts to analyze mixtures containing hydrogen, carbon monoxide, methane, ethylene and ethane were without success, fractionation was employed. The first three constituents pass through liquid nitrogen, ethylene and ethane being retained. In some of the runs enumerated later, hydrogen and carbon monoxide were determined directly and the methane by difference.

Since only rarely was ethylene found, the fraction of gas between −194° and −131°C was usually ethane. The formula for it was not determined in all cases, particularly in check runs, the volume alone being noted and recorded as C_xH_y.

RESULTS

The principal products found in all the work were methane, carbon monoxide and ethane. Traces of hydrogen and of ethylene were found in acetone photolysis at 250°C. The sec-butyl chloride fraction from acetone alone which was principally ethane gave carbon values higher than two. This has been interpreted as indicating

TABLE IV.

% CH_4 BY CONTRACTION	% CH_4 FROM CO_2 OBS.	% CH_4 FROM CO_2 CORR.
95.5	96.7	95.0
95.5	96.0	95.2
95.0	96.3	95.0
99.4	101.0	100.2
99.8	102.2	100.1
99.7	99.7	98.9

TABLE V.

VOL. GAS ANALYZED IN CC	1 0.426	2 0.556	3 0.359
% H_2 (by CuO—anhydrone)	17.6	17.4	16.5
% CO (by CuO—KOH)	49.8	49.5	49.5
% CH_4 from contraction	30.4	31.8(?)	30.4
% CH_4 from CO_2 obs.	31.7	30.6	31.1
% CH_4 from CO_2 corr.	30.3	30.2	30.4

TABLE VI.

VOL. CC	% C_2H_4	C_xH_y (OBS.)	C_xH_y (CORR.)
0.114	31.6	$C_{1.96}H_{6.18}$	$C_{1.92}H_{5.88}$
0.116	31.0	$C_{2.04}H_{6.78(?)}$	$C_{2.01}H_{(?)}$
0.120	32.7	$C_{1.94}H_{6.14}$	$C_{1.91}H_{5.84}$
0.104	30.1	$C_{2.08}H_{6.28}$	$C_{2.05}H_{5.97}$
0.128	31.1	$C_{2.08}H_{6.40}$	$C_{2.05}H_{6.07}$
0.097	28.6(?)	$C_{2.04}H_{6.32}$	$C_{2.01}H_{6.00}$

TABLE VII.

Acetone mm	Time min.	ΔP mm	Vol. in cc Total	Liq. N_2	−131°	% CO	% CH_4	% C_xH_y	C_xH_y		% Carbon Deficiency
				Temp. 200°C							
180	20	2.1	0.543	0.459	0.084	44.2	40.3	15.5	2.03	6.10	19
180	20	—	.517	.447	.070	43.7	42.8	13.5	2.13	6.85	18
90	30	2.6	.652	.514	.138	49.2	29.6	21.2	2.24	6.40	22
92	30	—	.631	.483	.148	47.2	29.4	23.4	—	—	—
46	30	0.9	.367	.272	.095	50.1	24.0	25.9	2.28	6.73	17
27	60	2.6	.513	.357	.156	51.7	17.8	30.4	2.07	6.06	22
				Temp. 100°C							
180	30	1.7	0.417	0.248	0.169	49.0	10.5	40.6	1.91	5.88	10
180	30	2.7	.640	.366	.274	48.4	8.7	42.8	2.02	6.10	2
90	30	1.6	.344	.192	.152	49.3	6.4	44.3	2.10	6.21	0
45	30	0.7	.245	.135	.110	50.6	4.5	44.9	2.22	6.23	0
25	30	0.3	.131	.073	.058	51.5	3.8	44.3	2.09	6.17	7
26	60	0.7	.287	.151	.136	49.3	3.8	47.4	2.12	6.18	0

the production of some propane by acetone photolysis. Assuming one molecule of carbon monoxide is formed for every molecule of acetone decomposed, the carbon found in all the hydrocarbons produced should be twice that in the carbon monoxide. Actually it is found to be less. This percentage carbon deficiency was calculated as follows:

$$\frac{2\,(\%\,CO)-(\%\,CH_4+x\cdot\%\,C_xH_y)}{2\,(\%\,CO)}\times 100.$$

Its value, which is quite specific for the particular system studied, whether acetone alone, acetone and mercury, or acetone and mercury dimethyl, indicates the production of a compound or compounds whose carbon to carbon monoxide ratio is greater than two.

In Table VII are recorded data showing the variation in the percentage composition of the products of acetone photolysis as a function of the pressure at two temperatures.

Since from the above table it can be seen that there is a less rapid change in the percentage products at pressures above 90 mm acetone all subsequent experiments were made at this pressure. Tables VIII–XI, which are self-explanatory, give the data found for the four systems examined at various temperatures.

For comparative purposes the data in Tables VIII–XI have been collected in the composite graph shown in Fig. 2 which illustrates very simply the similarity of behavior of the three systems when mercury is present in one form or other and the difference from that of acetone alone. Fig. 3 shows the variation of the carbon deficiency with temperature and although the actual values cannot be too accurate the general trend of them signifies a distinction in the behavior of the systems studied.

DISCUSSION

For purposes of discussion of the above results it will be convenient to set down a number of reactions which appear to be the major ones occurring in the various systems. The energies of activation of several reactions have already been estimated; the appropriate references are given with these values.

			$E_{act.}$	Ref.
System I. Acetone				
1.	CH_3COCH_3	$\xrightarrow{h\nu} CH_3+CH_3CO$		
2.	CH_3+CH_3CO	$\rightarrow CH_3COCH_3$	8	17
3.	CH_3+CH_3CO	$\rightarrow C_2H_6+CO$	6	
4.	$CH_3CO+(CH_3COCH_3)$	$\rightarrow CH_3+CO+(CH_3COCH_3)$	18	15
5.	$CH_3+CH_3COCH_3$	$\rightarrow CH_4+CH_2COCH_3$	16	17
6a.	$2CH_3COCH_3$	$\rightarrow (CH_3COCH_3)_2$		
6b.	$CH_3CO+CH_3COCH_3$	$\rightarrow CH_3COCH_2COCH_3$		
7.	$CH_3+CH_3COCH_3$	$\rightarrow C_2H_5COCH_3$	8	17
8.	$CH_3+C_2H_5COCH_3$	$\rightarrow CH_4+C_2H_4COCH_3$	<16	
9.	$C_2H_5COCH_3$	$\xrightarrow{h\nu}$ (CO, C_2H_6, C_2H_8, C_4H_{10})		11
System II. Acetone plus mercury				
10.	CH_3+Hg	$\rightarrow HgCH_3$		
11.	CH_3+HgCH_3	$\rightarrow Hg(CH_3)_2$		
12.	CH_3+HgCH_3	$\rightarrow CH_4+HgCH_2$	<13	
13.	CH_3+HgCH_3	$\rightarrow C_2H_6+Hg$		
System III. Acetone plus mercury dimethyl				
14.	$CH_3+Hg(CH_3)_2$	$\rightarrow CH_4+Hg(CH_3)CH_2$	13–14	
15.	$CH_3+Hg(CH_3)_2$	$\rightarrow C_2H_6+HgCH_3$		

together with 10, 11, 12 and 13.

If reactions 1 to 9 above represent the mechanism of acetone photolysis it is apparent that for each molecule of acetone decomposing (excluding the reverse reaction 2) one molecule of carbon monoxide is formed either by reaction 3 or 4. Regardless of which reaction predominates the volume of carbon monoxide produced should

TABLE VIII. *Variation of the composition of products with temperature from acetone. Pressure of acetone ~90 mm, time of radiation ~30 min.*

TEMP.	TOTAL	VOL. IN CC LIQ. N_2	−131°	CO	% CH_4	C_xH_y	C_xH_y x	C_xH_y y	% CARBON DEFICIENCY
250	0.869	0.765	0.104	44.2	43.9	12.0	1.93	5.94	24
225	.998	.812	.186	46.7	34.7	18.6	2.19	6.52	17
225	.568	.487	.082	46.2	39.5	14.4			
225	.913	.743	.169	46.7	34.8	18.5			
200	.652	.514	.138	49.2	29.6	21.2	2.24	6.40	17
200	.631	.483	.148	47.2	29.4	23.4			14[a]
175	.445	.322	.123	48.9	23.6	27.6	2.33	6.45	
175	.548	.384	.164	48.6	21.5	30.0			
150	.575	.370	.204	51.2	13.4	35.4			
150	.544	.352	.192	50.6	14.2	35.2	2.22	6.51	9
100	.344	.192	.152	49.3	6.4	44.3	2.10	5.94	0

[a] Calculated using $x = 2.2$ in C_xH_y.

TABLE IX. *Acetone photolysis in presence of mercury. Acetone pressure ~90 mm, time of radiation ~30 mm.*

TEMP.	TOTAL	VOL. IN CC LIQ. N_2	−131°	CO	% CH_4	C_xH_y	C_xH_y x	C_xH_y y	% CARBON DEFICIENCY
250	0.652	0.597	0.055	43.4	48.4	8.3			25[a]
225	.611	.535	.076	45.0	42.6	12.4	2.06	6.16	25
225	.520	.452	.068	45.0	42.0	13.0			24[a]
200	.276	.236	.040	47.5	38.1	14.5	1.88	6.03	
200	.510	.405	.105	48.1	31.4	20.6			25[a]
200	.551	.433	.118	47.8	30.8	21.4			23[a]
175	.587	.416	.171	49.8	21.2	29.2	1.97	6.25	20
175	.527	.378	.149	48.1	23.8	28.3			17[a]
150	.617	.396	.221	49.6	14.6	35.8	2.02	6.10	13
100[b]	—	—	—	49.8	5.0	44.0			7[a]

[a] Calculated using $x = 2.0$ in C_xH_y.
[b] Extrapolated from experiments not summarized here.

TABLE X. *Acetone photolysis in presence of mercury vapor. Acetone pressure ~90 mm, mercury pressure ~ 30–35 mm.*

TEMP.	TIME min.	TOTAL	VOL. IN CC LIQ. N_2	−131°	CO	% CH_4	C_xH_y	C_xH_y x	C_xH_y y	% CARBON DEFICIENCY
275	60	0.454	0.437	0.017[a]	39.0	57.3	3.7			18[b]
250	30	.354	.328	.026[a]	42.1	50.8	7.3			23[b]
250	60	.584	.544	.040[a]	41.7	51.6	6.8			22[b]
235	45	.999	.871	.128	44.7	42.5	12.8	1.92	5.88	24
227	60	.818	.718	.100	44.7	43.1	12.3	2.08	5.92	24
225	30	.495	.428	.067	45.5	41.0	13.5	2.12	6.39	24

[a] Too small to analyze. [b] Calculated using $x = 2.0$ in C_xH_y.

TABLE XI. *Acetone photolysis in presence of mercury dimethyl. Acetone ~90 mm, $Hg(CH_3)_2$ ~10 mm, radiation time ~30 min.*

TEMP.	TOTAL	VOL. IN CC LIQ. N_2	−131°	CO	% CH_4	C_xH_y	C_xH_y x	C_xH_y y	% CARBON DEFICIENCY
250	0.790	0.676	0.114	40.2	45.4	14.0	1.95	6.23	9
250	.540	.480	.060	39.4	49.4	11.1			9[a]
225	.549	.463	.086	42.7	41.6	15.6	2.09	6.23	15
225	.590	.493	.097	42.4	41.3	16.4			13[a]
225	.648	.537	.111	43.0	39.8	17.1			14[a]
225	.527	.445	.082	41.2	43.3	15.6			10[a]
200	.640	.489	.151	45.4	31.0	23.6	1.96	6.03	14
200	.558	.432	.126	44.6	32.8	22.6			13[a]
200	.690	.520	.170	45.4	30.0	24.6			13[a]
175	.490	.351	.139	45.8	25.8	28.4	2.01	6.12	10
175	.673	.452	.221	46.7	20.5	32.8			8[a]
150	.504	.319	.185	48.3	14.0	36.7	1.99	6.02	9

[a] Calculated using $x = 2.0$ in C_xH_y.

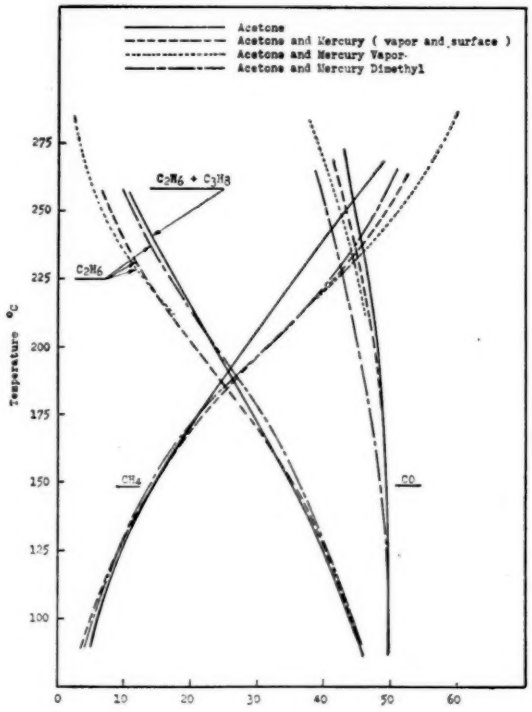

FIG. 2.

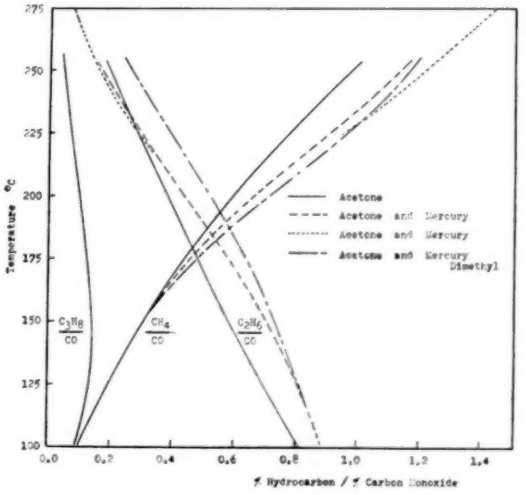

FIG. 3.

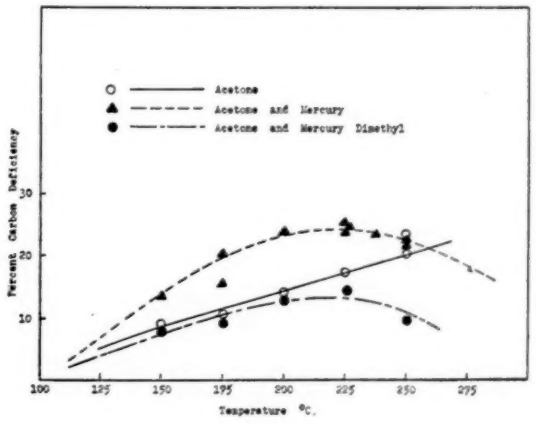

FIG. 4.

be constant and independent of temperature. The variations in light intensity of the lamp used in this work preclude a definite test of this, though the lack of any trend in the volumes of gas formed gives it support. On this assumption the relative quantities of hydrocarbon formed together with a fixed quantity of carbon monoxide have been calculated as a more desirable basis for comparison. The values are shown in Fig. 4. The C_xH_y fraction in acetone alone has been taken as a mixture of ethane and propane and although it is unlikely that all of the propane is pumped from the condensate at $-131°$, the trend of the C_3H_8/CO ratio with temperature is comparable with the results of Moore and Taylor.[11] They found a maximum percentage of propane in the photolysis of methyl ethyl ketone at 110–120°C. The propane shows a maximum here around 140°C.

The primary source of ethane in acetone photolysis has been taken to be reaction 3 rather than a combination of two methyl radicals[14] for if the energy of activation of the latter is 8 kcal. reaction 3 would offer effective competition. The energy of activation may be estimated by Eyring's method[15] using the C–C bond strength in acetyl as compared with the C–H bond strength in methane. The activation energy of the Walden inversion in methane was shown by Eyring to be 37 kcal. The C–C bond in acetyl was found by Gorin and by Herr and Noyes[16] to be about 18 kcal. and taking 95 kcal. as the C–H bond gives $E_3 = 37 \times 18/95 = 7$ kcal. Burton, Taylor and Davis[17] have calculated E_3 as 5.8

[14] See A. Gordon and H. A. Taylor, J. Am. Chem. Soc. In press.

[15] Gorin, Kauzmann, Walter and Eyring, J. Chem. Phys. **7**, 633 (1939).

[16] E. Gorin, J. Chem. Phys. **7**, 256 (1939); D. S. Herr and W. A. Noyes, J. Am. Chem. Soc. **62**, 2052 (1940).

[17] Burton, Taylor and Davis, J. Chem. Phys. **7**, 1080 (1939).

kcal. as the probable chain ending reaction in the decomposition of acetaldehyde induced by methyl radicals. The lower value 5.8 kcal. as compared with the calculated 7 kcal. is probably the better value since in Eyring's calculation the Walden inversion involved a C−H bond formation in methane whereas here the weaker bond C−C in ethane is being formed.

Methane production by reaction 5 for which 16 kcal.[18] seems to be a reasonable value would offer little competition to ethane production at low temperatures. It is observed that ethane predominates over methane at 100°C. Taking E_4 as 18 kcal. the increase in rate of reaction 4 with increasing temperature with its consequent increase in methyl radical concentration can account satisfactorily for the decrease in ethane and increase in methane as the temperature rises.

The production of acetonyl acetone was demonstrated by Rice, Rodowskas and Lewis[19] in the thermal decomposition of acetone at 350–400°C when one percent of mercury dimethyl was present. Its presence in the products of photolysis might explain the white deposit which is always observed in the condensation trap and which slowly sublimes. At the same time the ratio CH_4/CO must attain a value greater than unity at higher pressures at temperatures about 200°C judging by the trend of the results in Table VII. This can only occur if the acetonyl corresponding to CH_4 produced retains its CO in some such form as in acetonyl acetone and the CO does not appear in the gas phase.

The carbon deficiency observed is accounted for by reaction 7 with the formation of methyl ethyl ketone. The presence of this has recently been reported by Allen[20] in the high temperature photolysis of acetone. A carbon deficiency can only occur with the formation of a compound in which the carbon to carbon monoxide ratio is higher than that in acetone. The presence of propane in the products from acetone photolysis follows from reactions 7 and 9. Moore and H. S. Taylor have shown that propane is the predominant hydrocarbon in reaction 9 below 200°C. At the same time they point out that methane is formed more readily (reaction 8) from methyl ethyl ketone than from acetone suggesting that E_8 is somewhat less than 16 kcal.

Qualitatively the suggested reaction scheme 1 to 9 seems adequate to account for the observations. Quantitatively it is not completely satisfactory since the complexity precludes a complete calculation of the stationary free radical concentrations, and the relative importance of the subsequent reactions is difficult to establish. Inspection of the data in Table VII at 200°C shows that at higher pressures the ratio of CH_4/CO varies approximately as the two-thirds power of the acetone while the C_2H_6/CO ratio varies inversely approximately as the one-third power. This would require that the methyl radical concentration was roughly proportional to the two-thirds power of the acetone, a not impossible eventuality.

Turning now to the system in which mercury or mercury dimethyl is present, it is evident that a greater similarity in behavior exists between them than between any one of them and acetone alone. Particularly is this true so far as methane formation is concerned. The increase in the CH_4/CO ratio probably indicates new methane forming reactions other than 5 or 8. Since reaction 14 is the probable cause of methane formation from mercury dimethyl it would seem that this reaction or its alternative, reaction 12, must be proceeding in system II, acetone plus mercury, necessitating reactions 10 and 11. This is borne out by the observed greater carbon deficiency in the acetone-mercury system wherein methyl radicals are removed from the system as mercury methyl and thus do not appear as hydrocarbons. Further confirmation appears in the lesser carbon deficiency in the system containing mercury dimethyl wherein methyl radicals have a chance to react producing hydrocarbons, greater even than in acetone alone. The absence of propane in detectable amounts in systems II and III shows a more efficient methyl removal than in system I reducing thereby the possibility of reaction 7 to form methyl ethyl ketone. The small differences in the CH_4/CO ratios in systems II and III can probably be traced to differences in mercury methyl and dimethyl concentrations.

[18] *a*. F. O. Rice and K. Herzfeld, J. Am. Chem. Soc. **56**, 284, 488 (1934). *b*. Haden, Meibohm and O. K. Rice, J. Chem. Phys. **8**, 998 (1940).

[19] F. O. Rice, Rodowskas and Lewis, J. Am. Chem. Soc. **56**, 2497 (1934).

[20] A. O. Allen, J. Am. Chem. Soc. **63**, 708 (1941).

Considering the ratio C_2H_6/CO, it is observed that the value is greater in the mercury dimethyl experiments. This is to be expected since the mercury dimethyl concentration is relatively large favoring reaction 15. Conversely in the mercury experiments since methyl radicals are removed by reactions 10 and 11, their concentration is lower. There is some doubt concerning the source of ethane in these systems. Cunningham and Taylor[4] have suggested reaction 15, even attributing the value 1.5 kcal. obtained from the rate of increase of ethane production with temperature to its energy of activation. Simply from analogy with acetone, reaction 13 would seem to offer an even easier path. Although a Walden inversion type calculation as made above with acetone might not be quantitatively reliable, qualitatively it is significant. The Hg—C bond in mercury dimethyl is given by Terenin[21] as about 40–50 kcal. The bond in mercury methyl is probably considerably less, and thus ethane formation might be expected to be easier by reaction 13 than by 15. A decreasing concentration of $HgCH_3$ with increasing temperature would account for the low value 1.5 kcal. found by Cunningham and Taylor.

The crossing of the curves for the acetone and acetone-mercury systems at higher temperatures can be accounted for by the fact that if the propane found in acetone photolysis arises from methyl ethyl ketone decomposition, there would also be produced according to Moore and Taylor an approximately equivalent amount of ethane at these temperatures. If the total ethane found in the acetone system is reduced by an amount equal to the propane found, no crossing of curves would occur. It then follows that ethane is probably produced more easily by reaction 13 than by reaction 3.

From the data in Fig. 4 an approximate value of the relative activation energies of reactions 5 and 14 for methane production can be obtained. The CH_4/CO ratio for the acetone-mercury dimethyl system is about 1.2 times that for acetone alone in the temperature range 200 to 225°C. The ratio of acetone to mercury dimethyl in the former is 9 : 1. Hence approximately $1.2 = 1/9 . \exp(\Delta E/RT)$ whence $\Delta E = 2$–3 kcal. If E_5 is 16 kcal. then E_{14} is about 13–14 kcal. Since the ratio of mercury methyl to acetone in system II must be less than 1/9 the energy of activation of reaction 12 must be less than 13 kcal.

In conclusion it seems certain that mercury methyl, if not mercury dimethyl also, is formed by reaction between methyl radicals and mercury. From the general agreement of the results using liquid mercury with those where only mercury vapor is present, the reaction must involve mercury atoms.

[21] A. Terenin and N. Prilezhaeva, Acta Physicochim. U.S.S.R. **1**, 759 (1934).

Statistical Mechanics of Imperfect Gases*

ELLIOTT W. MONTROLL,† *Sterling Chemistry Laboratory, Yale University, New Haven, Connecticut*

AND

JOSEPH E. MAYER, *Chemistry Department, Columbia University, New York, New York*

(Received May 27, 1941)

The application of statistical mechanical equations to the calculation of thermodynamic properties of imperfect gases has been hindered by the occurrence of highly multiple integrals in these equations. By observing that some of these multiple integrals are related to the iterated kernels of an integral equation involving the potential energy function of a pair of molecules, a technique is developed which expresses these integrals in terms of the characteristic values of the integral equation. This technique is applied to the calculation of third virial coefficients and the molecular distribution function (which is essentially the probability of finding two specified molecules in two small volume elements a distance r from each other) at various temperatures for imperfect gases with Lennard-Jones potential energy functions.

I. INTRODUCTION

RECENTLY, using methods first investigated by Ursell,[1] formal expressions have been derived[2-7] for the physical properties of imperfect gases and condensing systems. In spite of the exactness of these equations, their use in making calculations has been limited by the fact that they are expressed in terms of so called "irreducible integrals"

$$\beta_n=\frac{1}{Vn!}\int\int\cdots\int\sum\prod_{n+1\geqq i>j\geqq 1}f_{ij}d\{\mathbf{n+1}\} \tag{1}$$

(sum over all products with all molecules more than singly connected)

and

$$H_{\nu m}\{\mathbf{v}\}=\frac{1}{m!}\int\int\cdots\int\sum_{\substack{m\geqq i>j\geqq 1\\ m\geqq k\geqq 1\\ \nu\geqq\kappa\geqq 1}}\prod_{(\nu>1)}f_{ij}f_{\kappa l}d\{\mathbf{m}\} \tag{2}$$

(sum over all connected products for which each molecule of the set $\{\mathbf{m}\}$ is connected to at least two of the set $\{\mathbf{v}\}$ by an independent path)

whose direct evaluation is a Herculean task. A fundamental statistical mechanical function, the Helmholtz free energy (from which all thermodynamic quantities can be calculated) is given by

$$A=RT\left[\log\left(\frac{h^2}{2\pi mkT}\right)\frac{1}{ev}-\sum_{n\geq 1}\frac{1}{n+1}\beta_n v^{-n}\right] \tag{3}$$

and the equation of state of the system is

$$\frac{Pv}{kT}=1-\sum_{n\geq 1}\frac{n}{n+1}\beta_n v^{-n}. \tag{4}$$

* Publication assisted by the Ernest Kempton Adams Fund for Physical Research of Columbia University.

† Sterling Research Fellow, Yale University.

[1] H. D. Ursell, Proc. Camb. Phil. Soc. **23**, 685 (1927).
[2] J. E. Mayer, J. Chem. Phys. **5**, 67 (1937).
[3] J. E. Mayer and P. G. Ackermann, J. Chem. Phys. **5**, 74 (1937).
[4] J. E. Mayer and S. F. Harrison, J. Chem. Phys. **6**, 87 (1938).
[5] S. F. Streeter and J. E. Mayer, J. Chem. Phys. **7**; 1025 (1939).
[6] B. Kahn and G. E. Uhlenbeck, Physica, **4**, 299 (1938).
[7] M. Born and K. Fuchs, Proc. Roy. Soc. **166**, 391 (1938).

As has become customary in empirical equations of state, the coefficient of v^{-n} (v is the volume per molecule) in (4) is called the $(n+1)$st virial coefficient. The distribution function $F_2\{\mathbf{2}\}$ (defined in such a manner that $F_2\{\mathbf{2}\}d\tau_1 d\tau_2/V^2$ is the probability that any specified molecule 1 is in the volume element $d\tau_1$ at the position x_1, y_1, z_1 at the same time 2 is in $d\tau_2$ at x_2, y_2, z_2) is given by [8,9]

$$F_2\{\mathbf{2}\}=\exp\left(-V(r_{12})/kT\right)\left[1+\sum_{m\geq 1} v^{-m}H_{2,m}\{\mathbf{2}\}\right]. \tag{5}$$

In Eqs. (1–5) $\{\mathbf{n}\}$ represents a set of n specified molecules and the set of $3n$ coordinates of these molecules:

$$\{\mathbf{n}\}=x_1, y_1, z_1, \cdots, z_n$$

$$d\{\mathbf{n}\}=d\tau_1 d\tau_2\cdots d\tau_n=dx_1\cdots dz_n;$$

$f(r_{ij})=f_{ij}=[\exp\{-V(r_{ij})/kT\}]-1$; and the integration extends over the volume V of the space in which the molecules of the system are confined. The mutual potential energy $V(r_{ij})$ of a pair of molecules whose distance of separation is r_{ij} becomes infinite as $r_{ij}\to 0$, has a negative minimum when r_{ij} is the equilibrium distance between the molecules, and rapidly approaches zero as the molecules separate from their equilibrium positions. k is Boltzmann's constant and T is the absolute temperature of the system at equilibrium.

The simplest irreducible integrals are

$$\beta_1=\int_0^\infty 4\pi r^2 f(r)dr, \quad \beta_2=\frac{1}{2V}\int\int\int f_{12}f_{23}f_{31}d\{3\}, \quad \beta_3=\frac{1}{3!V}(3\beta_{30}+6\beta_{31}+\beta_{32}), \tag{6}$$

where

$$\beta_{30}=\frac{1}{V}\int\int\int\int f_{12}f_{23}f_{34}f_{41}d\{4\}, \quad \beta_{31}=\frac{1}{V}\int\int\int\int f_{12}f_{13}f_{14}f_{23}f_{34}d\{4\},$$

$$\beta_{32}=\frac{1}{V}\int\int\int\int f_{12}f_{13}f_{14}f_{23}f_{24}f_{34}d\{4\}$$

and which correspond to "graphs"

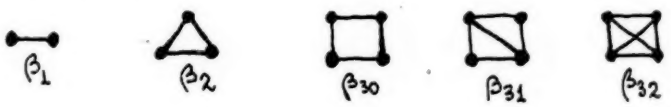

The corresponding H integrals leave at least two volume elements unintegrated. Graphs with every particle connected to exactly two others (for example, β_2 and β_{30}) are said to represent "ring integrals," the most general of which is a numerical factor multiplied by

$$p_n(0)=\frac{1}{V}\int\int\cdots\int f_{12}f_{23}\cdots f_{n,n+1}f_{n+1,1}d\tau_1\cdots d\tau_{n+1}. \tag{7}$$

Integrals whose graphs are linear chains with the positions of the two end particles fixed are called "chain integrals" and are of the form

$$p_n(r_{1,n+2})=\int\int\cdots\int f_{12}f_{23}\cdots f_{n,n+1}f_{n+1,n+2}d\tau_2\cdots d\tau_{n+1}. \tag{8}$$

Since the integration over the last volume element in Eq. (7) contributes V as a factor, as $r_{n+2}\to r_1$, $p_n(r_{1,n+2})\to p_n(0)$.

[8] J. E. Mayer and E. Montroll, J. Chem. Phys. **9**, 2 (1941).
[9] J. De Boer and A. Michels, Physica **6**, 97 (1939).

Inasmuch as β_1 is an integral over a single variable, its integration is not difficult;[10] however, passage to higher β's and H's introduces severe complications. Even the evaluation of β_2 necessitates the integration of a ninefold integral whose integrand is a rather complicated function.

The purpose of this paper is to demonstrate the applicability of some properties of integral equations and Fourier transforms to the calculation of the β's and H's. We shall calculate the third virial coefficient and the distribution function $F_2\{2\}$ for gases with Lennard-Jones potentials.

II. Mathematical Techniques

1. Development of $p_n(r)$ in terms of characteristic functions and characteristic values of a linear homogeneous integral equation. First consider the integration of $p_n(r_{1,\,n+2})$ to be taken over a cube with edges of length a. Then

$$p_n(r_{1,\,n+2})=\int_{-a/2}^{a/2}\int_{-a/2}^{a/2}\cdots\int_{-a/2}^{a/2} f_{12}f_{23}\cdots f_{n+1,\,n+2}\,d\tau_2\cdots d\tau_{n+1} \tag{9}$$

$$r_{ij}=[(x_i-x_j)^2+(y_i-y_j)^2+(z_i-z_j)^2]^{\frac{1}{2}}.$$

Now suppose f_{ij} is expanded as a bilinear form

$$f_{ij}=\sum_{\alpha,\,\beta} a_{\alpha\beta}\psi_\alpha(x_i,\,y_i,\,z_i)\psi^*_\beta(x_j,\,y_j,\,z_j) \tag{10}$$

of a complete set of functions $\{\psi_\alpha(x,\,y,\,z)\}$, orthonormal in the cube. The orthonormality condition means

$$\int_{-a/2}^{a/2}\int_{-a/2}^{a/2}\int_{-a/2}^{a/2}\psi_\alpha(i)\psi^*_\beta(i)\,d\tau_i=\delta_{\alpha\beta}$$

($\delta_{\alpha\beta}=1$ if $\alpha=\beta$ and zero otherwise).

By multiplying both sides of (10) by $\psi^*_\alpha(i)\psi_\beta(j)$ and integrating over the entire cubes, the orthonormality condition yields

$$a_{\alpha\beta}=\int\int f(r_{ij})\psi^*_\alpha(i)\psi_\beta(j)\,d\tau_i\,d\tau_j.$$

One might ask whether there exists a set $\{\psi_\alpha\}$ such that $a_{\alpha\beta}=0$ when $\alpha\neq\beta$. The answer is yes, for if $\{\psi_\alpha\}$ is the set of characteristic functions of the integral equation

$$\psi(x_i,\,y_i,\,z_i)=\lambda\int_{-a/2}^{a/2}\int_{-a/2}^{a/2}\int_{-a/2}^{a/2} f(r_{ij})\psi(x_j,\,y_j,\,z_j)\,d\tau_j, \tag{11}$$

then

$$a_{\alpha\beta}=\frac{1}{\lambda_\beta}\int_{-a/2}^{a/2}\int_{-a/2}^{a/2}\int_{-a/2}^{a/2}\psi^*_\alpha(i)\psi_\beta(i)\,d\tau_i=\frac{1}{\lambda_\beta}\delta_{\alpha\beta}.$$

Since the kernel $f(r_{ij})$ in gas theory is generally a function of $(x_i-x_j)^2+(y_i-y_j)^2+(z_i-z_j)^2$, its characteristic functions are[11]

$$\psi_{k,\,l,\,m}=a^{-1}\exp\left\{\frac{2\pi i}{a}(kx+ly+mz)\right\}, \qquad (k,\,l,\,m=0,\,\pm1,\,\pm2,\,\cdots). \tag{12}$$

---

[10] See, for example, Lennard-Jones, Proc. Roy. Soc. **106**, 463 (1924), where it is calculated for the potential energy function $V(r)=Ar^{-s}-Br^{-t}$.

[11] Cf. Hille and Tamarkin, Acta Math. **57**, 1 (1931).

This implies that $f(r)$ can be expanded formally as

$$f(x, y, z) \sim \sum_{k, l, m=-\infty}^{\infty} c_{k, l, m} a^{-\frac{3}{2}} \exp\left\{\frac{2\pi i}{a}(kx+ly+mz)\right\}, \tag{13}$$

where the coefficients $c_{k, l, m}$ can be evaluated by the usual method of multiplying both sides of (13) by $\psi^*_{k, l, m}$ and integrating over the entire cube. Thus

$$c_{k, l, m} = a^{-\frac{3}{2}} \int_{-a/2}^{a/2}\int_{-a/2}^{a/2}\int_{-a/2}^{a/2} f(x, y, z) \exp\left\{-\frac{2\pi i}{a}(kx+my+nz)\right\} dx dy dz. \tag{14}$$

Substituting (12) into (10), the characteristic values of $f(r_{12})$ are

$$\lambda_{k, l, m} = (1/a)^{\frac{3}{2}} c_{k, l, m}.$$

If we observe that (9) is the nth iterated kernel of the integral equation (11), we can express it in the well-known form[12]

$$\begin{aligned} p_n(r_{1, n+2}) &= \sum_{k, l, m=-\infty}^{\infty} \frac{\psi_{k, l, m}(1)\psi^*_{k, l, m}(n+2)}{\lambda^{n+1}_{k, l, m}} \\ &= \frac{1}{a^3} \sum_{k, l, m=-\infty}^{\infty} (a^{\frac{3}{2}} c_{k, l, m})^{n+1} \exp \frac{2\pi i}{a}\{kx_{1, n+2}+ly_{1, n+2}+mz_{1, n+2}\} \end{aligned} \tag{15}$$

($x_{i, j} = x_i - x_j$, etc.). The same result could have been achieved by merely substituting (12) into (9); however, by using the method given above, the theory of integral equations insures the convergence of the series as long as $n \geqslant 2$ and $\int\int |f(r_{12})|^2 d\tau_1 d\tau_2 < \infty$. This integrability condition is satisfied in most statistical mechanical problems, the most important exceptions being those involving Coulombic forces (electrolyte problems) in which cases the developments of this paper are not valid.

In general, a triple sum is inconvenient to handle, so (15) will now be reduced to a definite integral over one variable.

2. *Reduction of $p_n(r)$ to a simple integral.* First an expression for $c_{k, l, m}$ which is simpler and more useful than (14) will be derived. If $f(r) \sim 0$ when r is greater than some small fraction of a (as is the case in the theory of imperfect gases and condensing systems) the limits of integration on (14) can, with negligible error, be made infinite. Transforming to spherical polar coordinates yields

$$\begin{aligned} c_{k, l, m} = a^{-\frac{3}{2}} \int_0^{\infty} r^2 f(r) dr \int_0^{\pi} \left[\exp\left\{-\frac{2\pi i r m \cos\theta}{a}\right\}\right] \sin\theta d\theta \\ \times \int_0^{2\pi} \left[\exp\left\{-\frac{2\pi i r}{a} \sin\theta(k\cos\varphi + l\sin\varphi)\right\}\right] d\varphi \end{aligned} \tag{16}$$

but, as will be shown in the Appendix,

$$\begin{aligned} I &= \int_0^{\pi}\int_0^{2\pi} \exp\left\{-\frac{2\pi i r}{a}(k\cos\varphi\sin\theta + l\sin\varphi\sin\theta + m\cos\theta)\right\} \sin\theta d\varphi d\theta \\ &= \frac{2a}{r(k^2+l^2+m^2)^{\frac{1}{2}}} \sin\frac{2\pi r}{a}(k^2+l^2+m^2)^{\frac{1}{2}}. \end{aligned} \tag{17}$$

[12] Cf. R. Courant and D. Hilbert, *Methoden der Mathematischen Physik I* (Berlin, 1931), second edition, p. 116.

Therefore,

$$c_{k,l,m}=\frac{2}{a^{\frac{1}{2}}(k^2+l^2+m^2)^{\frac{1}{2}}}\int_0^\infty rf(r)\sin\left[\frac{2\pi r}{a}(k^2+l^2+m^2)^{\frac{1}{2}}\right]dr. \tag{18}$$

This equation shows that $c_{k,l,m}$ is a function of $(k^2+l^2+m^2)^{\frac{1}{2}}$ with spherical symmetry about the origin of a Cartesian k, l, m coordinate system. As has been mentioned before, the main contribution to $c_{k,l,m}$ originates from very small values of r (say when $r<10^{-6}a$). If k, l, m are small integers it is apparent that their corresponding terms in $p_n(r_{1,n+2})$ will be practically independent of k, l, m. Since the terms in the series which depend on k, l, m are those for which these integers are so large that the summand in (15) can be considered as a continuous function of k, l, m, the summation in (15) can be changed to an integration over k, l, m space. Writing

$$t=(2\pi/a)(k^2+l^2+m^2)^{\frac{1}{2}}, \tag{19a}$$

$$a^{\frac{1}{2}}c_{k,l,m}=4\pi\int_0^\infty r^2f(r)(\sin tr/tr)dr=g(t), \tag{19b}$$

the integral representation of $p_n(r_{1,n+2})$ becomes (in spherical polar coordinates)

$$p_n(r_{1,n+2})=\frac{1}{a^3}\int_0^\infty t^2g^{n+1}(t)dt\int_0^\pi\left[\exp\left\{-\frac{2\pi it}{a}z_{1,n+2}\cos\theta\right\}\right]\sin\theta d\theta$$
$$\times\int_0^{2\pi}\left[\exp\left\{-\frac{2\pi it\sin\theta}{a}(x_{1,n+2}\cos\varphi+y_{1,n+2}\sin\varphi)\right\}\right]d\varphi.$$

Applying (17) to the integration over the angle variables

$$p_n(r)=\frac{1}{2\pi^2}\int_0^\infty t^2g^{n+1}(t)(\sin tr/tr)dt \tag{20}$$

and as $r_{n+2}\to r_1$,

$$p_n(0)=(1/2\pi^2)\int_0^\infty t^2g^{n+1}(t)dt. \tag{21}$$

Thus the highly multiple chain and ring integrals have been reduced to simple integrals which have the same general form for all values of n. For very large n's one can derive an asymptotic expression for these integrals by the methods discussed in the next section.

3. Asymptotic formula for $p_n(r_{1,n+2})$. If $g(t)$ has a greatest maximum at $t=0$ (as it does in most cases of interest in the theory of condensing systems; see Fig. 1) we can find an asymptotic expansion[13] for $p_n(r)$ that is valid for large n. Defining

$$\mu_m=\int_0^\infty r^mf(r)dr,\quad g(t)=4\pi\sum_{m=0}^\infty\frac{(-1)^{m+1}t^{2m-2}\mu_{2m}}{(2m-1)!}. \tag{22}$$

Then, assuming that

$$g(t)=4\pi\mu_2\Big(\sum_{m=0}^\infty a_mt^m\Big)\exp\left(-\frac{t^2\mu_4}{6\mu_2}\right)$$

and comparing the coefficients of t^m with those in (22),

$$a_1=a_2=a_3=a_5=\cdots=a_{2n+1}=0$$

and

$$a_4=(\mu_6/5!\mu_2)-(\mu_4^2/72\mu_2^2).$$

[13] This approach is somewhat similar to that used in some problems in the theory of probability; cf. J. A. Carroll, Quart. J. Math. (Oxford series) **9**, 176 (1938).

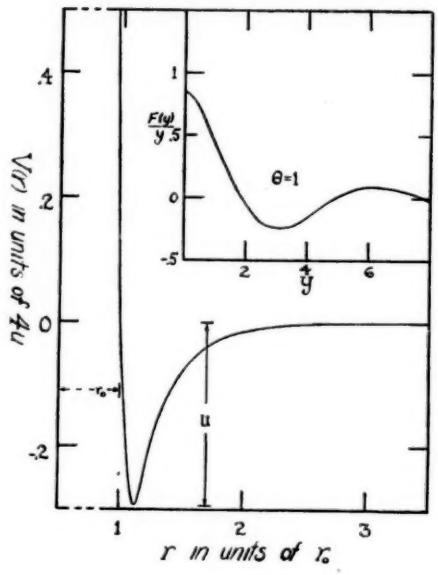

FIG. 1.

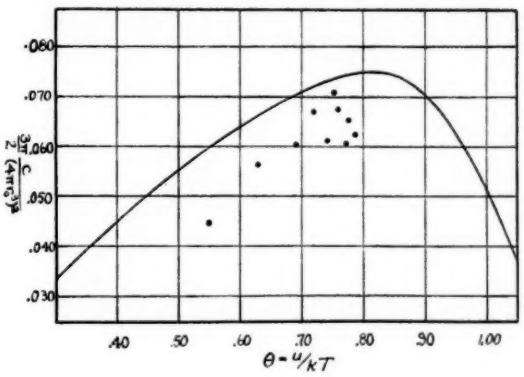

FIG. 2.

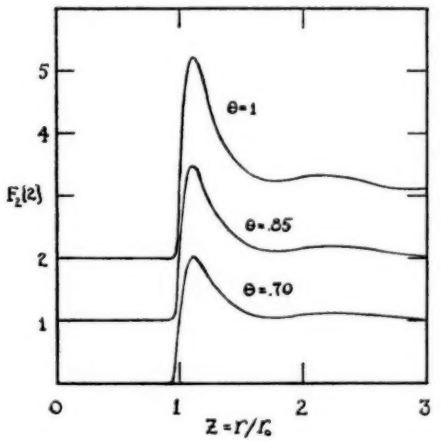

FIG. 3.

FIG. 1. Plot of the potential between pairs of molecules $V(r)$ Eq. (32), against r in units of r_0, and of $F(y)/y$, Eq. (35) against y.

FIG. 2. Plot of the third virial coefficient C in units of $(3\pi/2)/(4\pi r_0^3)^2$ against $\theta=u/kT$.

FIG. 3. The radial distribution function $F_2(r)$ as a function of $Z=r/r_0$ when the volume per molecule, v, is $2\pi r0^3/3$, which is about $(2/3)\,v$ (critical). $\theta=1$ corresponds to about $0.8\,T$ (critical).

Thus

$$g(t)=4\pi\mu_2(1+a_4t^4+\cdots)\exp(-t^2\mu_4/6\mu_2)$$

and

$$\frac{tg^{n+1}(t)}{(2\pi)^3}=\frac{t(4\pi\mu_2)^{n+1}}{(2\pi)^3}[1+(n+1)a_4t^4+\cdots]\exp\left\{-\frac{(n+1)t^2\mu_4}{6\mu_2}\right\}.$$

Substituting this in (20) and remembering that

$$\int_0^\infty t\exp(-Mt^2)\sin trdt=\frac{\pi^{\frac{1}{2}}}{4M^{\frac{3}{2}}}\exp(-r^2/4M),$$

$$\int_0^\infty t^5\exp(-Mt^2)\sin trdt=\frac{15\pi^{\frac{1}{2}}r\exp(-r^2/4M)}{16M^{7/2}}[1+0(1/M)],$$

we have

$$p_n(r_{1,n+1})\sim\frac{(2/\pi)^{\frac{1}{2}}(4\pi)^n3^{\frac{1}{2}}\mu_2^{n+5/2}}{[(n+1)\mu_4]^{\frac{3}{2}}}\exp\left[-\frac{3\mu_2r_{1,n+2}}{2(n+1)\mu_4}\right]\left[1+0\left(\frac{1}{n}\right)\right] \tag{23a}$$

and

$$p_n(0)\sim\left(\frac{2}{\pi}\right)^{\frac{1}{2}}\frac{(4\pi)^n3^{\frac{1}{2}}\mu_2^{n+5/2}}{[(n+1)\mu_4]^{\frac{3}{2}}}[1+0(1/n)]. \tag{23b}$$

The leading term of $0(1/n)$ in $p_n(0)$ is

$$\frac{135\mu_2^2}{(n+1)\mu_4^2}\left[\frac{\mu_6}{5!\mu_2}-\frac{\mu_4^2}{72\mu_2^2}\right].$$

4. More general integrals. Other components of irreducible integrals can be treated in a manner similar to that developed for ring and chain integrals. For example consider the part of β_4,

$$\frac{1}{V}\int\cdots\int f_{15}f_{12}f_{23}f_{34}f_{45}f_{13}d\{5\}, \tag{24a}$$

which corresponds to the graph of a square having one side in common with a triangle. This integral, which can be written as

$$\frac{1}{V}\int\int\int f(r_{12})f(r_{23})f(r_{31})p_2(r_{13})d\{3\}, \tag{24b}$$

is a special case of the more general class of integrals

$$s_n(0)=\frac{1}{V}\int\cdots\int f_0(r_{12})f_1(r_{23})\cdots f_n(r_{n+1,1})d\{n+1\}. \tag{25a}$$

Here, for all i, $f_i(r_{kl})=f_i(r_{lk})$, and each $f_i(r)$ is a function of the same type as $f(r)$. If, as before, we consider all the particles of the system as being contained in a cube with sides of length a,

$$s_n(r_{1,n+2})=\int_{-a/2}^{a/2}\cdots\int_{-a/2}^{a/2} f_0(r_{12})f_1(r_{23})\cdots f_n(r_{n+1,n+2})d\tau_2\cdots d\tau_{n+1}. \tag{25b}$$

The characteristic functions of the integral equations

$$\varphi(x_1, y_1, z_1; i)=\int_{-a/2}^{a/2}\int_{-a/2}^{a/2}\int_{-a/2}^{a/2} f_i(r_{12})\varphi(x_2, y_2, z_2; i)dx_2dy_2dz_2$$
$$(i=0, 1, 2\cdots, n)$$

are

$$\varphi_{k,l,m}(x, y, z; i)=a^{-\frac{3}{2}}\exp\{(2\pi i/a)(kx+ly+mz)\}$$
$$(k, l, m=0, \pm1, \pm2, \cdots).$$

So, if the development of $f_i(r)$ in terms of its characteristic functions is

$$f_i(r)=\sum_{k,l,m=-\infty}^{\infty} c_{k,l,m;i}a^{-\frac{3}{2}}\exp\{(2\pi i/a)(kx+ly+mz)\},$$

then

$$s_n(r_{1,n+2})=\frac{1}{a^3}\sum_{k,l,m}\prod_{i=0}^{n}(a^{-\frac{3}{2}}c_{k,l,m;i})\exp\frac{2\pi i}{a}[kx_{1,n+2}+ly_{1,n+2}, mz_{1,n+2}]. \tag{26}$$

Following the same procedure as in the case of all f's alike; if we let

$$a^{\frac{3}{2}}c_{k,l,m;i}=4\pi\int_0^\infty r^2f_i(r)(\sin tr/tr)dr=g_i(t) \tag{27}$$

and

$$t=\frac{2\pi}{a}(k^2+l^2+m^2)^{\frac{1}{2}},$$

we have

$$s_n(r)=\frac{1}{2\pi^2}\int_0^\infty\frac{t^2\sin tr}{tr}\prod_{i=0}^{n}g_i(t)dt \tag{28a}$$

and

$$s_n(0)=\frac{1}{2\pi^2}\int_0^\infty t^2\prod_{i=0}^{n}g_i(t)dt. \tag{28b}$$

Writing

$$g_0(t)=4\pi\int_0^\infty r^2 f(r)(\sin tr/tr)dr$$

and

$$g_1(t)=4\pi\int_0^\infty r^2 f(r)p_2(r)(\sin tr/tr)dr,$$

the special case (24a) becomes

$$\frac{1}{2\pi^2}\int_0^\infty t^2 g_0{}^3(t)g_1(t)dt,$$

and the original integration over fifteen variables has been converted to an integral over one variable.

An additional simplification is possible when the number of particles to be integrated over is large. If all the $g_i(t)$'s have their greatest maximum at $t=0$, it is easy to show, using reasoning similar to that of Section 3, that

$$s_n(r)=\frac{(4\pi)^{n+1}}{8\pi^2}\left(\prod_{i=0}^{n}\mu_{i,2}\right)\frac{\exp(-r^2/4M)}{M^{\frac{3}{2}}}\pi^{\frac{1}{2}}\left(1+\frac{15r^4}{4M^2}\sum_{i=0}^{n}a_{i,4}+\cdots\right). \tag{29}$$

Here

$$a_{i,4}=(\mu_{i,6}/5!\mu_{i,2})-(\mu_{i,4}^2/72\mu_{i,2}^2) \quad \text{and} \quad M=\sum_{i=0}^{n}(\mu_{i,4}/6\mu_{i,2}).$$

Suppose there is a largest $a_{i,4}$, and that its absolute value is A; also suppose there is a smallest $\mu_{i,4}/\mu_{i,2}$ and that its absolute value is a. Then

$$\left|\frac{\sum a_{i,4}}{M^2}\right|=\left|\frac{\sum a_{i,4}}{\frac{1}{36}\left(\sum\frac{\mu_{i,4}}{\mu_{i,2}}\right)^2}\right|\leqslant\frac{36nA}{n^2a^2}=O\left(\frac{1}{n}\right).$$

So, as $n\to\infty$, we have the asymptotic expressions

$$s_n(r)\sim\frac{(4\pi)^{n+1}}{8\pi^2}\left(\prod_{i=0}^{n}\mu_{i,2}\right)\frac{\exp(-r^2/4M)}{M^{\frac{3}{2}}}\pi^{\frac{1}{2}}\left[1+O\left(\frac{1}{n}\right)\right] \tag{30a}$$

and

$$s_n(0)\sim 3(6/\pi)^{\frac{1}{2}}(4\pi)^n\prod_{i=0}^{n}\mu_{i,2}\Big/\left(\sum_{i=0}^{n}\mu_{i,4}/\mu_{i,2}\right)^2. \tag{30b}$$

II. Application to the Calculation of Thermodynamic Functions

In order to calculate the thermodynamic properties of an imperfect gas it is sufficient to calculate

$$s_0=\sum_{k=1}^{\infty}\beta_k v^{-k}=4\pi v^{-1}\int_0^\infty r^2 f(r)dr+\sum_{k=2}^{\infty}\beta_{k,0}v^{-k}+\sum_{k=3}^{\infty}\beta_{k,1}v^{-k}+\cdots,$$

where the $\beta_{k,0}$'s are integrals over rings, the $\beta_{k,1}$'s correspond to rings with one internal connection, etc. By the proper number of differentiations and integrations of s_0 with respect to v, one can evaluate the Helmholtz free energy, the equation of state, and other thermodynamic functions.

Now, if n_{k+1} is the number of ways a $(k+1)$-membered ring can be constructed from $k+1$ molecules,

$$\beta_{k,0}=\frac{n_{k+1}}{Vk!}\int\cdots\int f_{12}\cdots f_{k+1,1}d\{\mathbf{k+1}\}.$$

4. More general integrals. Other components of irreducible integrals can be treated in a manner similar to that developed for ring and chain integrals. For example consider the part of β_4,

$$\frac{1}{V}\int\cdots\int f_{15}f_{12}f_{23}f_{34}f_{45}f_{13}d\{5\}, \tag{24a}$$

which corresponds to the graph of a square having one side in common with a triangle. This integral, which can be written as

$$\frac{1}{V}\int\int\int f(r_{12})f(r_{23})f(r_{31})p_2(r_{13})d\{3\}, \tag{24b}$$

is a special case of the more general class of integrals

$$s_n(0)=\frac{1}{V}\int\cdots\int f_0(r_{12})f_1(r_{23})\cdots f_n(r_{n+1,1})d\{n+1\}. \tag{25a}$$

Here, for all i, $f_i(r_{kl})=f_i(r_{lk})$, and each $f_i(r)$ is a function of the same type as $f(r)$. If, as before, we consider all the particles of the system as being contained in a cube with sides of length a,

$$s_n(r_{1,n+2})=\int_{-a/2}^{a/2}\cdots\int_{-a/2}^{a/2} f_0(r_{12})f_1(r_{23})\cdots f_n(r_{n+1,n+2})d\tau_2\cdots d\tau_{n+1}. \tag{25b}$$

The characteristic functions of the integral equations

$$\varphi(x_1, y_1, z_1; i)=\int_{-a/2}^{a/2}\int_{-a/2}^{a/2}\int_{-a/2}^{a/2} f_i(r_{12})\varphi(x_2, y_2, z_2; i)dx_2dy_2dz_2$$
$$(i=0, 1, 2\cdots, n)$$

are

$$\varphi_{k,l,m}(x, y, z; i)=a^{-\frac{3}{2}}\exp\{(2\pi i/a)(kx+ly+mz)\}$$
$$(k, l, m=0, \pm1, \pm2, \cdots).$$

So, if the development of $f_i(r)$ in terms of its characteristic functions is

$$f_i(r)=\sum_{k,l,m=-\infty}^{\infty} c_{k,l,m;i}a^{-\frac{3}{2}}\exp\{(2\pi i/a)(kx+ly+mz)\},$$

then

$$s_n(r_{1,n+2})=\frac{1}{a^3}\sum_{k,l,m}\prod_{i=0}^{n}(a^{-\frac{3}{2}}c_{k,l,m;i})\exp\frac{2\pi i}{a}[kx_{1,n+2}+ly_{1,n+2}, mz_{1,n+2}]. \tag{26}$$

Following the same procedure as in the case of all f's alike; if we let

$$a^{\frac{3}{2}}c_{k,l,m;i}=4\pi\int_0^\infty r^2f_i(r)(\sin tr/tr)dr=g_i(t) \tag{27}$$

and

$$t=\frac{2\pi}{a}(k^2+l^2+m^2)^{\frac{1}{2}},$$

we have

$$s_n(r)=\frac{1}{2\pi^2}\int_0^\infty\frac{t^2\sin tr}{tr}\prod_{i=0}^{n}g_i(t)dt \tag{28a}$$

and

$$s_n(0)=\frac{1}{2\pi^2}\int_0^\infty t^2\prod_{i=0}^{n}g_i(t)dt. \tag{28b}$$

Writing

$$g_0(t)=4\pi\int_0^\infty r^2f(r)(\sin tr/tr)dr$$

and

$$g_1(t)=4\pi\int_0^\infty r^2f(r)p_2(r)(\sin tr/tr)dr,$$

the special case (24a) becomes

$$\frac{1}{2\pi^2}\int_0^\infty t^2g_0{}^3(t)g_1(t)dt,$$

and the original integration over fifteen variables has been converted to an integral over one variable.

An additional simplification is possible when the number of particles to be integrated over is large. If all the $g_i(t)$'s have their greatest maximum at $t=0$, it is easy to show, using reasoning similar to that of Section 3, that

$$s_n(r)=\frac{(4\pi)^{n+1}}{8\pi^2}\left(\prod_{i=0}^{n}\mu_{i,2}\right)\frac{\exp(-r^2/4M)}{M^{\frac{3}{2}}}\pi^{\frac{1}{2}}\left(1+\frac{15r^4}{4M^2}\sum_{i=0}^{n}a_{i,4}+\cdots\right). \tag{29}$$

Here

$$a_{i,4}=(\mu_{i,6}/5!\mu_{i,2})-(\mu_{i,4}^2/72\mu_{i,2}^2)\quad\text{and}\quad M=\sum_{i=0}^{n}(\mu_{i,4}/6\mu_{i,2}).$$

Suppose there is a largest $a_{i,4}$, and that its absolute value is A; also suppose there is a smallest $\mu_{i,4}/\mu_{i,2}$ and that its absolute value is a. Then

$$\left|\frac{\sum a_{i,4}}{M^2}\right|=\left|\frac{\sum a_{i,4}}{\frac{1}{36}\left(\sum\frac{\mu_{i,4}}{\mu_{i,2}}\right)^2}\right|\leqslant\frac{36nA}{n^2a^2}=O\left(\frac{1}{n}\right).$$

So, as $n\to\infty$, we have the asymptotic expressions

$$s_n(r)\sim\frac{(4\pi)^{n+1}}{8\pi^2}\left(\prod_{i=0}^{n}\mu_{i,2}\right)\frac{\exp(-r^2/4M)}{M^{\frac{3}{2}}}\pi^{\frac{1}{2}}\left[1+O\left(\frac{1}{n}\right)\right] \tag{30a}$$

and

$$s_n(0)\sim 3(6/\pi)^{\frac{1}{2}}(4\pi)^n\prod_{i=0}^{n}\mu_{i,2}\Big/\left(\sum_{i=0}^{n}\mu_{i,4}/\mu_{i,2}\right)^2. \tag{30b}$$

II. Application to the Calculation of Thermodynamic Functions

In order to calculate the thermodynamic properties of an imperfect gas it is sufficient to calculate

$$s_0=\sum_{k=1}^{\infty}\beta_kv^{-k}=4\pi v^{-1}\int_0^\infty r^2f(r)dr+\sum_{k=2}^{\infty}\beta_{k,0}v^{-k}+\sum_{k=3}^{\infty}\beta_{k,1}v^{-k}+\cdots,$$

where the $\beta_{k,0}$'s are integrals over rings, the $\beta_{k,1}$'s correspond to rings with one internal connection, etc. By the proper number of differentiations and integrations of s_0 with respect to v, one can evaluate the Helmholtz free energy, the equation of state, and other thermodynamic functions.

Now, if n_{k+1} is the number of ways a $(k+1)$-membered ring can be constructed from $k+1$ molecules,

$$\beta_{k,0}=\frac{n_{k+1}}{Vk!}\int\cdots\int f_{12}\cdots f_{k+1,1}d\{\mathbf{k+1}\}.$$

Since $n_{k+1}=k!/2$ and $\beta_{k,0}=p_k(0)/2$, Eq. (21) implies that

$$\sum_{k=2}^{\infty}\beta_{k,0}v^{-k}=\frac{1}{4\pi^2}\int_0^\infty t^2\sum_{k=2}^{\infty}g^{k+1}(t)v^{-k}dt=\frac{1}{(2v\pi)^2}\int_0^\infty\frac{t^2g^3(t)dt}{1-g(t)/v}.$$

To find the contribution to s_0 of rings with one internal connection, we define

$$\gamma_{m,k}=\frac{1}{V}\int\cdots\int f_{12}\cdots f_{m+1,m+2}f_{m+2,1}d\{\mathbf{m+1}\}\int\cdots\int f_{m+2,m+3}\cdots f_{k+1,1}d\tau_{m+3}\cdots d\tau_{k+1}$$

and recall Eq. (19). Thus

$$\gamma_{m,k}=\frac{1}{V}\int\cdots\int f_{12}\cdots f_{m+1,m+2}f_{m+2,1}p_{k-m-1}(r_{1,m+2})d\{\mathbf{m+2}\}.$$

In s_0 each γ must be weighted with the number of ways it can be formed from $(k+1)$ molecules. This number is the product of the number of ways of forming a ring of $(k+1)$ molecules multiplied by the number of ways of inserting a single connecting bond of the desired type in the given ring. If $k+1\neq 2m+2$, this number is $(k+1)!/2$; and if $k+1=2m+2$, $(k+1)!/4$. Thus

$$\sum_{k=3}^{\infty}\beta_{k,1}v^{-k}=\sum_{k=1}^{\infty}\frac{(k+1)}{2}\gamma_{k,2k+1}v^{-(2k+1)}+\sum_{m=1}^{\infty}\sum_{k=2m+3}^{\infty}\frac{(k+1)}{2}\gamma_{m,k}v^{-k}.$$

But if we write

$$g_k(t)=4\pi\int_0^\infty r^2f(r)p_k(r)(\sin tr/tr)dr$$

and apply (28a),

$$\sum_{k=3}^{\infty}\beta_{k,1}v^{-k}=\sum_{k=1}^{\infty}\frac{k+1}{4\pi^2}v^{-(2k+1)}\int_0^\infty t^2g^{k+1}(t)g_k(t)dt+\sum_{m=1}^{\infty}\sum_{k=2m+1}^{\infty}\frac{(k+1)}{4\pi^2}v^{-k}\int_0^\infty t^2g^{m+1}(t)g_{k-m-1}(t)dt+\cdots.$$

In a similar manner expressions involving only functions of single integrals can be obtained for rings with more internal connections; however, one complication prevents the complete expansion of s_0 as a sum of simplified integrals. If one tries to apply the Fourier series method to configurations which are "tightly connected" (i.e., a bond connects every molecule in the configuration with every other one; for example β_{32}) new expressions result, but they are sums and integrals of the same "tightly connected" form in the reciprocal k, l, m space as the original ones in the x, y, z space.

To calculate the molecular distribution function $F_2\{2\}$ for imperfect gases, we will employ the expressions for chain integrals, (20) and (28a). Let the components of $H_{2,m}$ in (15) be ordered in sets $H^0_{2,m}$, $H^1_{2,m}$, $\cdots$, such that the H^0's correspond to integrals over chains without internal connections, H^1's to those with one internal connection, etc. Since the integral over a chain with n doubly connected molecules and two singly connected end molecules is $p_{n+1}(r_{12})$ when the distance between the two singly connected end molecules is r_{12}, and since this integral remains invariant under any of the $n!$ interchanges of the internal molecules,

$$H^0_{2,n}=p_{n+1}(r_{12})=\frac{1}{2\pi^2}\int_0^\infty\frac{t^2g^{n+1}(t)\sin tr_{12}}{tr_{12}}dt.$$

Thus

$$\begin{aligned}F_2\{2\}&=\exp(-V(r_{12})/kT)\left[1+\frac{1}{2\pi^2}\int_0^\infty\frac{t^2\sin tr_{12}}{vtr_{12}}\sum_{m=0}^{\infty}v^{-m}g^{m+2}(t)dt+\sum_{m=2}^{\infty}v^{-m}H^1_{2,m}+\cdots\right]\\&=\exp(-V(r_{12})/kT)\left[1+\frac{1}{2\pi^2v}\int_0^\infty\frac{t^2g^2(t)}{1-g(t)/v}\frac{\sin tr_{12}}{tr_{12}}dt+\sum_{m=2}^{\infty}v^{-m}H^1_{2,m}+\cdots\right].\end{aligned}\tag{31}$$

TABLE I. *$F(y, \theta)/y$ as a function of θ and y.*

y	$\theta=1$	$\theta=0.85$	$\theta=0.754$	$\theta=0.695$	$\theta=0.55$	$\theta=0.40$	y	$\theta=1$	$\theta=0.85$	$\theta=0.754$	$\theta=0.695$	$\theta=0.55$	$\theta=0.40$
0.00	0.8460	0.6342	0.5082	0.4409	0.2695	0.1042	5.00	0.0096	0.0111	0.0116	0.0117	0.0101	0.0100
0.50	.7191	.5320	.4262	.3544	.2042	.0613	5.50	.0618	.0540	.0492	.0464	.0399	.0332
1.00	.4569	.3194	.2581	.2004	.0810	−.0207	6.00	.0838	.0715	.0632	.0601	.0509	.0417
1.50	.1745	.0952	.0467	.0191	−.0443	−.1010	6.50	.0785	.0665	.0596	.0562	.0452	.0380
2.00	−.0516	−.0831	−.1015	−.1114	−.1335	−.1532	7.00	.0541	.0456	.0416	.0382	.0324	.0272
2.50	−.1930	−.1875	−.1846	−.1840	−.1764	−.1692	7.50	.0218	.0185	.0167	.0159	.0140	
3.00	−.2374	−.2171	−.2027	−.1946	−.1743	−.1547	8.00	−.0098	−.0070	−.0059	−.0052	−.0034	
3.50	−.2193	−.1899	−.1716	−.1623	−.1394	−.1181	8.50	−.0300	−.0243	−.0216	−.0193	−.0150	
4.00	−.1506	−.1268	−.1127	−.1049	−.0872	−.0701	9.00	−.0454	−.0327	−.0289	−.0266	−.0217	
4.50	−.0570	−.0534	−.0459	−.0416	−.0330	−.0259							

The sum over $H^1_{2,m}$ can be treated in the same manner as that over $\beta_{k,1}$ but inasmuch as it will not be used in the calculations of the next section, we do not write it out explicitly. In fact, it is possible to sum most of the series that do not involve "tightly connected" configurations, but the resulting expressions are very complicated.

III. IMPERFECT GASES WITH LENNARD-JONES POTENTIALS

The mutual potential energy function, $V(r)$, between two molecules whose distance of separation is r becomes infinite as $r\rightarrow 0$, has a negative minimum when r is the equilibrium distance of the molecules, and rapidly approaches zero as the molecules tend to infinite separation. London[14] has shown from quantum-mechanical considerations that the potential energy contribution of the attractive forces between two molecules with no permanent electric moment has a dominant term proportional to r^{-6}. Since, to find the total potential energy, a repulsive term that becomes infinite at $r=0$ must be added, Lennard-Jones[15] assumed this term to be proportional to r^{-m}. Then after calculation of the theoretical second virial coefficient from

$$B(T)=\tfrac{1}{2}\int_0^\infty 4\pi r^2(1-e^{-V(r)/kT})dr$$

with such a general $V(r)$, he found the proportionality constants and m values that gave the best agreement with experiments. Here m will be chosen to be 12 (this number gives the best results for the most kinds of molecules). Thus if u and r_0 are constants for a given molecular species

$$V(r)=4u[(r_0/r)^{12}-(r_0/r)^6], \tag{32}$$

in which the minimum value of $V(r)$ is $-u$ and occurs at $r=(\sqrt[6]{2})r_0$. The potential $V(r)$ is zero at $r=r_0$, positive for $r<r_0$ and negative for $r>r_0$. For argon[15] $r_0=3.408$ A.U. and $u=165.0\times 10^{-16}$ erg; for neon $r_0=2.743$ A.U. and $u=48.81\times 10^{-16}$ erg. With this potential function,

$$f(r)=\exp\left[-4\theta(z^{-12}-z^{-6})\right]-1, \tag{33a}$$

and

$$g(t/r_0)=(4\pi r_0^3/t)\int_0^\infty z\{\exp\left[-4\theta(z^{-12}-z^{-6})\right]-1\}\sin tz dz, \tag{33b}$$

where $\theta=u/kT$ and $z=r/r_0$. The complexity of the integrand in (33b) makes the analytical evaluation of $g(t/r_0)$ difficult, so numerical integration is resorted to.

One of the simplest quantities which can be calculated from $g(t/r_0)$ and which can be compared with experimental data is the third virial coefficient. By definition this quantity (which shall henceforth be designated by C) is given by the equation

$$Pv/kT=1+B/v+C/v^2+\cdots,$$

[14] For an up-to-date review see H. Margenau, Rev. Mod. Phys. **11**, 1, 25 (1939).
[15] J. E. Lennard-Jones, Physica **4**, 941 (1937).

TABLE II. *Values of* $\int_0^\infty y^2\left\{\frac{F(y,\theta)}{y}\right\}^2\frac{\sin yz}{yz}\,dy$.

z	$\theta=1.0$	$\theta=0.85$	$\theta=0.70$	z	$\theta=1.0$	$\theta=0.85$	$\theta=0.70$
1.0	0.150	0.075	0.041	2.2	0.147	0.084	0.042
1.2	.068	.010	−.014	2.4	.134	.080	.044
1.4	.023	−.023	−.046	2.6	.086	.055	.030
1.6	.020	−.013	−.049	2.8	.051	.034	.016
1.8	.059	−.006	−.023	3.0	.036	.012	
2.0	.115	.055	.015				

from which it follows (Eq. (4)) that $C=-2\beta_2/3$. But

$$\beta_2=\tfrac{1}{2}p_2(0)=\int_0^\infty t^2g^3(t)dt/4\pi^2.$$

therefore

$$C=-\frac{2}{3}\frac{(4\pi r_0^3)^2}{\pi}\int_0^\infty y^2\left\{\frac{F(y,\theta)}{y}\right\}^3dy, \tag{34}$$

where

$$F(y,\theta)=\int_0^\infty z\{\exp\left[-4\theta(z^{-12}-z^{-6})\right]-1\}\sin yz dz, \tag{35}$$

and $y=tr_0$. The integration of $F(y,\theta)$ is described in the Appendix and $F(y,\theta)/y$ is tabulated for various values of θ in Table I. The function

$$3\pi C/2(4\pi r_0^3)^2$$

as calculated from (34) is plotted in Fig. 2 as a function of $\theta=u/kT$, and is compared with the corresponding quantity obtained from the experimental third virial coefficients of argon.[16] Considering that the experimental C values are the result of least squaring isotherm data to fit an equation with a small number of virial coefficients while the theoretical ones are terms in an infinite series, the agreement is as good as can be expected. Actually, the deviations are of the same order as those resulting from the comparison of the data of different experimentalists. Also, a small error in r_0 would cause a rather large error in converting an experimental C to $(3\pi/2)C/(4\pi r_0^3)^2$ because r_0 is raised to such a high power in the conversion factor.

Another fundamental quantity that can easily be calculated from the $F(y,\theta)/y$ tables is the distribution function $F_2\{2\}$. Since Eqs. (31) and (35) imply (here z is written for r_{12}) that

$$F_2\{2\}=e^{-V(z)/kT}\left[1+\frac{4\pi r_0^3}{\pi v}\int_0^\infty y^2\left\{\frac{F(y,\theta)}{y}\right\}^2\frac{\sin yz}{yz}dy+\cdots\right], \tag{36}$$

the values of the integral

$$\int_0^\infty y^2\left\{\frac{F(y,\theta)}{y}\right\}^2\frac{\sin yz}{yz}dy$$

as tabulated in Table II can be used to calculate $F_2\{2\}$ up to fairly high densities. The graphs of $F_2\{2\}$ in Fig. 3 (note that the curve for $\theta=0.85$ has been raised one unit and that for $\theta=1$ by two units) behave qualitatively in the manner one would expect from physical considerations. The first peak results from the tendency of nearest neighbors of any molecule to be at a distance which corresponds to the minimum in the potential well of Fig. 1 and which is smoothed out a bit by thermal agitation. The second peak corresponds to the tendency of next nearest neighbors to occupy positions that correspond to the minimum in their mutual potential energy well with respect to the first nearest neighbors. As θ increases, the peaks sharpen as one would expect from the diminishing of thermal

[16] J. Otto, *Wien-Harms Handbuch der Experimentalphysik* (Leipzig, 1929), Vol. VIII–2, p. 151.

agitation. Experimentally, $F_2\{2\}$ is related to the Fourier transform of the intensity of x-rays scattered from the gas.[17] The plot is made at a density greater than the critical, for which, at the lower temperatures, the equations are not expected to be valid, since the series of Eq. (31) diverge.

The authors wish to thank Dr. F. Nachod for his aid with some of the calculations.

Appendix I

Integration of $I=\int_0^{\pi}\int_0^{2\pi}\exp(-2\pi ir/a)(k\cos\varphi\sin\theta+l\sin\varphi\sin\theta+m\cos\theta)\sin\theta d\theta d\varphi$.

If one defines a vector

$$\mathbf{h}=\frac{k}{a}\mathbf{i}+\frac{l}{a}\mathbf{j}+\frac{m}{a}\mathbf{k}, \qquad \exp[-(2\pi ir/a)(k\cos\varphi\sin\theta+--)]=\exp(-2\pi i\mathbf{r}\cdot\mathbf{h}).$$

Choosing a new polar coordinate system with h as polar axis, $\mathbf{r}\cdot\mathbf{h}=rh\cos\gamma$,

$$h=(1/a)(k^2+l^2+m^2)^{\frac{1}{2}}$$

and

$$I=\int_0^{\pi}\int_0^{2\pi}\exp(-2\pi irh\cos\gamma)\sin\gamma d\varphi' d\gamma=2\pi\int_{-1}^{+1}\exp(-2\pi irhy)dy=(2/rh)\sin 2\pi rh.$$

For this method of integration, which is simpler than that originally proposed, the authors are indebted to Professor Kirkwood.

Appendix II

Evaluation of $F(y,\theta)/y$

By definition

$$F(y,\theta)=\int_0^{\infty}z\{\exp[-4\theta(z^{-12}-z^{-6})]-1\}\sin yzdz.$$

It is possible to obtain an asymptotic expression when y is small by writing

$$\sin yz=yz-y^3z^3/3!+(\sin yz-yz+y^3z^3/3!),$$

for in that case (say $y<0.4$)

$$F(y,\theta)/y\sim\mu_2-\mu_4y^2/3!.$$

In a manner described by Lennard-Jones,[10] if $n\leq 4$

$$\mu_n=\int_0^{\infty}z^n\{\exp[-4\theta(z^{-12}-z^{-6})]-1\}dz=\frac{(4\theta)^{(1+n)/12}}{12}\sum_{l=0}^{\infty}\frac{(4\theta)^{l/2}}{l!}\Gamma\left(\frac{l}{2}-\frac{n+1}{12}\right).$$

For larger values of y it seems most convenient to divide the range of integration into three parts

$$F(y,\theta)=\int_0^{0.85}+\int_{0.85}^{a}+\int_a^{\infty}=I_1+I_2+I_3.$$

When $z\leq .85$, $\{\exp[-4\theta(z^{-12}-z^{-6})]-1\}\sim -1$ and

$$I_1=-(1/y^2)(\sin 0.85y-0.85y\cos 0.85y).$$

If α is fairly large one can write

$$I_3=\int_a^{\infty}z(4\theta z^{-6}-4\theta(1-2\theta)z^{-12}+\cdots)\sin yzdz.$$

The α can be chosen to make the integral involving z^{-12} as small as the error (say ϵ) desired in $F(y,\theta)$. This choice is made by noting that

$$\epsilon=\left|\int_a^{\infty}z^{-11}\sin yzdz\right|\cdot|4\theta(1-2\theta)|<\int_a^{\infty}z^{-11}dz\cdot|4\theta(1-2\theta)|=|4\theta(1-2\theta)|/10\alpha^{10}$$

and

$$\alpha<[2\theta|(1-2\theta)|/5\epsilon]^{1/10}.$$

With such a choice of α, integration by parts yields[18]

$$I_3=4\theta\int_a^{\infty}z^{-5}\sin yzdz=\frac{\theta}{\alpha}\left\{\frac{\sin\alpha y}{\alpha}\left[\frac{1}{\alpha^2}-\frac{y^2}{6}\right]+\frac{y\cos\alpha y}{3}\left[\frac{1}{\alpha^2}-\frac{y^2}{2}\right]+\frac{y^4\alpha}{6}\int_a^{\infty}\frac{\sin yz}{z}dz\right\}.$$

When y is large, integration by parts in the "other direction" gives the asymptotic expression

$$I_3\sim\frac{4\theta}{y\alpha^5}\left\{\cos\alpha y\left[1-\frac{5\cdot 6}{(\alpha y)^2}+\frac{5\cdot 6\cdot 7\cdot 8}{(\alpha y)^4}\right]+5\frac{\sin\alpha y}{\alpha y}\left[1-\frac{6\cdot 7}{(\alpha y)^2}+\frac{6\cdot 7\cdot 8\cdot 9}{(\alpha y)^4}\right]+\varphi\frac{5\cdot 6\cdot 7\cdot 8\cdot 9}{(\alpha y)^5}\right\},$$

where $|\varphi|<1$.

Unfortunately it has not been possible to find simple analytical expressions for I_2, so it must be integrated numerically.

[17] Zernicke and Prins, Zeits. f. Physik **41**, 184 (1927); Debye and Mencke, Physik. Zeits. **31**, 797 (1932).

[18] The integral $\int_a^{\infty}\sin yzdz/z$ is obtainable from $Si(ay)$ tables, cf. *Mathematical Tables* (British Association for the Advancement of Science, London, 1931). Vol. 1.

The Mechanism of Reactions Involving Excited Electronic States

II. Some Reactions of the Alkali Metals with Hydrogen[1]

JOHN L. MAGEE AND TAIKEI RI*
Princeton University, Princeton, New Jersey
(Received May 22, 1941)

Some chemiluminescent and quenching reactions of the alkali metals are considered. The reaction which leads to the luminescence of sodium in atomic hydrogen is seen to be adiabatic, and a model potential energy surface, constructed by the semi-empirical method, is found to be in qualitative agreement with the experimental observations. The lowest electronic states of the system Na^*H_2 are considered in an attempt to understand the mechanism of the non-adiabatic reaction which quenches the sodium D line. It is shown that two crossing points should occur, one of them involving a polar state. The rate of the quenching reaction is discussed in terms of the absolute reaction rate theory.

I. INTRODUCTION

IN this paper we shall be concerned with two types of reactions,

$$M+2H\rightarrow M^*+H_2, \quad (1)$$

$$M^*+H_2\rightarrow M+H_2'. \quad (2)$$

M denotes an alkali metal; the asterisk indicates electronic excitation and the prime, vibrational excitation. Reaction (1) has been studied experimentally a number of times.[2,3] It takes place readily with sodium at 200°C, slightly with potassium, and apparently not at all with rubidium and cesium. The energies of excitation for the D line (first excited level) of these four elements are 48.2, 37, 36 and 32 kcal., respectively; so there is not a *direct* relationship between magnitude of excitation and ease of occurrence. Kaplan[4] has suggested that the determining factor is the position of the vibrational levels in the H_2 molecule relative to the alkali metal energy levels. We shall see in Section II that these reactions are best understood in terms of the potential surfaces on which they occur.

The quenching reaction (2) has been studied for M = Na.[5,6] It takes place with a fairly high efficiency.

Reaction (1) is "adiabatic,"† while (2) is not. This observation is more clear on examination of Fig. 1 in which the electronic levels of the two sides of the reaction are given schematically. The zero of energy is taken as the separated atoms, and the number of doublet states at each level is given. The connection lines indicate how these reactions take place "adiabatically." In reaction (1) the M atom can gain excitation "adiabatically" due to the degeneracy of the initial state. In order for reaction (2) to take place there must be some configuration of the complex MH_2 for which the first and second electronic levels have equal energy. In Section III of this paper we shall consider small configurations of MH_2 in an effort to determine the exact mechanism of this reaction.

II. THE POTENTIAL SURFACE FOR REACTION (1)

We shall construct a model potential surface for the particular reaction with M = Na by means of the semi-empirical method. There is added simplification for linear configurations and we only consider the linear mechanism.

For the linear mechanism there are four states which must be considered, namely, the two

[1] Paper I deals with reactions of the alkali metals and halogens, J. L. Magee, J. Chem. Phys. **8**, 687 (1940).
* Assistant Professor, Kyoto Imperial University.
[2] K. F. Bonhoeffer, Zeits. f. physik. Chemie **113**, 199 (1924); **116**, 391 (1925).
[3] F. L. Mohler, Phys. Rev. **29**, 419 (1927).
[4] J. Kaplan, Phys. Rev. **31**, 997 (1928).
[5] R. Mannkopf, Zeits. f. Physik **36**, 315 (1926).
[6] V. Kondratjew and M. Siskin, Physik. Zeits. Sowjetunion **8**, 644 (1936).
† The use of this term has not always been clear. The discussion which follows will serve to define its meaning in this paper, and what we believe to be correct usage.

pairs of doublet states for Na−H−H and Na*−H−H ($^2\Sigma$). The II states do not interact with these. Thus we have a fourth-order secular equation to solve,

$$\begin{vmatrix} H_{11}-E & H_{21} & H_{31} & H_{41} \\ H_{12} & H_{22}-E & H_{32} & H_{43} \\ H_{13} & H_{23} & H_{33}-E & H_{43} \\ H_{14} & H_{24} & H_{34} & H_{44}-E \end{vmatrix} = 0. \quad (3)$$

We take

$$\Psi_1 = (\mathrm{Na}-\mathrm{H}\quad \mathrm{H})$$
$$\Psi_2 = (\mathrm{Na}\quad \mathrm{H}-\mathrm{H})$$
$$\Psi_3 = (\mathrm{Na}^*-\mathrm{H}\quad \mathrm{H})$$
$$\Psi_4 = (\mathrm{Na}^*\quad \mathrm{H}-\mathrm{H})$$

as the four bond functions.[7] Since the calculation is only to give a *model* potential surface we make a further simplification: the neglect of matrix elements between the two different degrees of excitation of Na. This reduces the problem to a solution of two quadratic equations involving Ψ_1 and Ψ_2, Ψ_3 and Ψ_4, respectively. Each of these has roots which are given by the London formula,[8]

$$E = Q \pm [\tfrac{1}{2}\{(\alpha-\beta)^2+(\alpha-\gamma)^2+(\beta-\gamma)^2\}]^{\frac{1}{2}}, \quad (4)$$

where Q is the Coulombic energy; α, β and γ are the exchange integrals for the three pairs of atoms. The energies were obtained in the customary semi-empirical manner,[9] taking the Coulombic energy as 0.2 the Morse curve energy and the exchange integral as 0.8. The data used in constructing the Morse curves are given in Table I.

It is actually just the neglected interaction (probably fairly strong) between the two states of excitation which allows reaction (1) to occur readily. This method of calculation should give the correct general form of the potential surfaces, and approximately the correct positions. There will not actually be "crossings," since there will be matrix elements to prevent it.

Figure 2(I) shows the contour surface calculated in this manner. This is the *second* surface for all configurations. The cross sections of the surface for infinite separation of H and Na, respectively, are given in 2(II) and 2(III). These show the relationship of the surface which is given in 2(I) to the other three roots of the secular equation. The curves corresponding to the contour surface are in heavy lines. The reaction path is indicated in I by means of arrows. In IV a cross section is given which goes down the reaction path and through the activated state (from *a* to *b* of 2(I)).

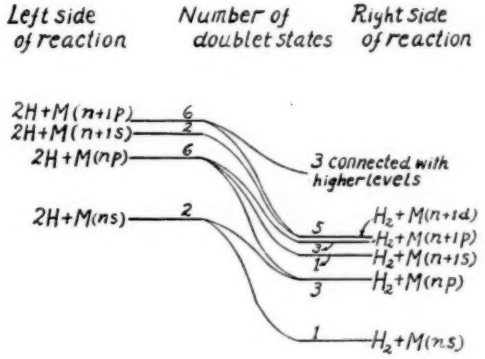

FIG. 1. Adiabatic connection of energy levels for the reactions, 2H+M (various excitations)→H_2+M (various excitations). Because of the greater degeneracy of the left side of the reaction, the M atom frequently can gain electronic excitation adiabatically.

We have stated that the method used in this work is not expected to give reliable *quantitative* results, and at this point we shall discuss briefly its shortcomings. In the first place a Morse curve is particularly poor approximation of the excited Na*−H molecule. Mulliken[10] gives evidence that this curve is actually made up of three different types of states: first Na*−H changing to a mixture of Na^+-H^- and Na−H at equilibrium separation and finally becoming pure Na−H in the repulsive region. In order to use as few states as possible we have neglected the polar states except insofar as they are represented in the Morse curve. The potential for Na*−H could have been approximated better, but in view of other errors it was not deemed necessary.

The second fault is that the approximation of the upper surfaces using the London formula is too low at infinite separation of one of the atoms. The upper (triplet) curves for H_2 in 2(III) are

[7] For discussions of bond functions see J. C. Slater, Phys. Rev. **38**, 1109 (1931); and H. Eyring and G. E. Kimball, J. Chem. Phys. **1**, 239 (1933).

[8] F. London, Zeits. f. Elektrochemie **35**, 552 (1929).

[9] H. Eyring, Trans. Faraday Soc. **34**, 3 (1937). This paper gives a detailed discussion of the semi-empirical technique and many references to earlier papers.

[10] R. S. Mulliken, Phys. Rev. **50**, 1028 (1936).

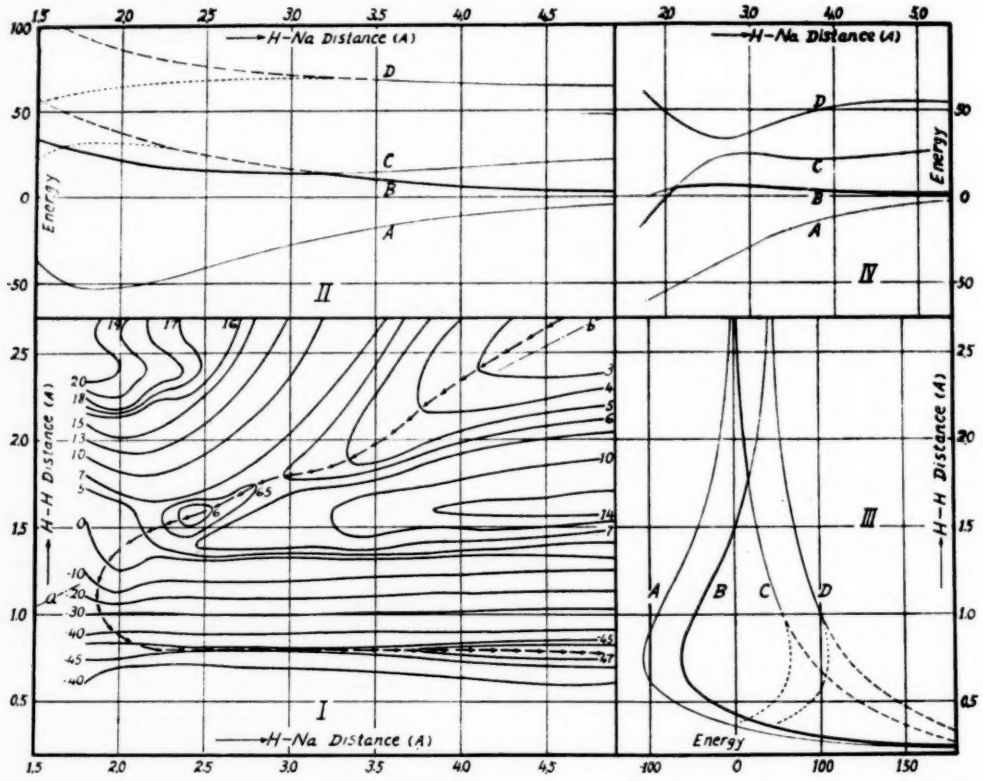

FIG. 2. In this figure, I shows the contour surface for the reaction, $2H+Na \rightarrow H_2+Na^*$. The cross sections for infinite separation of H and Na, respectively, are shown in II and III. These show the relationship of the surface given in I to the other three roots of the secular equation. A cross section going through the activated state (from *a* to *b* of I) is shown in IV.

much too low.[11] Furthermore, the approximation breaks down completely for separations smaller than equilibrium; in 2(II) and 2(III) the dotted lines show that the calculated upper states of each pair become lower in energy as $r \rightarrow 0$ whereas the actual energy rises (dashed lines are schematic).

In spite of these obvious imperfections the qualitative features of the actual potential surface should be evident from our calculated surface.

Now let us consider the luminescent reaction. One must remember that it must always *compete* with the reaction on the lower surface which combines H atoms without exciting Na, i.e.,

$$2H+Na \rightarrow H_2+Na. \qquad (4)$$

There will be no luminescence at all if the activation energy of (1) is sufficiently high. This is probably the reason for the nonluminescence of Rb and Cs. The low activation energy (calculated value $\sim$6.5 kcal.) for $2H+Na$ is a result of the strong interaction between H and Na. This interaction should decrease for the alkali metals in the order K, Rb, Cs, as evidenced by the strength of the M−H bonds. Other factors are also involved, such as polarity, differences in percentage of Coulombic energy, etc., but not much activation energy difference is necessary to account for the observed result: At 200°C, 6.0 kcal. makes a thousandfold difference in rate.

The ratio of the rates of the two reactions can be given as the ratio of the rate constants,

$$k_1'/k_4' = a \exp(-E_1/RT). \qquad (5)$$

Reaction (4) has no activation energy. The factor a is for the most part κ_1/κ_4, the ratio of the "kappa factors"[12] of the two reactions. A good

[11] James, Coolidge and Present, J. Chem. Phys. **4**, 187 (1936).

[12] κ corrects for the systems crossing the activated state and then returning to the initial state. See paper I.

estimate of κ_1 is unity. κ for the reaction,

$$3H \rightarrow H_2 + H, \qquad (6)$$

has been estimated by Eyring, Gershinowitz and Sun[13] as $\frac{1}{8}$. Taking $\kappa_4 = 0.1$ (from analogy with (6)) and the calculated activation energy 6.5 kcal. (which gives $\exp(-E_1/RT) = 10^{-6.5/2.3}$), we have

$$k_1'/k_4' = 10^{-6.5/2.3}/0.1 = 0.015.$$

This prediction is that 15 Na atoms are excited electronically for 1000 which gain only thermal energy of translation. For bright luminescence the ratio should probably be larger than this.

Mohler[3] reports a bright luminescence of an Na, H mixture at 200°C, a very slight luminescence of a K, H mixture, and none for Rb, H and Cs, H. Only the first level of excitation (D line) is observed for Na and K, as one would expect if the potential surfaces are well separated. To get higher lines there must be crossings of surfaces. The higher excitations probably do not occur because reaction (1) is so much faster; the potential surface leading to Na* ($3p$) is so much simpler than others that practically all systems going by the upper route find their way along it.

The actual mechanism may involve the formation of a triangular activated state. This seems reasonable because the part of the surface leading to the activated state is rising because of H−H repulsion. The little valley up which the reaction path runs is a result of this Na−H attraction. Having *two* strong Na−H bonds should lower this energy still further.

III. The Quenching Reaction

A. Classification of states

Let us consider the crossing of the lowest two surfaces in an attempt to determine the exact mechanism of the quenching process. It is likely that there are crossings as a result of special symmetries: The two possible cases are linear and isosceles triangular. It is easy to be sure that there are no crossings for linear configurations, since the Π surfaces must remain higher in energy than the Σ surfaces. The possibility for the isosceles triangular case is much greater since there are surfaces of different symmetries which involve strong interaction between the Na* atom and H_2.

There is a threefold orbital degeneracy for the Na*−H_2 states; two are even with respect to reflection in the plane of the three atoms, and one is odd. There is no possibility for a quenching reaction involving the odd state since this symmetry must be preserved. It corresponds to an electronic angular momentum for the complex as a whole.

Figure 3 shows the triangular system in coordinate axes. The states which we shall consider are indicated schematically for infinite Na−H_2 separation in Fig. 4. A_1 is the Schoenfliess notation (symmetry group C_{2v}) indicating the totally symmetric representation; B_1 indicates oddness with respect to the yz plane.

The lowest state—and consequently the final state for the quenching process—is 1. In order to have a chance of crossing to this from the upper states, the initial upper state must have B_1 symmetry. Let us now consider the possibility for a B_1 state having an energy lower than state 1 for some particular configuration.

Figure 5 illustrates schematically the expected behavior of states 1, 2 and 3. Briefly, it appears that for some configuration the polar B_1 state should be the lowest for the system. The electron affinity of H_2 has been estimated to be −46.5 kcal.[14] and the ionization potential of Na is 118 kcal. We calculate that at 2A separation the polar state has zero energy relative to Na−H_2 infinitely separated. The lowest A_1 state is certainly higher than this due to the exchange repulsion. Figure 5 is not accurate in that H_2 and H_2^- have different radii. H_2^- has an r_0 value twice as large as H_2;[14] so H_2+Na* cannot

TABLE I. *Morse curve constants.*
$E = D'\{\exp[-2a(r-r_0)] - 2\exp[-a(r-r_0)]\}$

Molecule	D' (kcal.)	a	r_0(A)
H−H	108.6	1.94	0.74
Na−H	53.3	1.047	1.888
Na*−H	34.37	0.373	3.03

[13] Eyring, Gershinowitz and Sun, J. Chem. Phys. **3**, 786 (1935).

[14] Hirschfelder, Taylor and Eyring, J. Chem. Phys. **4**, 479 (1937).

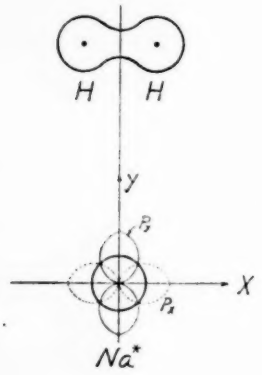

FIG. 3. The NaH_2 system in coordinate axes.

actually go smoothly to $H_2^- + Na^+$ at the point *a* of Fig. 5 on approaching. There is a connection made to indicate that the reaction is adiabatic; the nuclei must actually come in closer and the H atoms must separate considerably. In all probability the system can reach the lowest point with little or no activation energy. At the point *b* there is resonance of state 1 with state 4. There are probably two places where transition can be made between the lowest B_1 and A_1 surfaces: at *c* and *d* in Fig. 5.

The transition is strictly forbidden for isosceles triangular configuration, but is allowed for slightly distorted triangular complexes.

Now let us consider briefly the reasons for believing the pure $Na^* - H_2$ states to be attractive. Calculations by the Heitler-London method for three hydrogen-like atoms, two in *s* states and one in a *p* state, led to this result.[15] Both A_1 and B_1 triangular complexes were very stable. The reason for this result was partly because of the increased importance of the Coulombic binding: The fraction of Coulombic energy was found to be about 0.5 (rather than 0.2 used earlier in this paper). Using the semi-empirical method and 0.5 Coulombic energy, a binding energy of 15 kcal. is calculated for the complex Na^*H_2 (with respect to dissociation into $Na^* + H_2$).

Thus it appears possible that the mechanism of the quenching reaction is first the formation of a Na^*H_2 complex followed by an "internal quenching" and dissociation into $Na + H_2$. A more detailed consideration of the rate of reaction may throw more light upon the question.

[15] J. L. Magee, J. Chem. Phys. **8**, 677 (1940).

B. Rate of the quenching reaction

In order to calculate the rate of the reaction we should know the activated state. Two possibilities present themselves: (a) the formation of the M^*H_2 complex is rate determining; or (b) the transfer between the two surfaces is rate determining. We shall only consider a rate expression for case (a), since not enough of the details of the surfaces are known for case (b) calculation. Actually, it is possible to calculate the rate of a reaction by considering the rate of systems passing any point on the reaction path, provided this can be properly corrected (with a κ factor). Since all complexes quench with definite probability it seems that the rate of the association reaction is a good way to consider the problem.

Since the Na^*H_2 complex is most likely exothermic (see above) this problem is similar to that of atomic association discussed by Eyring, Gershinowitz, and Sun.[13] Gorin[16] has discussed the association of free radicals. For these reactions there is an activated state due to the rotational energy of the complex. The potential of the rotational energy acts against the attractive potential and creates a maximum which is at a different separation for each rotational quantum number. If we assume that a potential $E(r)$ which depends only upon the distance between Na^* and the center of H_2 acts between H_2 and Na^*, and that the properties of H_2 remain the same at the activated state, we get for the rate constant,

$$k_2' = (\tfrac{1}{3})\kappa \frac{kT}{h} \frac{h^3}{(2\pi\mu kT)^{\frac{3}{2}}} \cdot Z, \qquad (7)$$

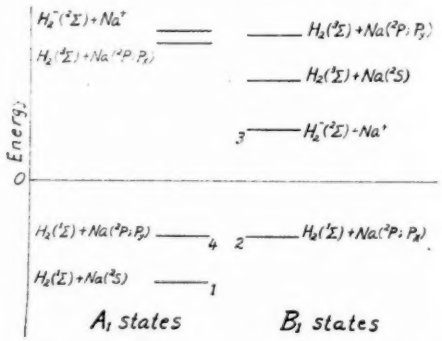

FIG. 4. Schematic representation for some of the lower electronic states of $Na - H_2$, given for infinite $Na - H_2$ separation.

[16] Gorin, Acta Physicochimica, USSR, **9**, 681 (1938).

where

$$\mu = m_{H_2} \cdot m_{Na}/(m_{H_2}+m_{Na});$$

and

$$Z=\sum_{J=1}^{J_m}(2J+1)\exp-\left\{\frac{J(J+1)h^2}{8\pi^2\mu r_e^2}-E(r_e)\right\}\Big/kT,$$

r_e is the separation H_2-Na at the activated state and depends upon J. J_m is the maximum rotational quantum number which will permit complex formation. κ corrects for the complexes which dissociate without quenching, and the $\frac{1}{3}$ factor is statistical: of the three possible states which may be formed only the B_1 state can lead to quenching (see Part A of this section).

It is interesting to compare this formula to ordinary collision theory, on which we obtain

$$k_2' = 2r^2(2\pi kT/\mu)^{\frac{1}{2}}. \qquad (8)$$

Setting

$$\kappa Z/3 = 8\pi^2\mu r^2 kT/h^2 \qquad (9)$$

in (7) one, of course, obtains (8). Thus we can use (9) to define a radius r and cross section πr^2 for the process. Z is to be evaluated graphically.[13]

For $E(r)$ we use the Morse curve,

$$E(r_e) = 15.0\{\exp[-0.746(r_e-3.0)] - 2\exp[-0.373(r_e-3.0)]\}. \qquad (10)$$

Energy is in kcal. and distance in angstrom units. The part in the braces is practically the same as for Na^*-H (see Table I).

The temperature used in Kondratjew's[6] quenching experiments was about 750° absolute. Using our calculated value of $r=7.64$A (under the assumption that $\kappa=1$), we calculate a cross section of $18.34\cdot10^{-15}$ cm². The experimental value is $1.57\cdot10^{-15}$ cm². The calculated value is about a factor of ten too large, and the discrepancy must be put on κ, i.e., $\kappa \cong \frac{1}{10}$.

The kinetic theory cross section is $3.12\cdot10^{-15}$ cm². The larger value which we obtained was, of course, due to the attractive potential. This calculation indicates the possibility of obtaining cross sections for quenching processes which are far in excess of the kinetic theory values. Although smaller for Na^*+H_2, observed values frequently are larger than kinetic theory cross section by a factor of ten.

Let us consider κ in more detail. This is the probability that there will be an internal quenching once the complex is formed, and should depend upon J. Large rotational energies of the complex destroy the interaction among the various vibrations and decrease the life of the complex. If we assume that $\kappa=1$ for values of J which give the complex less than $2kT$ rotational energy, and $\kappa=0$ for all larger values of J, we calculate $r=2.5$A, $\pi r^2 = 1.97\cdot10^{-15}$ cm².

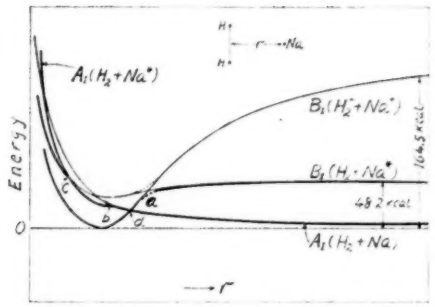

FIG. 5. Schematic illustration of the behavior of the lowest A_1 state and the two lowest B_1 states. The polar B_1 state is actually for a larger H_2 separation and does not join smoothly with the other at the point a; the connection is, of course, adiabatic. At the point b, another A_1 state (state 4 in Fig. 4) becomes lowest, and we have only shown this state for small $Na-H_2$ separations to avoid complication. It appears that crossing between A_1 and B_1 states which can lead to transfers between them (and consequently a successful quenching reaction) occur at the points c and d. In all probability, either of these points can be reached without activation energy.

Increasing the value of the attractive energy increases the cross section. If the 15 kcal. of Eq. (10) are increased to 30, r becomes 8.75A and $\pi r^2 = 24.09\cdot10^{-15}$ cm². Decreasing this energy to 3 kcal. gives $r=4.59$A, $\pi r^2 = 6.61\cdot10^{-15}$.

Kondratjew and Siskin[6] have shown that the quenching effectiveness for a number of molecules (O_2, N_2, CO, NO, I_2) is related in a general way to the strength of the bonds which the atom in the molecules make with Na.

Other factors which could vary the cross section on this model are: a of the Morse potential, and μ the reduced mass. The cross section appears to be practically insensitive to variation in μ, but changes considerably with a. However, this factor should remain about the same for a given degree of excitation of an atom, independent of the quencher.

C. Other quenching reactions

The quenching reactions of K, Rb, and Cs with H_2 have not been studied. The interaction

of H_2 with these metals is presumably weaker (see Section II) than with Na, and consequently one expects a smaller cross section for quenching. The potential surfaces should be qualitatively the same for all alkali metals.

There are quenching mechanisms which are strictly adiabatic. For example,

$$Hg(^3P_1)+H_2 \rightarrow Hg+2H, \qquad (11a)$$

$$\rightarrow HgH+H. \qquad (11b)$$

These do not take place by the mechanism discussed above (IIIA), but are chemical reactions of the type of reaction 1, and the potential surface is qualitatively similar to that shown in Fig. 2. The activation energy is most likely small, if not zero. It is, of course, impossible to choose between (11a) and (11b) without calculation, since they both take place on the same potential surface. The most abundant product depends upon the nature of the potential surface. It is probable, however, that most of the HgH molecules which would be formed by (11b) would have enough vibrational energy to dissociate.

The quenching reaction of Na,

$$Na^*+H_2 \rightarrow 2H+Na, \qquad (12)$$

requires an activation energy ($\sim$56 kcal. from Fig. 2) and is consequently of no importance.

The crossing of potential surfaces which was discussed in IIIA does not depend as heavily on the symmetry arguments as might be supposed at first. The nature of crossing points has been discussed by Neumann and Wigner[17] and more recently by Teller.[18] They show that, in general, two parameters must be varied to bring about a crossing. In the symmetrical case discussed above the two parameters were: (1) the *kind* of triangle which the system forms, (2) the *size* of the triangle. To cause a crossing we first chose an isosceles triangle so that two exchange integrals (α, β) would be equal. All matrix elements which contained ($\alpha-\beta$) as a factor then vanished and states were divided into noncombining A_1 and B_1 classes. Now a variation of the height of the triangle changed the relative positions of the diagonal terms and was found to bring about crossings between non-interacting surfaces.

For unsymmetrical systems (such as $CO-Na^*$) it is not for isosceles triangular configurations that these same matrix elements vanish, nor do they vanish all at once as for the symmetrical case; but for some particular kind of triangle each of these same nondiagonal matrix elements vanishes, and a variation of the size of the triangle can bring about crossing points.

Teller[18] has discussed the rate of change from one surface to another in terms of the varied parameters.

We would like to thank Professor Henry Eyring for advice and criticism of this work, and also Professor G. K. Rollefson for reading the manuscript and offering suggestions. One of us (J. L. M.) would like to acknowledge valuable discussions with Professor Eugene Wigner.

[17] J. Neumann and E. Wigner, Physik. Zeits. **30**, 467 (1929).
[18] E. Teller, J. Phys. Chem. **41**, 109 (1937).

Semi-Empirical Calculations of Activation Energies

JOSEPH O. HIRSCHFELDER
Department of Chemistry, University of Wisconsin, Madison, Wisconsin
(Received May 16, 1941)

The predictions of the Eyring semi-empirical scheme for calculating activation energies are compared with the existing experimental data. It is found that in most cases this agreement is satisfactory. However, the experimental data are not sufficiently accurate to make this scheme appear unique. The experimental activation energies seem to be functions only of the binding energies and do not depend in an important way on either the size of the atoms or on the diatomic force constants. If the reaction $a+bc\rightarrow ab+c$ is exothermic, it is found that the activation energy is $0.055D'_{bc}$, where D'_{bc} is the energy of the bond bc. This formula is derived from the semi-empirical scheme on the assumption that the attraction between the distant atoms a and c is zero. For exothermic four atom reactions $ab+cd\rightarrow ac+bd$, it is found that the activation energy is $0.28(D'_{ab}+D'_{cd})$. The numerical factor was adjusted to fit the H_2+I_2 reaction and although, in most cases, this gives activation energies in agreement with the semi-empirical values no mathematical connection has been made.

THE development of semi-empirical schemes for calculating the activation energies of chemical reactions is an attempt to place the intuition of the skilled organic chemists on a mathematical basis. The ideal formulation would use strict quantum-mechanical reasoning to relate the activation energies to simpler and more easily measurable physical properties. But molecular quantum mechanics has not yet advanced sufficiently far for this purpose and we must be content with determining the functional relationships from a rough theoretical treatment and evaluate the proportionality constants empirically. The method, as developed by Eyring and his co-workers, is sufficiently flexible so that it can be made consistent with any set of chemical facts and still agree with the basic principles of quantum mechanics. Its use is purely as an interpolation formula and its justification must be based on the accuracy of its predictions. The results appear to be as satisfactory as the experimental data permit. Within the last ten years about a hundred activation energies have been calculated and it is only in a few exceptional cases that these values do not agree with the experimental data to within ten kilocalories. However, there are very few reactions in which the mechanism is certain and the activation energy is well known.

For example, the thermal reaction of H_2 and I_2 is the only four-atom reaction which kineticists would place in this class. Thus the semi-empirical scheme awaits further experimental observations to test its accuracy. The purpose of this paper is to examine the present empirical status of the semi-empirical scheme in search for systematic errors. As a by-product we find two simple rules for calculating activation energies which give as good agreement with experiments as do the more laborious calculations.

The semi-empirical scheme requires two basic assumptions:

(1) The first-order perturbation method is adequate for calculating the interactions between atoms and molecules.

(2) The integrals which occur in the first-order perturbation scheme do not involve more than two atoms at a time and they may be related to corresponding integrals belonging to hypothetical diatomic molecules.

At the present time, the first-order perturbation method provides the most satisfactory quantum-mechanical theory of valence. The more rigorous theories tend to obscure the importance of a chemical bond. Unfortunately, the variational calculations of Coolidge and James,[1] and of Hirschfelder, Eyring and Rosen[2] have shown that the first-order perturbation scheme is not applicable for the reaction of a hydrogen

[1] A. S. Coolidge and H. M. James, J. Chem. Phys. **2**, 811 (1934).

[2] J. Hirschfelder, H. Eyring and N. Rosen, J. Chem. Phys. **4**, 121 and 170 (1936); J. Hirschfelder, H. Diamond and H. Eyring, J. Chem. Phys. **5**, 695 (1937); D. Stevenson and J. Hirschfelder, J. Chem. Phys. **5**, 933 (1937); J. Hirschfelder, J. Chem. Phys. **6**, 795 (1938).

atom with a hydrogen molecule. Furthermore, we may see from the work of Ikehara and Rosen[3] that the overlap integrals for Li_2, Na_2, and K_2 are almost as large as the overlap integral for H_2 so that we have the same objection to this approximation in the case of the alkalis as we have in the case of the hydrogen reactions. Perhaps, reactions involving carbon are better adapted to the use of the first order perturbation method, or at least this question will bear further investigation. The best evidence that this might be the case is that this method has been singularly successful in predicting the energy of resonance between various Lewis configurations. The second assumption is really the keystone of the semi-empirical scheme. London[4] was the first one to approximate the complicated integrals of molecular systems by two atom integrals. Here again, the variational calculations for $H+H_2$ have shown this approximation to be untenable and, here again we must raise the question whether perhaps the one system we have studied is not an exception. The two assumptions may or may not be justifiable, but at least they provide the most plausible basis for a semi-empirical scheme. The paper of Gorin, Walter and Eyring[5] on reactions of a hydrogen atom with methane provides the best example of how these assumptions can be used to calculate activation energies.

Most semi-empirical calculations require additional and less palatable assumptions in the interests of computational facility. The most usual of these is due to Eyring. He assumed:

(3) The Coulombic energy is a certain fraction of the total binding energy of a diatomic molecule. This fraction, n, is the same for all internuclear distances and is usually taken to be the same for all diatomic molecules.

This assumption permits all of the integrals for a complicated molecule to be expressed in terms of the spectroscopically observed binding energies of diatomic molecules. The calculation of activation energies then becomes a simple task. Whole energy surfaces can be constructed and the intimate details of intermolecular actions become apparent. Regardless of ultimate validity, this assumption has already served to uncover many qualitative features of reaction kinetics. For example, Albert Sherman was able to show that the distances between the atoms and molecules determined the catalytic activity of a surface. Then Henry Eyring predicted that hydrogen and fluorine would not explode without a catalyst—a notion which seemed like heresy until it was subsequently verified by experiment. Eyring developed the idea of a constant fraction of Coulombic energy after studying the calculations of Heitler-London and of Sugiura[6] of the Coulombic and exchange energies of the H_2 molecule. Figure 1 shows the variation of the ratio of the Coulombic to the total binding energy as a function of the internuclear separation. When the atoms are at their equilibrium separation, the Coulombic energy vanishes. As the atoms are pulled apart, the Coulombic energy rises abruptly to 0.14 of the total binding energy and remains approximately the same until very large separations are reached. The notion of a constant percentage Coulombic energy, at least in the case of hydrogen, seems to be justified when the system is expanded, as it is near the activated state during a chemical reaction. The fact that the approximation breaks down at small separations results in spurious minima in the potential energy surfaces which have been criticized repeatedly.[7] The fact that n is equal to 0.14 for H_2, of course, tells us nothing about reactions involving some other diatomic molecule. All too generally, it has been assumed that for all molecules this fraction must remain 0.14. The fallacy of this assumption is borne out in the case of the alkalis where we have the calculations of Ikehara and Rosen similar to those of Heitler-London and Sugiura for H_2 to show that for Li_2, n should be 0.23; for Na_2, n should be 0.32; and for K_2, n should be 0.38. Similarly the calculations of Voge[8] for the C−H bond show that in that case n should be approximately 0.63. It was the intention of Eyring and of his coworkers to use one value for n, say $n=0.14$, for the sake of simplicity and let the empirical

[3] N. Rosen and S. Ikehara, Phys. Rev. **43**, 5 (1933).
[4] F. London, Zeits. f. Physik **46**, 455 (1928); **50**, 24 (1928).
[5] E. Gorin, J. Walter and H. Eyring, J. Am. Chem. Soc. **61**, 1876 (1939).
[6] Y. Sugiura, Zeits. f. Physik **45**, 484 (1927).
[7] L. S. Kassel, *Kinetics of Homogenous Gas Reactions* (Chemical Catalog Company, 1932), p. 57.
[8] H. Voge, J. Chem. Phys. **4**, 581 (1936).

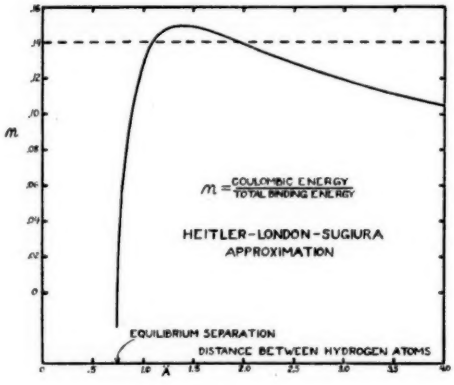

FIG. 1.

agreements of their activation energy calculations indicate what changes should be made. Unfortunately the experimental activation data at the present time are so incomplete and uncertain that this has not been feasible.

There are two more assumptions which are sometimes made in semi-empirical calculations which should be regarded as dangerous:

(4) All valence bonds are treated on the same footing regardless of whether they involve *s*, *p*, or *d* electrons.

(5) Neighboring groups do not influence the activation energy appreciably.

Organic chemists have some feeling for the second of these approximations and can even estimate for us the error made on this account. Much work is in progress to estimate the effect of neighboring groups from a quantum-mechanical standpoint. However, we have little feeling for the effect which different types of valence electrons have on the course of a chemical reaction. For example, the work of Magee[9] indicates that the activated state for a three atom reaction in which one of the valence electrons is in the *p* state may be triangular instead of linear as had previously been supposed. Thus the nature of the binding electrons may completely change the shape of the potential energy surfaces. This interesting possibility will bear considerable further investigation. However, this point should not be stressed because the experimental activation energies for three atom reactions involving *p* electrons seem to be in no way different in magnitude from those where only *s* electrons are involved.

[9] J. Magee, J. Chem. Phys. **8**, 677 (1940).

Even if all of the above assumptions were valid, it would be necessary to use an accurate expression for the potential energy of the various diatomic molecules. The Morse functions have been used for this purpose. If w_{ab} is the energy of the diatomic molecule ab in which the nuclei are separated a distance r_{ab}, the Morse functions give:

$$w_{ab}=D'_{ab}[-2\exp(a_{ab}(r_{ab}-(r_0)_{ab}))+\exp(-2a_{ab}(r_{ab}-(r_0)_{ab}))]. \quad (1)$$

Here D'_{ab}, $(r_0)_{ab}$, and a_{ab} are constants which are usually determined from spectroscopic data. The three constants of the Morse functions are adjusted so as to represent accurately the potential energy of the diatomic molecule in the vicinity of the equilibrium separation. It is well known that these functions do not correspond closely to the true energy of the diatomic molecules for large separations. Thus Hylleraas,[10] Rydberg,[11] Coolidge, James and Vernon,[12] Hulburt and Hirschfelder,[13] etc., have been working on improved forms for the potential energy, and it is tacitly understood that these functions should be incorporated in the semi-empirical calculations as soon as they are generally available. The error which the Morse functions make in the activation energy for three atom reactions is usually small since the neighboring atoms are close together where the Morse functions are accurate and the distant atoms are too far apart to make an appreciable energy contribution. However, errors of the order of ten kilocalories can be expected in four atom reactions where some of the internuclear separations are for intermediate distances where the Morse functions have the greatest error.

I. Reactions Between an Atom and a Diatomic Molecule

In order to calculate the activation energy for the exothermic reaction

$$ab+c\rightarrow a+bc, \quad (2)$$

[10] E. Hylleraas, Zeits. f. Physik **96**, 661 (1935).
[11] R. Rydberg, Zeits. f. Physik **73**, 376 (1932); **80**, 514 (1933).
[12] A. S. Coolidge, H. M. James and E. L. Vernon, Phys. Rev. **54**, 726 (1938).
[13] H. M. Hulburt and J. Hirschfelder, J. Chem. Phys. **9**, 61 (1941).

TABLE I.

REACTION $a+bc \rightarrow ab+c$	HEAT OF REACTION	Eactivation (EXPERIMENTAL)	$0.055D_{bc}'$	PUBLISHED SEMI-EMPIRICAL CALCULATIONS OF E_{act} $n=0.10$	$n=0.14$	$n=0.20$
$H+H_2 \rightarrow H_2+H$	0	6.2 ± 1[1] {6.0[2] 7.0±.5[3]	6.0	10,[12] 11[13]	7.9[14]	7.63[15]
$H+HCl \rightarrow H_2+Cl$	+7.7	4.5[1] {6±1[4] 4.2±.3[5]	5.6	14.7,[16] 12.7[13] 16.3[14]	11.4[14]	10.3[17]
$H+HBr \rightarrow H_2+Br$	+16.4	1.2[1] {1.2[6] 1.3[7]	4.7	9.5,[13] 13.9[14]	10.4[14]	7.0[17]
$H+HI \rightarrow H_2+I$	+32.7	1.5[8]	3.9	10.6[14]	7.7[14]	
$H+Cl_2 \rightarrow HCl+Cl$	+44.8	2[1] {4.9±1[4] 2.2±.3[5]	3.1	0,[13] 3,[16] 4[14]	2.7[14]	
$H+Br_2 \rightarrow HBr+Br$	+41.1	1.2[9]	2.5	0,[13] 3[14]	2.1[14]	
$H+I_2 \rightarrow HI+I$	+34.6	0[8]	1.9	0,[13] 2.5[14]	1.8[14]	
$F+H_2 \rightarrow HF+H$	+82	7.5±1.5[10]	6.0	5,[13] 10.6[14]	6.3[14]	
$H+HO \rightarrow H_2+O$	+2.5	4.5±2[11]	5.8	7.5[14]		

[1] H. J. Schumacher, *Chemische Gasreaktionen* (Theodor Steinkopff, 1938).
[2] A. Farkas, Zeits. f. physik. Chemie **B10**, 419 (1930).
[3] K. H. Geib and P. Harteck, Zeits. f. physik. Chemie (Bodenstein Festband), p. 849 (1931).
[4] W. H. Rodebush and W. C. Klingelhöfer, J. Am. Chem. Soc. **55**, 130 (1933).
[5] See A. Sommer, Dissertation (Berlin, 1934) together with L. van Müffling, Dissertation (Berlin, 1936).
[6] M. Bodenstein and Lutkemeyer, Zeits. f. physik. Chemie **114**, 208 (1924).
[7] F. Bach, K. F. Bonhoeffer and Moelwyn-Hughes, Zeits. f. physik. Chemie **B27**, 71 (1934).
[8] K. F. Bonhoeffer and L. Farkas, Zeits. f. physik. Chemie **132**, 235 (1928).
[9] M. Bodenstein and S. C. Lind, Zeits. f. physik. Chemie **57**, 168 (1907).
[10] M. Bodenstein and Jockusch, Zeits. f. anorg. allgem. Chemie **231**, 24 (1937).
[11] H. von Hartel and M. Polanyi, Zeits. f. physik. Chemie **B11**, 97 (1930).
[12] H. Eyring and M. Polanyi, Naturwiss. **18**, 914 (1930).
[13] H. Eyring, J. Am. Chem. Soc. **53**, 2546 (1931). No corrections for zero-point energies.
[14] A. Sherman and H. Eyring (unpublished paper presented at Washington Meeting of American Chemical Society 1933). Presumably the zero-point energies were neglected.
[15] J. Hirschfelder, H. Eyring, and B. Topley, J. Chem. Phys. **4**, 170 (1936). This value of the activation energy agrees with experiment when corrected for the zero-point energies.
[16] G. Kimball and H. Eyring, J. Am. Chem. Soc. **54**, 3876 (1932). No corrections for zero-point energies.
[17] A. Wheeler, B. Topley, and H. Eyring, J. Chem. Phys. **4**, 178 (1936).

it is necessary to know the total energy, E, of the system of three atoms a, b, and c for all of their internuclear separations r_{ab}, r_{bc}, and r_{ac}. According to the constant percentage Coulombic scheme (CPC), this energy is:

$$E=n(w_{ab}+w_{bc}+w_{ac})-(1-n)[w_{ab}^2+w_{bc}^2+w_{ac}^2 - w_{ab}w_{bc}-w_{ab}w_{ac}-w_{bc}w_{ac}]^{\frac{1}{2}}+D_{ab}'. \quad (3)$$

Here n is the fraction of the total energy which is Coulombic and w_{ab}, etc., have the same significance as before. It is easy to show from this equation that for any particular value of r_{ab} and r_{bc} the energy of the system is lowest when the three atoms are in a line. Thus the activated state is a linear configuration. Of course, corrections are always made in calculating the absolute rate of a chemical reaction for the systems which react by paths other than the energetically easiest reaction path. The zero-point energy does not vary appreciably (by more than one or two kilocalories) as we proceed along the reaction path, so that it will be safe in this discussion to assume that the zero-point energy is the same in the initial state as it is in the activated state. This simplifies the calculations without affecting the conclusions. Table I shows how the calculated activation energies compare with the experimental values. Of the nine reactions for which accurate experimental data are known, the semi-empirical scheme with $n=0.14$ gives satisfactory agreement in six cases and poor agreement in three cases. The poor agreement is for the reactions of halogen acids with a hydrogen atom, where the central atom (hydrogen) is so small that according to the Morse curves the energy of interaction between the outside atoms is appreciable. In the six cases where the semi-empirical calculations agree with experiment, the interaction between the most distant atoms is very small. This suggests that the error may arise from the Morse curves giving too much interaction energy for atoms which are far apart, and this is shown independently by the potential energy curves of Hulburt and Hirschfelder.

Perhaps, if we take the energy of interaction between the outside atoms to be zero, i.e., $w_{ac}=0$, we would arrive at a better approximation to reality than is given by the Morse curves.

In any case this assumption leads to an interesting simplication of the semi-empirical scheme. With $w_{ac}=0$, the energy according to Eq. (2) becomes

$$E=n(w_{ab}+w_{bc})-(1-n)(w_{ab}^2+w_{bc}^2-w_{ab}w_{bc})^{\frac{1}{2}}+D'_{ab}.$$

Figure 2 shows how the energy depends on w_{ab} and on w_{bc}. The stationary states are determined by the two conditions:

$$\frac{\partial E}{\partial r_{ab}}=\left[n-\left(\frac{1-n}{2}\right)\frac{2w_{ab}-w_{bc}}{(w_{ab}^2+w_{bc}^2-w_{ab}w_{bc})^{\frac{1}{2}}}\right]\frac{\partial w_{ab}}{\partial r_{ab}}=0,$$
$$\frac{\partial E}{\partial r_{bc}}=\left[n-\left(\frac{1-n}{2}\right)\frac{2w_{bc}-w_{ab}}{(w_{ab}^2+w_{bc}^2-w_{ab}w_{bc})^{\frac{1}{2}}}\right]\frac{\partial w_{bc}}{\partial r_{bc}}=0. \quad (4)$$

There are three solutions to these equations, one minima and two saddle points. The higher of these two saddle points is the activated state.

If the reaction $ab+c$ is exothermic, the activated state is given by the conditions:

$$\frac{\partial w_{ab}}{\partial r_{ab}}=0, \quad n-\left(\frac{1-n}{2}\right)\frac{2w_{bc}-w_{ab}}{(w_{ab}^2+w_{bc}^2-w_{ab}w_{bc})^{\frac{1}{2}}}=0. \quad (5)$$

The solution to these equations is

$$w_{ab}=-D'_{ab}, \quad w_{bc}=-D'_{ab}/2\left[1-n\left(\frac{3}{1-2n}\right)^{\frac{1}{2}}\right]. \quad (6)$$

So that

$$E_{\text{act}}=D'_{ab}/2[2-3n-(3(1-2n))^{\frac{1}{2}}]. \quad (7)$$

The activation energy for an exothermic reaction then only depends on the strength of the bond broken and the fraction of the energy which is assumed to be Coulombic. Thus, if $n=0.14$

$$E_{\text{act}}=0.055D'_{ab}. \quad (8)$$

Table I shows that this simple rule for activation energies gives good agreement with experiment for all nine reactions. Figure 3 shows how the activation energy varies with the fraction of the total energy which is assumed to be Coulombic. Thus reactions involving the alkalis which have M between 0.23 and 0.38 may be expected to have very small activation energies and this is borne out qualitatively by experiment.

The other saddle point is found by interchanging ab and bc in Eqs. (6). The energy of the

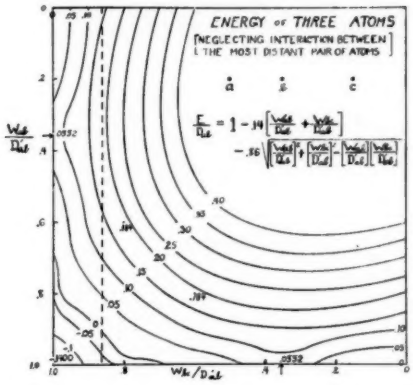

FIG. 2.

system for this configuration is:

$$E_{\text{sad}}=D'_{ab}-D'_{bc}/2[3n+(3(1-2n))^{\frac{1}{2}}], \quad (9)$$

so that if $n=0.14$

$$E_{\text{sad}}=0.055D'_{bc}-(D'_{bc}-D'_{ab}). \quad (10)$$

The requirement that the reaction as written be exothermic insures that this energy is lower than the activation energy.

Between these saddle points there is a position of minimum energy which may correspond to a metastable triatomic molecule. It is given by the conditions:

$$\frac{\partial w_{ab}}{\partial r_{ab}}=0, \quad \frac{\partial w_{bc}}{\partial r_{bc}}=0, \quad (11)$$

which have the solutions:

$$w_{ab}=-D'_{ab} \quad \text{and} \quad w_{bc}=-D'_{bc}.$$

So that

$$E_{\min}=-n(D'_{ab}+D'_{bc})-(1-n)(D'^2_{ab}+D'^2_{bc}-D'_{ab}D'_{bc})^{\frac{1}{2}}+D'_{ab}.$$

The existence of these minima are a very characteristic feature of the semi-empirical scheme and are not just due to our neglect of W_{ac}. If we had included the interactions between the distant atoms in our calculations r_{ab} and r_{bc} would be expanded slightly beyond their equilibrium values and the depth of the minimum would not be as pronounced. The variational calculations for the energy of $H+H_2$ do not show the existence of a minimum, but these calculations are not sufficiently accurate to rule out completely the possibility for its existence. These minima could

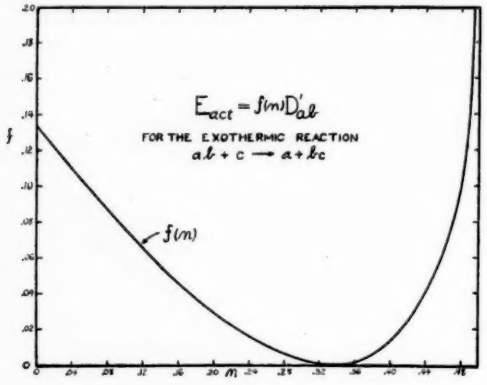

FIG. 3.

be spurious owing to the breaking down of the CPC at the small separations. However, if the minima do exist, they would have a profound effect on the reaction kinetics of atomic and free radical reactions. The lifetime of the collision complexes would be extremely long. It is interesting to examine this possibility quantitatively. The mean lifetime is the reciprocal of the specific rate of decomposition of the metastable molecules. This rate may be computed by means of the Eyring theory of absolute reaction rates. For this purpose we must calculate all of the vibration frequencies, energies, moments of inertia, etc., from our calculated potential energy surface. Assuming $n=0.14$ and taking into account the interaction between the distant atoms (in accordance with the Morse curves) we find the data in Table II. These lifetimes would have been even longer had we taken $w_{ac}=0$. The experimental evidence for the existence or nonexistence of these triatomic molecules is not conclusive. If it can be shown experimentally that these calculated lifetimes are too long, then the potential energy surfaces must be changed accordingly.

The calculations of Gorin, Walter, and Eyring indicate that free radicals stick to hydrocarbons. Their calculations do not require the CPC assumption, but their results seem to be on the same footing as the above metastable molecules.

II. Reactions Between Diatomic Molecules

The next simplest type of chemical reactions involves two diatomic molecules:

$$uv+xy \rightarrow ux+vy.$$

It will be convenient to consider the reaction in the exothermic direction. The CPC semi-empirical scheme gives the same expression for the energy of the four atom systems as for the three atoms, Eq. (2) except that

w_{ab} is replaced by the sum $w_{uv}+w_{xy}=\alpha$

w_{bc} is replaced by the sum $w_{ux}+w_{vy}=\beta$

w_{ac} is replaced by the sum $w_{uy}+w_{vx}=\gamma$

D'_{ab} is replaced by the sum $D'_{uv}+D'_{xy}$.

It is easy to see from a qualitative examination of this formula that the energy of the system is lowest when the four atoms lie in a plane. Other features of the reaction path are obscured by the complicated dependence of the energies on the internuclear distances. The calculation of the energy surfaces and activation energies for these reactions are best accomplished by means of the nomographs discussed by Altar and Eyring. We mounted onto stainless steel rules scales for the energy of the diatomic molecules as a function of their internuclear separation. These rulers were fastened together with screws and slides so that the energy of the diatomic molecules can be read directly for any desired nuclear configuration. Figure 4 will make this clear. The energies α, β, and γ are obtained by adding the scale readings for the corresponding pairs of diatomic molecules. The other nomograph makes use of the principle that if a quadrilateral has two neighboring interior angles equal to 60° and three of the sides are α, β, and γ the fourth side is equal to

$$S=(\alpha^2+\beta^2+\gamma^2-\alpha\beta-\alpha\gamma-\beta\gamma)^{\frac{1}{2}}$$

which is the square root which occurs in our energy expression. Four stainless steel rulers were fastened together so as to form a quadrilateral consistent with the 60° constraints. Three separate scales are graduated on each of the rulers. The scales in black correspond to α, β, γ, and S; the ones in red give 0.14α, 0.14β, 0.14γ, and

TABLE II.

Molecule	Activation Energy $ab+c$	Energy at Minimum	Mean Life of Metastable Molecule
F_3	7.7 kcal.	−6.6 kcal.	5.4×10^{-5} sec.
Cl_3	5.3	−6.7	2.8×10^{-6} sec.
Br_3	3.6	−5.7	5.5×10^{-8}
I_3	2.5	−4.6	2.2×10^{-10}

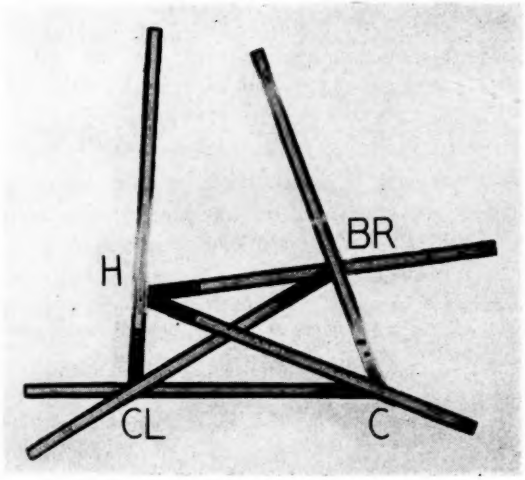

FIG. 4.

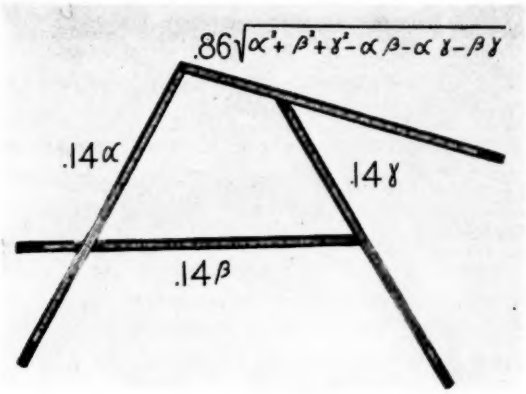

FIG. 5.

0.86S; and the ones in blue give 0.20α, 0.20β, 0.20γ, and $0.80S$. Figure 5 shows this instrument. To calculate the energy of a four atom system, it is only necessary to set the rulers for α, β, and γ, according to the black numerals, and read all four rulers according to the red or to the blue scales. The energy of the system for $n=0.14$, i.e., 14 percent Coulombic, is the sum of the four numbers in red. Similarly the energy for $n=0.20$ is the sum of the four numbers in blue. These instruments make it very easy to carry out a CPC semi-empirical calculation of the activation energies.

The substitution reaction, HBr+CCl→HCl +CBr will serve to make the activation energy calculations more clear. For each value of α' and for β there is a lowest value of the energy of the system. This can be found by trial and error, between thirty and forty settings of the nomograph suffice to determine one such energy. The lowest values of the energy are then mapped as a function of α and of β (see Fig. 6). The reaction path is easily recognized as the energetically easiest way of getting from the initial state characterized by $\alpha=\alpha_0$, $\beta=0$ to the final state characterized by $\alpha'=0$, $\beta=\beta_0$. It is interesting to examine the configurations of the atoms as the reaction proceeds along the reaction path. In Fig. 7 this is illustrated. (a) In the beginning of the reaction, the HBr approaches the Cl head on. Both the H and the Br are repelled from the C to which they are not bound. (b) After the HBr

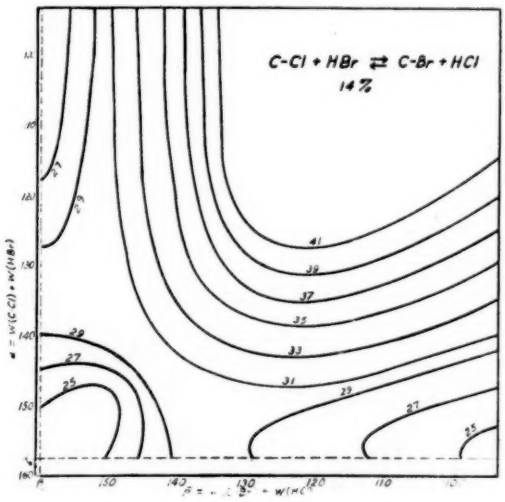

FIG. 6.

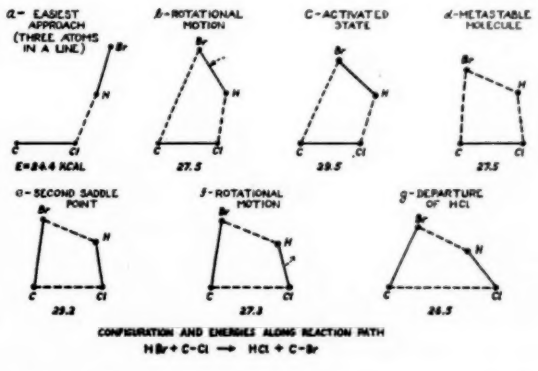

FIG. 7. Configuration and energies along reaction path HBr+C−Cl→HCl+C−Br.

TABLE III.

Reaction $X_2+Y_2\rightarrow 2XY$	Heat of Reaction	E_{act} Experiment	$0.28E_i$	Semi-empirical E_{act} $n=0.10$	Semi-empirical E_{act} $n=0.14$	Semi-empirical E_{act} $n=0.20$
$H_2+I_2\rightarrow 2HI$	+3.5	40[1,2]	40.5	48.0[3], 47.2[4]	48.3[3], 35.8[4] 37.5*	21.5[5]
$H_2+Br_2\rightarrow 2HBr$	+24.5	>43	43.3	45[3], 46[4]	36.4[4], 39*	26.5*
$H_2+Cl_2\rightarrow 2HCl$	+43.2	>39	46.6	54[3]	44.5*	29.5*
$H_2+F_2\rightarrow 2HF$	+126.8	>25	48.7	50[3]		
$H_2+H_2\rightarrow 2H_2$	0	>58	60.9	96[3], 84.2[4]	68.7[4]	
$I_2+Cl_2\rightarrow 2ICl$	+6.9	>15	26.2	12[3]	14.4*	10.4*

* Calculations of Hirschfelder for the purpose of this paper. These calculations all take the zero-point energy of the initial state equal to that at the activated state.

[1] M. Bodenstein, Zeits. f. physik. Chemie **29**, 295 (1898).
[2] G. B. Kistiakowsky, J. Am. Chem. Soc. **50**, 2315 (1928).
[3] H. Eyring, J. Am. Chem. Soc. **53**, 2537 (1931).
[4] A. Sherman and H. Eyring, paper presented at Washington Meeting of American Chemical Society.
[5] A. Wheeler, B. Topley and H. Eyring, J. Chem. Phys. **4**, 178 (1936). Unfortunately an erroneous value of the energy of dissociation of HI was used in this calculation according to a private communication with these authors.

TABLE IV. *Complex reactions.*

$ab+cd\rightarrow ac+bd$	Heat of Reaction	E_{act} Experiment	$0.28E_i$	Semi-Empirical E_{act} $n=0.10$	Semi-Empirical E_{act} $n=0.14$	Semi-Empirical E_{act} $n=0.20$
$H_2+ICl\rightarrow HI+HCl$	+19.9	>33.9[1]	42.6		39,[2] 40.5*	24.9,[3] 24*
$H_2+C_2H_4\rightarrow C_2H_6$	+33.3	+43.2[4,5]	46.6	51.5[6]	43.5[7]	
$Br_2+C_2H_4\rightarrow C_2H_4Br_2$	+30.4	<30,[8] >23[7,8]	28.9	40.6[7]	31.3,[7] 24.4[9]	
$I_2+C_2H_4\rightarrow C_2H_4I_2$	+11.30[10]	>18.2[10]	26.1		30[8]	
$CI+HI\rightarrow CH+I_2$	for methyl	33.4[11]	31.8		20.3*	10.4*
	for ethyl	29.8[11]	31.8		20.3*	10.4*
	for propyl	29.2[11]	31.8		20.3*	10.4*
$C_2H_4+HI\rightarrow C_2H_5I$	+19.0	24[11]	36.5			
$C_2H_4+HBr\rightarrow C_2H_5Br$	+19.0	34[12]	41.0			

* Calculations of Hirschfelder for the purpose of this paper.
[1] Bonner, Gore and Jost, J. Am. Chem. Soc. **57**, 2723 (1935).
[2] A. Sherman and N. Li, J. Am. Chem. Soc. **58**, 690 (1936).
[3] W. Altar and H. Eyring, J. Chem. Phys. **4**, 661 (1936).
[4] R. Pease, J. Am. Chem. Soc. **54**, 1876 (1932).
[5] G. Egloff and C. Parrish, Chem. Rev. **19**, 145 (1936).
[6] A. Sherman and H. Eyring, J. Am. Chem. Soc. **54**, 2661 (1932).
[7] A. Sherman and H. Eyring, paper presented before the Washington Meeting, American Chemical Society, 1933.
[8] A. Sherman and C. H. Sun, J. Am. Chem. Soc. **56**, 1096 (1934).
[9] A. Sherman, O. T. Quimby and R. O. Sutherland, J. Chem. Phys. **4**, 732 (1936).
[10] M. Polissar, J. Am. Chem. Soc. **52**, 956 (1930).
[11] R. A. Ogg, J. Am. Chem. Soc. **56**, 526 (1934).
[12] F. Daniels and P. L. Veltman, J. Chem. Phys. **7**, 756 (1939).

has approached to the point where the H−Cl distance is almost the equilibrium separation, the HBr performs a rotary motion with the Br approaching the C. (c) In the activated state, the H−Br and the C−Cl bonds are still resolved and the distances H−Cl and C−Br are slightly expanded. (d) The four atoms have a slight tendency to form a metastable molecule with the four principle internuclear distances corresponding to their equilibrium separations. (e) The H−Br and the C−Cl distances increase until the energy of the system is almost the same as for the activated state. (f) The HCl makes a rotary motion until the Br−H−Cl are once more in a line. (g) The HCl departs to complete the reaction.

In Tables III and IV, the experimental activation energies are compared with the semi-empirical calculations. As is customary for semi-empirical calculations, the reactions of complex molecules are idealized by considering only the atoms which are involved in the bond changes. The lack of accurate experimental data is appalling. The activation energy for H_2-I_2 is the best known. Here agreement is obtained by taking $n=0.14$. In most of the reactions, only a lower limit can be placed on the activation energy because we know only the kinetics for a competing mechanism which is more favorable. It will be observed that while the activation energy of three atom systems was mildly affected by changes in the fraction of the total energy

which is assumed to be Coulombic, the activation energy for the four atom reactions is greatly changed. The value of $n=0.14$ seems to give the best agreements.

We might seek a simple rule for the activation energies which would give rough agreement with experiment and with the semi-empirical calculations. As a first approximation, we might suppose that the activation energy is proportional to the strength of the bonds broken since this would be a logical extension of the rule for three atom reactions. Indeed:

$$E_{act}=0.28(D'_{uv}+D'_{xy})$$

is in accord with experiment as can be seen from Tables III and IV. Here the constant 0.28 has been adjusted to fit the activation energy for H_2+I_2. This rule is very similar to the one proposed by Eyring[14] in 1930. The principal objection to both these rules seems to be lack of experimental checks. One curious feature of both of these rules is that the relative sizes of the atoms do not enter into the energy considerations. The fact that rough agreement is obtained with these rules shows that at least the relative sizes of the atoms do not enter in an important way. At the present time the experimental data are not sufficiently accurate to distinguish between the activation energy of the 28 percent rule and the results of the semi-empirical scheme.

The author wishes to express his appreciation to the Wisconsin Alumni Foundation for financial assistance throughout the course of this work.

[14] H. Eyring, Zeits. f. physik. Chemie **B7**, 244 (1930).

AUGUST, 1941 JOURNAL OF CHEMICAL PHYSICS VOLUME 9

The Inductive Mechanism of Dipole Interaction and the Estimation of Molecular Dipole Moments

A. EDWARD REMICK
Department of Chemistry, Wayne University, Detroit, Michigan

(Received May 5, 1941)

The problem of calculating molecular dipole moments from constant bond moments is impractical since bond moments are greatly altered by their environment. As an alternative method it is proposed that molecules be considered as substitution products of a simple system of reference compounds whose bond moments are altered by the substitution. Equations for calculating these dipole interactions are developed on the assumption that only the inductive mechanism of electron displacement is operative in saturated molecules. The values of the dipole moments of polyhalogeno-paraffins calculated by means of these equations are found to be in rough accord with the facts. The agreement is much improved by empirical alterations of the values for the electronic polarizations of certain electron groups.

I. INTRODUCTION

IT has long been recognized that serious difficulties prevent the accurate calculation of dipole moments of molecules from the "bond moments" of their constituent bonds. In the first place, bond moments do not have constant values but are greatly altered by their intramolecular environment. Then there are the additional difficulties of locating the points within a molecule from which given dipoles may be considered to act or be acted upon and of giving adequate recognition to the fact that bond polarizabilities have both longitudinal and transverse components.[1] Fortunately bond polarizabilities are but little affected by their environment.[1] The problem has been attacked by Smallwood and Herzfeld,[2] Smyth and McAlpine,[3] and Groves and Sugden.[4] All of these investigators set up models in which the effects of intramolecular induction were considered to be

[1] K. G. Denbigh, Trans. Faraday Soc. **36**, 936 (1940).
[2] H. M. Smallwood and K. F. Herzfeld, J. Am. Chem. Soc. **52**, 1919 (1930).
[3] C. P. Smyth and K. B. McAlpine, J. Chem. Phys. **1**, 190 (1933).
[4] L. G. Groves and S. Sugden, J. Chem. Soc. 1992 (1937).

transmitted from the assumed position of a given primary dipole to any polarizable portion of the molecule *directly across the intervening space*. An alternative and simpler treatment is suggested by the concept of the "inductive mechanism" used qualitatively with great success by the English school of organic chemists.[5] According to this concept, substitution of an atom in a molecule results in the primary displacement of the bonding electron pair at the point of substitution. This primary displacement is considered to be relayed through the molecule *along the lines of the valence bonds* in proportion to their polarizabilities. Now it seems to the present author that it would be a mistake to consider the "effect" operating by the inductive mechanism and the one operating directly across space to be two independent agencies, since the alteration of the effective kernel charge of the central atom (which is considered responsible for the operation of the inductive mechanism) is thought to be due to the altered screening effect of the primary electron pair, i.e., to its altered repulsion of other electron pairs attached to the same central atom. This repulsion would be expected to operate directly across space and hence is the same repulsion as that involved in the second "effect" mentioned above. The important point to be grasped with respect to the inductive mechanism is that it does not ignore the *direct* interaction of the electron pairs attached to the same central atom but replaces this interaction by an equivalent alteration in the effective kernel charge of the central atom. The fact that the concept of the inductive mechanism has proved highly successful in giving qualitative solutions to problems in organic chemistry[5] gives one the courage to believe that it may be at least as reliable and useful a picture as the one used by the above-mentioned authors to represent the extremely complicated interactions which take place between the parts of a molecule.

The present paper shows that if it be assumed that intramolecular dipole interaction takes place in saturated molecules exclusively by the "inductive mechanism" a simple mathematical method may be developed by means of which the dipole moments of alkyl halides and polyhalides may be calculated with fair success from the moments of the corresponding monohalogeno-methanes.

II. Development of Equations

In order to calculate polarizability effects, the following well-known equation[6] may be used.

$$P_E=\frac{n^2-1}{n^2+2}\cdot\frac{m}{d}=\frac{4\pi N}{3}\sum\frac{e^2}{f}. \tag{1}$$

In this equation P_E is the electronic polarization, n the refractive index, m the molecular weight, d the density, N Avogadro's number, e the charge on an electron and f the restoring force constant. Two more well-known relationships

$$e\Delta F=-f\Delta x \tag{2}$$

and

$$\Delta F=\Delta q/r^2 \tag{3}$$

may now be combined to give

$$f=-\Delta qe/r^2\Delta x, \tag{4}$$

in which ΔF is the change in the intensity of the electric field at a given point which results from a change Δq in the charge q located at a point r cm away from the point in question, and Δx is the resultant displacement of an electron from its equilibrium position which is located at the point in question. The minus sign was introduced into Eq. (2) to make all equations consistent with the following convention: If the "reference atom" A be linked to another atom B, the dipole moment μ_{AB} will be considered positive if its positive end lies toward A. Any further displacement Δx of the bonding electron pair away from A will be considered positive. Equation (4) will be accurate only if Δx is so small that the intensity of the field may be considered constant during the displacement. We will assume, as a first approximation, that this condition is fulfilled.

Let us now define the "partial charges" $+\bar{q}_A$ and $-\bar{q}_A$ as the charges which, if placed respectively on atoms A and B, would give rise to the same moment in the bond A–B as that which actually exists. If A is a carbon atom it would be considered to bear four partial charges each one of which contributes directly to the

[5] C. K. Ingold, Chem. Rev. **15**, 225 (1934).

[6] C. P. Smyth, *Dielectric Constant and Molecular Structure* (Chemical Catalog Company, 1931), p. 143.

moment of only one bond. (Indirectly each partial charge affects all bonds by interaction, a point which will be considered below.) The following equation, in which r_{AB} is the distance between the centers of the atoms A and B, is consistent with the above definition.

$$\mu_{AB} = \bar{q}_A r_{AB} = 2ex_{AB}. \quad (5)$$

Here x_{AB} is considered to be the average distance of the bonding electron pair from the midpoint of the bond A−B in a direction toward B.

We are now in a position to attack the question of the inductive interaction of bonds. Let us assume that this interaction occurs only by the inductive mechanism.

In dealing with carbon compounds it is convenient to choose CH_3Y as a "reference molecule" and refer to its four component moments as "standard bond moments," symbolized by μ^0_{CH} and μ^0_{CY}. The carbon atom is chosen as the reference atom. Next let three hydrogen atoms of CH_3Y be substituted respectively by T_1, T_2 and T_3 (symbolized collectively as T). This substitution will increase the positive charge on C by an amount Δq_C. According to the theory of the inductive effect C−Y will be altered by the substitution through the accompanying change in the kernel charge of C, *viz.*, $\Delta q_C^{\#}$ which is effective ($\#$) in attracting the electrons of the C−Y bond. Changes in q_C produced by the substitution of any one bond may be considered to be distributed between the other bonds of the reference atom so that its effect on any one bond, say on C−Y, is

$$\Delta q_C^{\#} = K_p \Delta q_C, \quad (6)$$

where K_p is a partition constant whose existence is justified by the fact that the whole of Δq_C will not be effective in polarizing C−Y since Δq_C will be counterbalanced by shifts induced in three bonds. Thus no one bond is altered as much as though it alone were being altered. As a first approximation we might, therefore, take $K_p = \frac{1}{3}$.

The exact evaluation of Δq_C is very difficult if not impossible with our present knowledge. The difficulty arises from the circumstance that, by Eq. (5), $\bar{q}$ is zero for any non-polar bond, regardless of its length. Hence, if one H of CH_4 were replaced by a larger atom and if the resultant bond were still equally polar, $\Delta\bar{q}_C$ would be zero although the screening effect must have decreased causing an accompanying increase in the effective nuclear charge of the carbon atom. Manifestly the latter cannot be measured accurately by $\Delta\bar{q}_C$. We may, however, give formal recognition to the difficulty by considering that the effective charge on C is made up of four portions, each ascribable to one bond, and that Z_{CX} would be the portion contributed by the C−X bond if the average position of its electron pair were half-way between the C and X atoms. Accordingly, when CH_3Y is substituted by T, we may write

$$\Delta q_C = \sum_{T=T_1,T_2,T_3} [(\bar{q}_{CT} + Z_{CT}) - (\bar{q}^0_{CH} + Z^0_{CH})]. \quad (7)$$

The difference $Z_{CT} - Z^0_{CH}$ does not contribute directly to the value of $\Delta\bar{\mu}$ of the bond being substituted but it does contribute to the alteration of the other three bonds of the molecule by induction. As an example of this effect one may consider the transformation of CH_4 into $(CH_3)_3CH$ and C_2H_2, respectively. In each case Δq_C is the same since, as will be shown later, $\Delta\bar{\mu} = 0$ in each case; but Δq_C apparently is not zero if we may ascribe the higher force constant found for the C−H bond in acetylene (from Raman spectra) to a higher kernel charge on the carbon atom.

Equations (5), (6) and (7) may now be combined to express the effect of the total substitution of the three hydrogen atoms of CH_3Y.

$$\Delta q_C^{\#} = K_p \sum_{T=T_1,T_2,T_3} [(\bar{\mu}_{CT}/r_{CT}) - (\bar{\mu}^0_{CH}/r_{CH}) + Z_{CT} - Z^0_{CH}]. \quad (8)$$

This change in the charge on C results in displacing the C−Y electrons a distance Δx_{CY} away from their position in the reference molecule. Thus the "equilibrium position" alluded to in discussing Eq. (4) is seen to be the position of the electron pair in the reference molecule. If, furthermore, $\bar{\mu}_{CY}$ represents the moment of the bond C−Y in the substituted molecule, it follows from Eq. (5) that

$$\bar{\mu}_{CY}/2e = \bar{\mu}^0_{CY}/2e + \Delta x_{CY}. \quad (9)$$

By substituting appropriate values from Eqs. (1) and (4), Δx_{CY} of Eq. (9) may be replaced; also N

TABLE I. *Electronic polarizations (P_E) of electron groups.*

GROUP	P_E	LITERATURE
H : H	2.035	*a*
C : H	1.61	*a*
C : C	1.41	*a*
C : F :	1.82	*a*
C : Cl :	6.57	*b*
C : Br :	9.47	*b*

[a] Calculated from the data of Watson and Ramaswamy, Proc. Roy. Soc. **A156**, 144 (1936).
[b] Reference 6, p. 152.

may be taken as 6.03×10^{23} and e as 4.80×10^{-10} e.s.u., and it may be assumed as a first approximation that r of Eq. (4) is $r_{CY}/2$ and that f_{CY} is a constant independent of the substituents T.[1] When these substitutions are made into Eq. (9) we get

$$\bar{\mu}_{CY}-\bar{\mu}^0_{CY}=-1.583\times10^{-24}(P_E')_{CY}\Delta q_C^{\#}/r_{CY}^2. \quad (10)$$

In this equation P_E' is the polarization of an electron *pair*.

Equation (10) has been found to work out rather well with the halogens, but not with the C−H bond. For the latter better results are obtained if r_{CH} instead of $r_{CH}/2$ is taken as r in Eq. (4). This gives us:

$$\bar{\mu}_{CH}-\mu^0_{CH}=-0.557\times10^{-8}\Delta q_C^{\#}, \quad (11)$$

in which $(P_E')_{CH}$ was taken as 1.61 cm^3 and r as 1.07A.

III. THE CALCULATION OF DIPOLE MOMENTS

Equations (10) and (11) are our working equations. The values of $\Delta q_C^{\#}$ may be obtained from Eq. (8). The difference between the Z terms in Eq. (8) will have to be neglected until a method of approximating its value is found.

As a starting point in the calculation of the dipole moments of molecules, it is necessary to know the value of μ^0_{CH} in methane. Trieschmann,[7] from dipole moment measurements in combination with x-ray and electron beam results, and Timm and Mecke[8] from the strength of absorption bands, arrive at a value of about $+0.3\times10^{-18}$ e.s.u. for $\bar{\mu}_{CH}$, while Smyth[9] maintains that the correct value is -0.3×10^{-18} e.s.u. Rollefson and Havens[10] get the same numerical value but do not indicate the direction of the moment. The present author is not qualified to pass judgment on this controversy but the only explanation of the zero moments of branched chain saturated hydrocarbons, such as the isomeric heptanes,[11] which is consistent with the picture already set up in this communication is the assumption that $\mu^0_{CH}=0$. Accordingly this value will be used in the following calculations.

The method of applying Eqs. (10) and (11) may now be illustrated by showing the steps in the calculation of the dipole moment in CH_2Cl_2. First, $\bar{\mu}^0_{CCl}$, which refers to the "reference compound" CH_3Cl, must be obtained by taking H as Y and Cl as T_1. Since Y is H the reference compound now becomes CH_4. Appropriate substitutions are now made in Eq. (10) using the values in Table I for P_E' and Pauling's covalent bond radii[12] for the computation of the interatomic distances, r_{CH} and r_{CCl}, and it is solved simultaneously with the following equation, which represents the vector addition of the bond moments.

$$\mu_{CH_3Cl}=\bar{\mu}_{CCl}-\bar{\mu}_{CH}=1.86\times10^{-18} \text{ e.s.u.}$$

1.86×10^{-18} is the experimental value of the dipole moment of CH_3Cl. Values of "standard

TABLE II. *Standard bond moments.*

BOND	REF. COMPD.	$\mu_{CH_3Y}\times10^{18}$	LITERATURE	$\bar{\mu}^0_{CY}\times10^{18}$
C−H	CH_4	0.00		0.000
C−H	C_2H_6	0.00		0.000
C−H	CH_3Cl	1.86	*a*	−0.135
C−H	CH_3Br	1.80	*b*	−0.121
C−H	CH_3F	1.80	*b*	−0.160
C−C	C_2H_6	0.00		0.000
C−Cl	CH_3Cl	1.86	*a*	1.73
C−Br	CH_3Br	1.80	*b*	1.68
C−F	CH_3F	1.80	*b*	1.64

[a] Reference 6, page 201.
[b] See reference 3 in text.

[7] H. G. Trieschmann, Ber. d. Deutsch. Chem. Ges. **32**, 22 (1936).
[8] B. Timm and R. Mecke, Zeits. f. physik. Chemie **98**, 363 (1935).
[9] C. P. Smyth, J. Phys. Chem. **41**, 209 (1937).
[10] R. Rollefson and R. Havens, Phys. Rev. **57**, 710 (1940).
[11] C. P. Smyth and W. N. Stoops, J. Am. Chem. Soc. **50**, 1883 (1928).
[12] L. Pauling, *The Nature of the Chemical Bond*, first edition (Cornell University Press, 1939), p. 154.

bond moments" thus obtained are listed in Table II.

It should be remarked that, from the point of view of Eq. (10), the only significance of a substituent is the shift it produces in the electron pair binding it to the reference atom. Since the introduction of a substituent T causes shifts in the C−H electrons, this latter effect is thus equivalent to substituting the actually remaining hydrogen atoms. Thus in every case it is considered that the three initial hydrogen atoms of the reference compound, CH_3Y, are substituted either by atoms other than hydrogen or by altered hydrogen atoms.

The next step in the calculation of μ for CH_2Cl_2 is to set up two equations as follows. (1) Taking Cl as Y, the reference compound becomes CH_3Cl and T=Cl, H, H. Then from Eq. (10):

$$\bar{\mu}_{CCl}-1.73\times10^{-18}=\frac{-1.583\times10^{-24}\times6.57}{(1.76\times10^{-8})^2}\times\left[\frac{2}{3}\left(\frac{\bar{\mu}_{CH}}{1.07\times10^{-8}}+\frac{0.135\times10^{-18}}{1.07\times10^{-8}}\right)+\frac{1}{3}\left(\frac{\bar{\mu}_{CCl}}{1.76\times10^{-8}}+\frac{0.135\times10^{-18}}{1.07\times10^{-8}}\right)\right]. \quad (12)$$

(2) Taking Y as H, the reference compound becomes CH_4 and T=Cl, Cl, H. Then using Eq. (11) for $\bar{\mu}_{CH}$, proceed as above to set up another equation, which is solved simultaneously with Eq. (12) to give values for $\bar{\mu}_{CH}$ and $\bar{\mu}_{CCl}$. Finally the vector addition of two C−H and two CCl dipoles (assuming the angles between any two bonds to be tetrahedral angles, *viz.*, 109° 28′) gives the value of μ for CH_2Cl_2. Table III summarizes values thus found under the heading "first method."

Considering the crude assumptions that went into the first method, the results are gratifying. Of these assumptions, probably the one which introduces the greatest error is the use of the molar refractions of the complete halogen octets for P_E'. Only two electrons of such an octet are at the assumed distance, $r_{CX}/2$, from the reference atom; hence the polarizability effect calculated by the use of these P_E' values is too large. These considerations seem to justify the empirical lowering of the P_E' values for the carbon-halogen linkages. An empirical increase of P_E' for the C−C bond also seems justified inasmuch as it was found necessary, in dealing with substituent methyl groups, first to calculate μ_{CC} in the usual way and then to treat this value as a constant in a second calculation in which the methyl carbon was taken as the reference atom. Thus the interaction of the induced dipoles in the C−H links of the methyl group back on the C−C bond was neglected. If this back-induction had been taken into consideration it would have increased the C−C moment. On this basis the empirical increase in the polarizability of the C−C bond is justified.

TABLE III. *Calculated values of molecular dipole moments.*

COMPOUND	$\mu\times10^{18}$ (CALCULATED) FIRST METHOD	SECOND METHOD	$\mu\times10^{18}$ OBSERVED	LITERATURE
Me_2CHCl	2.02	2.09	2.15	*a*
Me_3CCl	2.06	2.19	2.13	*b*
$MeCHCl_2$	1.54	1.86	2.07, 2.06	*c, d*
EtCl	1.94	1.99	2.05	*a*
EtBr	1.87	1.93	2.01, 2.02	*a, b*
EtF	1.82	1.91	1.92	*e*
$MeCCl_3$	1.10	1.52	1.77, 1.79	*b, c*
CH_2Cl_2	1.42	1.59	1.58, 1.59, 1.62	*c, f, g*
CH_2Br_2	1.26	1.43	1.43	*c*
CHF_2Cl	1.77	1.40	1.39	*h*
$CHFCl_2$	1.36	1.24	1.29	*h*
$CHCl_3$	0.89	1.07	1.01, 1.02, 1.05	*i, c, h*
$CFCl_3$	1.23	0.78	0.45	*h*

[a] Groves and Sugden, J. Chem. Soc. 158 (1937).
[b] R. H. Wiswall Jr. and C. P. Smyth, J. Chem. Phys. **9**, 356 (1941).
[c] Maryott, Hobbs and Gross, J. Am. Chem. Soc. **63**, 659 (1941).
[d] Ghosh, Mahanti, Mukherjee, Zeits. f. Physik **58**, 711 (1929).
[e] C. P. Smyth and K. B. McAlpine, J. Chem. Phys. **2**, 499 (1934).
[f] Sanger, Physik. Zeits. **27**, 556 (1926).
[g] Mahanti, J. Ind. Chem. Soc. **5**, 673 (1928).
[h] See reference 3 in text.
[i] Ramaswamy, Proc. Indian Acad. Sci. **A4**, 108 (1936).

Accordingly a "second method" was employed in which the following empirical values for P_E' were used: C−Cl=5.1; C−Br=7.5; C−C =1.80. The value for C−H remained unaltered and it was found unnecessary to change $(P_E')_{CF}$, indicating that the polarizability of the unshared electrons of the fluorine atom must be very low. The dipole moments calculated by this second method are listed in the third column of Table III.

IV. Discussion of Results

Although the values of dipole moments calculated by the first method leave much to be desired, the general sequence of calculated moments is sufficiently correct to give one the

feeling that the induction picture, as used by the English organic chemists, is essentially correct. This feeling becomes stronger when it is found that the use of reasonable empirical values for the polarizability effects gives (second method) excellent quantitative agreement in all but two cases and yields the correct sequence of molecular dipole moments except that Me_3CCl, $MeCHCl_2$ and $MeCCl_3$ are out of line respectively by 0.10, 0.14 and 0.08 Debye units.

In comparing the results of this paper with those of previous investigators in the field, it should be remarked that Smallwood and Herzfeld made no attempt to calculate the "back induction" of an induced dipole on the primary dipole and they had no success in dealing with methane derivatives. The method of Groves and Sugden is only applicable to the calculation of dipoles induced in non-polar parts of the molecule and hence is apparently inapplicable to polyhalides. Smyth and McAlpine calculated the "back induction" from only one bond by a method of successive approximation. In this regard our method seems to be an improvement, since it takes into consideration the mutual inductive interactions of all four bonds of a carbon atom. Smyth and McAlpine only gave the results of calculations involving considerations of bond polarizabilities for two compounds, in which cases the differences between calculated and observed values are about the same as obtained by the "first method" of this paper.

Of related interest is the fact that only a few months ago the following comment was written by Maryott, Hobbs and Gross:[13] ". . . the increment in going from $CHCl_3$ to CH_3CCl_3 is approximately 0.8 D whereas the increment in going from CH_2Cl_2 to CH_3CHCl_2 is approximately 0.5 D and from CH_3Cl to CH_3CH_2Cl the increment is only 0.2 D. On the basis of any simple induction picture this sequence of increments must be regarded as very anomalous if not inexplicable." In view of these remarks it is gratifying to find that our method gives the above sequence.

It is possible, of course, that the empirical corrections of the P_E' values are over-corrections which in part compensate for the errors inherent in the development of the equations; indeed it is also probable that the special Eq. (11) required for dealing with the polarizability effect of the C−H bond falls in the same category. One obvious weakness of the method lies in the fact that the effective kernel charge cannot rigorously be shown to be equal to the sum of the partial charges as defined. This relationship must be recognized as a reasonable guess, the justification for which must be sought in the accord achieved between calculated and experimental results. The success achieved with reasonably altered polarizabilities gives one some justification for hoping that the "first method" may ultimately be improved without recourse to empirical adjustments by introducing into the mathematical development of Eq. (10) considerations of the longitudinal and transverse components of P_E', the disentanglement of the polarizabilities of shared and unshared electrons and the more accurate evaluation of r in Eq. (4) and of K_p in Eq. (10). Pending such refinements the "second method" should be useful for the empirical estimation of defects from additivity of bond moments, and the "first method," since it is based on an induction picture which has proved successful in making rough comparisons of reaction speeds and equilibrium points on the basis of alterations in effective kernel charge resulting from substitution, may reasonably be hoped to furnish a semi-quantitative refinement in such theoretical methods.

[13] Maryott, Hobbs and Gross, J. Am. Chem. Soc. **63**, 659 (1941).

Letters to the Editor

THIS section will accept reports of new work, provided these are terse and contain few figures, and especially few halftone cuts. The Editorial Board will not hold itself responsible for opinions expressed by the correspondents. Contributions to this section should not exceed 600 words in length and must reach the office of the Managing Editor not later than the 15th of the month preceding that of the issue in which the letter is to appear. No proof will be sent to the authors. The usual publication charge ($3.00 per page) will not be made and no reprints will be furnished free.

The Experimental Determination of the Intensities of Infra-Red Vibration-Rotation Absorption Bands of Gases

A. J. WELLS AND E. BRIGHT WILSON, JR.
Mallinckrodt Chemical Laboratory, Harvard University, Cambridge, Massachusetts
June 23, 1941

BECAUSE the finite resolution of available infra-red spectrometers is insufficient to follow the variations of the true absorption coefficient in a vibration-rotation absorption band, the apparent integrated absorption coefficient may differ from the true integrated absorption coefficient by several hundred percent. This is true even with the highest resolutions now obtainable for bands with sharp rotational lines. Bourgin[1] obtained reasonably accurate results for HCl by using a spectrometer capable of resolving the rotational structure and extrapolating the integral of the fraction absorbed to zero path length. Bartholomé[2] got a very different result by using a spectrometer of very low resolving power and a very high pressure of HCl, such that no rotational structure remained. His method has been criticized by Kemble,[3] whose conclusions have since been justified by the dispersion measurements of Rollefson and Rollefson.[4]

We have tested a method, related to both of the above, which seems to be very easy to apply even with a spectrometer of quite low resolving power. We extrapolate to zero *partial* pressures of absorbing gas the integral of the apparent absorption coefficient divided by partial pressure. This is measured in a cell containing a sufficiently high pressure of non-absorbing *foreign* gas to eliminate rotational fine structure. Mathematically,

$$\int \alpha d\nu = \lim\ (p \to 0)(1/pl) \int \ln\ (D/D_0) d\nu,$$

in which α is the true absorption coefficient at unit pressure, ν is the frequency, p is the pressure, l the cell length, D and D_0 the observed intensities with and without the absorbing gas, and the integrals are over the given band.

The foreign gas reduces the variation in true intensity across the band. There remains, however, the effect of the shape of the envelope. This is taken care of by the extrapolation, as can be shown mathematically. In principle it is not necessary to remove the fine structure, but in practice the extrapolation then needs to be carried too far for accuracy. However, for gases as complicated as propylene, for example, the addition of a foreign gas has no effect at reasonable pressures[5] and is therefore unnecessary, presumably because the line spacing is already less than the line width under the pressure of the absorbing gas.

TABLE I. *Intensities for bands of N_2O and C_2H_4. (Units: cm^{-1} per cm length per mm Hg pressure.)*

	Nitrous oxide		
Band	590	1285	2224 cm^{-1}
Intensity	0.043	0.37	2.1
	Ethylene		
Band	950*	1444	3050 cm^{-1}*
Intensity	0.36	0.061	0.22

* These bands consist of two unresolved fundamentals.

The above method has been applied to the fundamental bands of N_2O and C_2H_4. The results obtained are given in Table I. These figures should be considered as preliminary; greater accuracy requires special arrangements for measuring the absorption of low pressures.

Dr. R. Rollefson[6] of the University of Wisconsin very kindly sent us the infra-red dispersion curve which he has obtained for ethylene. From our own interpretation of this curve we believe that the two methods are in agreement to within 20 percent or better on the three intensities. Furthermore, these results agree well with the dielectric constant measurements of Smyth and Zahn,[7] on ethylene. Similarly, our results on nitrous oxide give 0.49 for the atomic polarization, whereas from dielectric constant and refractive index (visible) measurements, Czerlinsky[8] gives 0.46 and Watson and Ramaswamy[9] give 0.41.

A detailed description of the theory of this method and further results will be published later.

[1] D. G. Bourgin, Phys. Rev. **29**, 794 (1927).
[2] E. Bartholomé, Zeits. f. physik. Chemie **B23**, 131 (1933).
[3] E. C. Kemble, J. Chem. Phys. **3**, 316 (1935).
[4] R. Rollefson and A. H. Rollefson, Phys. Rev. **48**, 779 (1935).
[5] Eva von Bahr, Ann. d. Physik **29**, 780 (1909); **33**, 585 (1910); P. C. Cross and F. Daniels, J. Chem. Phys. **2**, 6 (1934).
[6] For the method used, see R. Rollefson and R. Havens, Phys. Rev. **57**, 710 (1940).
[7] C. P. Smyth and C. T. Zahn, J. Am. Chem. Soc. **47**, 2501 (1925).
[8] E. Czerlinsky, Zeits. f. Physik **88**, 515 (1934).
[9] H. E. Watson and K. L. Ramaswamy, Proc. Roy. Soc. **A156**, 144 (1936).

The Estimation of Intensities from X-Ray Films

JOSEPH S. LUKESH
Massachusetts Institute of Technology, Cambridge, Massachusetts
July 10, 1941

FOR the purposes of crystal structure determinations it is often enough to obtain a rough scale of relative intensities of the various x-ray reflections. Indeed, in many cases, visual comparison will suffice. In some instances, however, it is desirable to have a less arbitrary set of values which still need not be as precise as a microphotometer record. Such a case was encountered recently, and a rapid and easy method was developed which gave excellent results. In this method, prints were made of the film at various exposure times, all prints being developed simultaneously. The exposure time required to just produce

darkening of a given spot was taken as a measure of the intensity of the diffracted x-ray beam producing the spot.

The exposure required to produce a density ρ is given by the product Et, where E is the illumination and t the time. The product Et is a constant for a given density as long as the development time is constant, but both E and t may vary. Letting ρ equal the density of silver deposit which is just visible, Et is the exposure necessary to produce darkening which is just observable.

If a film be printed for such a time t_1 that one of the reflections, 200 for instance, just begins to be darkened, and for such a time t_2 that another reflection, 400, just begins to be darkened, then the relative densities of the spots are given by the ratio of t_1 to t_2. That is, if t_1 is twice t_2, then 200 is twice as dense as 400. This result follows from the fact that the product E_1t_1 must be equal to E_2t_2. Any variation in t must be accompanied by an inverse variation in E. The illumination E is inversely proportional to the density of the spot, and therefore the density is directly proportional to the time t required to produce an observable darkening. To a first approximation, the density of the silver deposit is directly proportional to the intensity of the diffracted x-ray beam. Thus, it is apparent that a measure of the intensity of any reflection relative to all others on the same film is given by the time required to bring out a silver deposit just visible to the eye.

There are, of course, limitations to this procedure. The density of a reflection is not uniform over the spot. Some one part must be chosen as a reference point, the center being the easiest. The scale of values obtained does not represent the true intensities since the intensities are not integrated over the entire spots. However, the results are highly satisfactory when only a relative scale is needed.

It should be pointed out that a printing paper which can be developed to a high contrast should be used. The higher the contrast, the greater the resolution of the spots. A paper manufactured by the Eastman Kodak Company under the trade name "Kodolith" was found suitable when developed for ten minutes.

The author is indebted to A. C. Hardy of the Massachusetts Institute of Technology for suggestions which led to the development of this method of estimating intensities.

The Vapor Pressure and Heat of Vaporization of N^{15}*

ISIDOR KIRSHENBAUM
Department of Chemistry, Columbia University, New York, New York
June 25, 1941

INTEREST in the separation of isotopes and in the theory of vapor pressures of non-polar liquids has led to the investigation of the vapor pressures of various isotopic substances. This is a preliminary report on the vapor pressure difference between natural nitrogen and nitrogen containing 34.6 percent N^{15}, with the equilibrium amounts of N^{14}_2, $N^{14}N^{15}$, and N^{15}_2.

The differential method and the apparatus used in making these measurements are similar to those used by Thode[1] but differ in several essential details which will be described in a later paper. The nitrogen samples were obtained by circulating ammonia over hot copper oxide. The ammonia was prepared from C.P. ammonium chloride. The various samples of nitrogen were purified by the use of liquid nitrogen traps and were analyzed for purity and isotopic content on a Bleakney type mass spectrometer. Two samples of natural nitrogen were also tested by measuring the differences in vapor pressure between them from 64°K to 75°K. These differences were in no case larger than the experimental error.

TABLE I.

P_1 cm	Temp. °K	P_1-P_2 cm	P_1/P_2
11.250	64.11	0.0480	1.00428
19.900	67.50	0.0771	1.00389
25.100	69.00	0.0921	1.00368
31.110	70.46	0.1081	1.00349
42.022	72.61	0.1368	1.00327
54.500	74.61	0.1646	1.00303

Table I briefly summarizes the results. Two different samples of natural nitrogen and of the concentrated nitrogen were used in obtaining these results. P_1 is the pressure of natural nitrogen and P_2 is the pressure of the nitrogen containing 34.6 percent N^{15}. Each P_1-P_2 is an average of at least four determinations on the samples, where each determination is the average of at least ten readings taken two minutes apart. The absolute temperature was deduced from the observed vapor pressure of the ordinary nitrogen using the data of Henning and Otto[2] and is correct to $\pm 0.01°$. The experimental error in P_1-P_2 is in all cases less than ± 1.4 percent of the difference, usually being ± 1 percent.

The vapor pressure data for the liquids can be represented by an equation of the form, $\log_{10}(P_1/P_2)=A/T+B$. Using this, $\Delta H_2-\Delta H_1$ was calculated to be 1.13 calories. Assuming that the difference in the heats of vaporization is a linear function of the mole fraction, the heat of vaporization of pure N^{15}_2 was found to be 3.27 calories higher than the heat of vaporization of ordinary nitrogen.

A more detailed report of these results, together with the results of work on more concentrated samples of N^{15} and extending over a somewhat larger temperature range, will be reported later. The author gratefully acknowledges his indebtedness to Professor H. C. Urey for suggesting these experiments and for his helpful advice throughout the course of the work.

[1] Harry G. Thode, J. Am. Chem. Soc. **62**, 581 (1940).
[2] Henning and Otto, Physik. Zeits. **37**, 634 (1936).
* Publication assisted by the Ernest Kempton Adams Fund for Physical Research of Columbia University.

Thermodynamics of High Polymer Solutions

PAUL J. FLORY
Esso Laboratories, Chemical Division, Standard Oil Development Company, Elizabeth, New Jersey
July 14, 1941

THE abnormal thermodynamic properties of solutions containing high polymers have been explained quantitatively by Meyer[1] in terms of an idealized model in which elements of the polymer chains replace molecules

of solvent in a quasi-solid lattice. Entropies of mixing exceeding the classical "ideal" values are attributed to the numerous configurations which the polymer molecules are free to assume. Huggins[2] has reported an approximate treatment of dilute polymer solutions, apparently assuming a model equivalent to that of Meyer. Some time ago the writer carried out, on the basis of Meyer's model, a general statistical treatment applicable to high polymer solutions at all concentrations. The entropy of mixing n solvent and N polymer molecules, each of which possesses x elements which may replace β molecules of solvent in the liquid lattice is found to be

$$\Delta S_{\text{mixing}} = k\left[-n' \ln\left(\frac{n'}{n'+xN}\right) - N \ln\left(\frac{N}{n'+xN}\right) + (x-1)N \ln\left(\frac{\gamma-1}{e}\right) - N \ln 2\right], \quad (1)$$

where $n' = n/\beta$ and γ is the coordination number for a polymer chain element in the liquid lattice. This equation differs markedly from the familiar expression for the entropy of mixing equal sized molecules. However, (1) reduces to the latter when $x = 1$, provided that the last term, which takes into account the indistinguishability of one end of the polymer molecule from the other, is omitted. Very recently Huggins[3] has derived an analogous relationship for the case $\beta = 1$.

The partial molal entropy of dilution, obtained from (1), is

$$\Delta\bar{S}_1 = -(R/\beta)[\ln(1-v_2) + (1-1/x)v_2], \quad (2)$$

where $v_2 = xN/(n'+xN)$ is the volume fraction of polymer in solution. Series expansion gives

$$\Delta\bar{S}_1 = (R/\beta)(v_2/x + v_2^2/2 + v_2^3/3 + \cdots). \quad (2')$$

Osmotic pressure data[4] for dilute solution of rubber in toluene ($\Delta\bar{H}_1 \leqq 0$) agree with (2') if one lets $\beta = 6$. Data for concentrated solutions ($v_2 > 0.5$) require a value of β in the vicinity of unity. Equation (2) predicts, in agreement with experiments,[5] that the partial pressure of solvent in a concentrated solution of a high polymer will be practically independent of molecular weight.

Assuming[6] a heat of dilution given by $\Delta\bar{H}_1 = B\bar{V}_1 v_2^2$ where $\bar{V}_1$ is the partial molar volume of the solvent, the critical condition for complete miscibility when $\beta = 1$ is found to be $B\bar{V}_1/RT = (1+x^{\frac{1}{2}})^2/2x$; the critical concentration, which is given by $v_2 = 1/(1+x^{\frac{1}{2}})$, lies close to $v_2 = 0$ for high polymers. Detailed calculations of the composition of the phases in equilibrium for $x = 1000$ when $B\bar{V}_1/RT$ exceeds slightly the critical value (i.e., slightly below the critical solution temperature) show that there will be negligible amounts of polymer in the solvent phase, even when the polymer phase contains as much as 80 percent of solvent. Thus, the statistical mechanical treatment of polymer solutions explains the results of Brønsted and Volqvartz,[7] who found that polystyrene was capable of taking up several times its weight of propyl laurate at 20° without dissolving to a perceptible extent in the excess solvent. A discussion of the bearing of this work on fractional separation of non-homogeneous polymers will be included in a forthcoming publication.

From (1) it can also be shown that, according to Meyer's model, the molar entropy change for the conversion of completely oriented polymer to a state of random entanglement is given by

$$R \ln(x/2) + R(x-1) \ln[(\gamma-1)/e]. \quad (3)$$

[1] Meyer, Helv. Chim. Acta **23**, 1063 (1940).
[2] M. L. Huggins, J. Chem. Phys. **9**, 440 (1941).
[3] M. L. Huggins, paper presented before the Wilder D. Bancroft Colloid Symposium, Ithaca, New York, June 20, 1941.
[4] Meyer, Wolff, and Boissonnas, Helv. Chim. Acta **23**, 430 (1940).
[5] Stamberger, J. Chem. Soc. 2318 (1929).
[6] G. Scatchard, Chem. Rev. **8**, 321 (1931).
[7] J. N. Brønsted and K. Volqvartz, Trans. Faraday Soc. **35**, 576 (1939); **36**, 619 (1940).